UNIMORE
UNIVERSITÀ DEGLI STUDI DI
MODENA E REGGIO EMILIA

UNIVERSITÀ DEGLI STUDI
DI MODENA E REGGIO EMILIA

Dottorato di ricerca in "Physics and nano sciences"

Ciclo XXXVIII

GRAPHENE ELECTRIC DOUBLE-LAYER TRANSISTORS FOR LABEL-FREE DETECTION OF BIOMARKERS

Candidato: ARSLAN LIAQUAT

Relatore (Tutor): Prof. Francesco Rosselaa

Coordinatore del Corso di Dottorato: Prof. Marco Affronte

ACKNOWLEDGEMENT

*"**Indeed, with hardship comes ease."***— **Al-Qur'an 94:6**

"If I have seen further, it is by standing on the shoulders of giants."- Isaac Newton

The journey of knowledge is never walked alone; it is illuminated by the guidance, support, and kindness of those who believe in us.First and foremost, I would like to express my deepest gratitude to my supervisor, **Prof. Francesco Rossella**, for his continuous guidance, encouragement, patience, and invaluable scientific insights throughout the course of this research work. His constructive discussions, critical feedback, and constant support have been fundamental to the successful completion of this thesis. I am sincerely thankful for the opportunity to work under his supervision and benefit from his expertis during my research. His professionalism, scientific vision, and dedication to research have greatly inspired me throughout my PhD journey.

I would also like to express my sincere appreciation to **Dr. Leonardo Martini**, who co-supervised my research work. I am deeply indebted to him for the extensive experimental training he provided me in Raman spectroscopy, nanofabrication, electron beam lithography, and electrical transport measurements, which became the strong technical foundation of my research. His way of mentoring was truly inspiring-always patient, supportive, and willing to explain every step with clarity and precision. The practical skills and confidence I gained under his guidance played a crucial role in shaping my development as a researcher.

I would also like to gratefully acknowledge **Prof. Enrique Diez**, Head of the Nanotechnology Group at the University of Salamanca, Spain, where I had the privilege to spend my abroad research period. I am extremely thankful to him and his research group for providing me with the opportunity to work in such an advanced and stimulating scientific environment, as well as for granting me access to the cleanroom facilities and experimental infrastructure. This experience significantly broadened my scientific perspective and enriched my research experience both academically and personally.

I would especially like to thank **Vito** for his valuable discussions and technical suggestions related to lithography processes, which were extremely helpful during my experimental work. My sincere thanks also go to **El Hadj Abidi** for introducing me to heterostructure fabrication concepts and accompanying me during transport measurements, from whom I learned many important practical aspects of experimental nanotechnology research.

I am equally thankful to **Javier, Sahil, Krishna, Ana, and Namrita** for the enjoyable discussions, shared experiences, and memorable moments during lunch breaks and research interactions. These

conversations brought positivity, friendship, and balance during demanding periods of research work.

My sincere thanks are extended to all my colleagues, collaborators, and fellow researchers for their support, cooperation, and encouragement throughout this journey. I would especially like to thank the **NanoFaber group** and my lab colleagues, particularly **Luca**, for always helping with laboratory-related matters and providing useful technical insights related to my research project. I would also like to thank **Isram, Alberta, Federico, Miriam, and Ghaseem** for their kindness, and support. Their companionship created a positive, motivating, and collaborative atmosphere that made this journey much more meaningful and enjoyable.

Finally, and most importantly, I would like to express my heartfelt gratitude to my beloved family for their unconditional love, endless prayers, patience, and unwavering support throughout every stage of my academic journey. I am especially grateful to my parents, whose sacrifices, encouragement, and constant motivation have always been the greatest source of strength in my life. As an international student living far from home, pursuing a PhD alone was never an easy journey, but every conversation with them renewed my determination and gave me the courage to continue forward.

I would also like to express my sincere love and gratitude to my brothers and sisters, especially my elder sister, who has always been a great source of inspiration and emotional support for me. Her encouragement helped me overcome many difficult moments during this journey.

A very special thanks goes to my beloved wife for her patience, sacrifices, understanding, and unwavering support throughout my PhD journey. I am deeply thankful to her for allowing and encouraging me to pursue my academic goals abroad while always standing beside me during the challenges of this path.Lastly,

I would like to dedicate this PhD thesis to my beloved children, **Zahra Fatima** and **Muhammad Zaviyar Ali**. Their innocence, love, and smiles have always brought peace and motivation to my heart, even during the most difficult times. They remain my greatest inspiration and the true joy behind every achievement.

ARSLANLIAQUAT

ABSTRACT

Graphene-based electrolyte-gated field-effect devices have emerged as promising platforms for label-free biosensing owing to their high carrier mobility, large surface-to-volume ratio, and strong sensitivity to electrolyte-mediated carrier modulation and interfacial transport perturbations. In particular, graphene electric double-layer transistors (GEDLTs) enable enhanced coupling between the electrolyte and graphene channel through nanometer-scale electric double-layer capacitance, allowing sensitive electrical detection of biomolecular interactions under liquid-gated conditions. However, the coupled influence of ionic screening, biomolecular adsorption, interfacial charge redistribution, and carrier transport on the sensing response remains insufficiently understood. In particular, the relationship between adsorption-induced interfacial perturbations and transport behaviour in graphene biosensors requires further physical clarification.

This thesis investigates the sensing mechanisms of graphene electric double-layer transistors for label-free biomarker detection through experimental characterization, continuum electrostatic analysis, and atomistic adsorption modelling. Experimental investigation, supported by modelling-assisted interpretation, was employed to examine coupled transport and interfacial sensing phenomena occurring near the graphene–electrolyte interface.

Continuum electrostatic analysis was employed to investigate electric double-layer formation, ionic screening, and electrolyte-mediated carrier modulation in graphene transistor structures. The simulations supported interpretation of the sensing behaviour under varying electrolyte and pH conditions, demonstrating that electrolyte-gated graphene transistors exhibit strong sensitivity to local interfacial transport perturbations because of the high electric double-layer capacitance. The analysis indicated that electrolyte conditions and ionic screening strongly influence carrier modulation near the graphene surface.

Experimental characterization of human serum albumin sensing revealed systematic evolution of the transfer characteristics, transconductance, carrier mobility, and transport broadening with increasing biomolecular concentration. The graphene electric double-layer transistor platform

exhibited concentration-dependent electrical response with a calculated limit of detection of **0.0087 mg mL^{-1}.** The sensing response demonstrated that biomolecular adsorption modifies not only carrier density but also the graphene transport uniformity through adsorption-induced disorder and carrier scattering effects.

Brownian Dynamics simulations were employed to support interpretation of the sensing response. The atomistic analysis revealed that albumin adsorption occurs through heterogeneous molecular orientations and dynamically distributed adsorption configurations rather than a single preferred adsorption geometry. Different adsorption states generated spatially varying interfacial perturbations near the graphene surface, providing physical insight into the observed transport broadening and mobility suppression during sensing.

The combined experimental and modelling-assisted analysis demonstrates that graphene electric double-layer transistor biosensors operate through coupled ionic, adsorption-induced, and transport-mediated interfacial mechanisms spanning continuum and atomistic scales. These findings indicate that transport-sensitive analysis provides a physically meaningful approach for interpreting adsorption-induced disorder and heterogeneous biomolecular interactions in electrolyte-gated graphene biosensors. Overall, this thesis provides a physically grounded understanding of coupled transport and interfacial sensing mechanisms in graphene-based label-free biosensors.

Contents

LIST OF FIGURES

produces localized electrostatic perturbations and transport disorder, leading to carrier mobility suppression and amplified transport-sensitive electrical response.

CHAPTER 1
INTRODUCTION, MOTIVATION, AND STATE OF THE ART

1.1 Introduction

The rapid advancement of biosensing technologies has substantially influenced modern healthcare, environmental monitoring, and biochemical analysis. In particular, there is growing demand for sensing platforms capable of rapid, selective, and highly sensitive detection of chemical and biological species under physiologically relevant conditions. Such requirements are especially important in applications related to early disease diagnostics, point-of-care testing, and continuous health monitoring, where conventional analytical techniques often remain time-consuming, expensive, and dependent on complex laboratory infrastructure [1-3].

Among the different sensing approaches currently under investigation, electrochemical and field-effect transistor (FET)-based biosensors have attracted considerable attention due to their compatibility with miniaturized electronic systems and their capability for real-time, label-free detection [4]. In these devices, molecular interactions at the sensing interface can directly modulate electrical transport properties in the active channel, enabling high-sensitivity electrical transduction of biochemical events. The continuous development of nanoscale materials and low-dimensional electronic systems has further accelerated progress in this field by improving interfacial sensitivity and reducing detection limits [4].

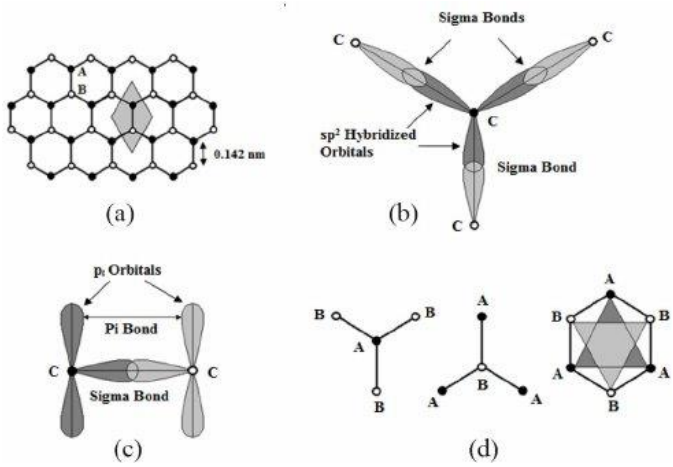

Figure 1.1: Evolution of graphene-based electronic devices and applications highlighting the emergence of graphene as a multifunctional electronic material. Adapted from Dash et al. (2014) Ref.5

Graphene has emerged as one of the most intensively investigated nanomaterials for electronic biosensing applications owing to its unique structural and electrical properties [6, 7]. It consists of a two-dimensional hexagonal lattice of sp^2-bonded carbon atoms and exhibits exceptionally high carrier mobility, large specific surface area, optical transparency, and remarkable electrostatic tunability [6]. Since every atom in graphene is exposed to the surrounding environment, the material is highly sensitive to local electrostatic perturbations induced by ionic species, charged biomolecules, and interfacial adsorption processes [8]. These characteristics make graphene particularly attractive for electrolyte-based sensing platforms where electrical response is strongly governed by surface interactions.

Graphene field-effect transistors (GFETs) have therefore become an important class of biosensing devices capable of converting local electrochemical variations into measurable electrical signals [9–11]. In electrolyte-gated configurations, the graphene channel is electrostatically modulated through an electrolyte medium, allowing efficient capacitive coupling between ionic redistribution within the electrolyte and carrier transport in graphene. Under these conditions, the formation of an electric double layer (EDL) near the graphene–electrolyte interface produces extremely high interfacial electric fields over nanometric distances, enabling strong electrostatic gating at relatively low operating voltages [9].

The sensing behaviour of electrolyte-gated GFETs is closely associated with interfacial electrostatic phenomena occurring at the solid–liquid interface. Parameters such as ionic strength, electrolyte composition, pH, Debye screening length, and surface charge density can substantially influence the local electrostatic environment surrounding the graphene channel [12]. As a result, variations in interfacial ionic distribution may directly affect graphene carrier concentration, channel conductance, and Dirac voltage response, as well as transport-related parameters such as carrier mobility and scattering behavior. Understanding these coupled electrostatic interactions is therefore essential for improving the sensitivity, operational stability, and interpretation of graphene-based biosensors operating in electrolyte environments [13].

Despite substantial progress in graphene biosensing technologies, several challenges remain in understanding the relationship between molecular adsorption, ionic screening, and electrical transport modulation under realistic physiological conditions. In concentrated electrolytes, strong

Debye screening can significantly suppress long-range electrostatic interactions between charged biomolecules and the graphene surface, thereby complicating the interpretation of sensing signals [14]. Furthermore, many experimental studies report electrical sensing responses without fully correlating interfacial electrostatics, ionic transport, and adsorption-mediated carrier modulation across multiple physical length scales [12].

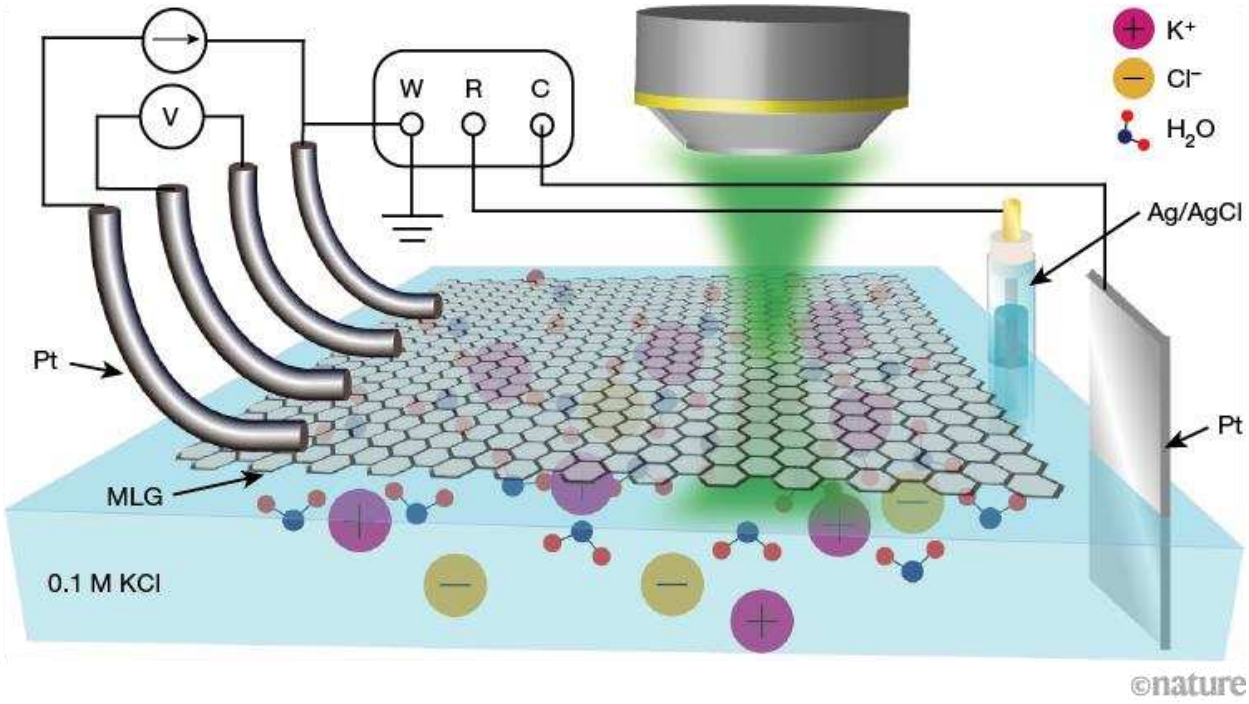

Figure 1.2: Conceptual illustration of microscopic processes occurring at electrode–electrolyte interfaces relevant to electrochemical and graphene-based sensing systems. Adapted from Xu et.al (2023) Ref. (15)

For this reason, increasing attention has recently been directed toward combined experimental and modelling approaches capable of correlating electrostatic interactions with measurable transport behavior [16]. Such approaches can provide deeper physical insight into how nanoscale ionic and molecular interactions influence measurable electronic behaviour in electrolyte-gated graphene devices

The present thesis investigates electrolyte-mediated transport modulation and sensing behaviour in electrolyte-gated graphene field-effect transistors through a combined modelling and experimental framework. Particular emphasis is placed on understanding the influence of electric double-layer formation, ionic screening, pH-dependent electrostatic interactions, and biomolecular

adsorption on the electrical transport characteristics of graphene devices operating in electrolyte environments. Continuum finite-element modelling, atomistic considerations, and experimental transport measurements are integrated to provide a broader interpretation of electrolyte-mediated sensing mechanisms in graphene-based transistor platforms.

Within electrolyte-gated graphene devices, the sensing response is strongly influenced by electrostatic coupling at the graphene–electrolyte interface, where ionic redistribution and carrier modulation jointly determine the measured electrical behaviour. The following chapters therefore progressively develop the theoretical background, modelling framework, experimental methodology, and transport analysis required to investigate electrolyte-mediated sensing phenomena in graphene-based electronic systems.

1.2 Research Motivation and Objectives

1.2.1 Research Motivation

The increasing demand for rapid, reliable, and miniaturized biochemical detection technologies has accelerated the development of electronic biosensors capable of operating in complex electrolyte environments. Among the various sensing platforms currently under investigation, graphene-based field-effect transistors have emerged as promising candidates due to their high carrier mobility, low intrinsic noise, and strong sensitivity to surface electrostatic perturbations [9–11]. In particular, electrolyte-gated graphene field-effect transistors (EG-GFETs) have attracted considerable interest for applications involving pH sensing, ion detection, and biomolecular recognition under physiologically relevant conditions [9,].

Despite substantial progress in graphene biosensor development, several fundamental challenges remain unresolved in understanding the physical origin of sensing behaviour in electrolyte-gated devices. Under electrolyte conditions, the sensing response is not governed solely by biomolecular adsorption, but rather by the coupled interaction between ionic screening, electric double-layer formation, interfacial electrostatics, and graphene carrier modulation [12–14]. Furthermore, electrolyte-mediated disorder and scattering effects may significantly influence carrier mobility and transport behavior, particularly near the Dirac regime, yet these effects remain comparatively underexplored in graphene biosensing literature.These effects become especially important in

physiological electrolytes, where high ionic concentrations significantly reduce the effective range of electrostatic interactions through Debye screening [14].

As a consequence, experimentally measured electrical signals in graphene transistors often cannot be interpreted exclusively in terms of direct charge transfer from adsorbed biomolecules. Variations in ionic strength, pH, electrolyte composition, surface charge density, and adsorption configuration may simultaneously contribute to the observed transport response. This complexity has led to continuing discussion regarding the dominant mechanisms responsible for signal modulation in electrolyte-gated graphene sensing platforms.

Another important limitation in the current literature is the partial separation between experimental observations and theoretical interpretation. Many experimental studies report transfer characteristics and sensing responses without fully correlating these measurements with interfacial electrostatics or ionic transport phenomena. Conversely, several theoretical studies focus primarily on continuum electrostatic analysis while neglecting experimentally relevant adsorption behaviour and transport characteristics. Consequently, a comprehensive understanding of how nanoscale interfacial interactions influence measurable electrical transport behaviour remains incomplete [16].

In addition, much of the existing graphene biosensing literature primarily emphasizes sensitivity enhancement, while comparatively less attention is directed toward understanding the underlying physical mechanisms governing electrolyte-mediated sensing response. For biosensors intended to operate in physiological environments, this limitation becomes particularly significant because electrolyte composition and ionic screening strongly affect sensing stability, reproducibility, and selectivity[17,18].

These considerations motivate a combined experimental and modelling investigation aimed at establishing physically consistent relationships between electrolyte-mediated interfacial interactions, carrier transport modulation, and experimentally measurable sensing response. Such an approach is necessary for establishing clearer relationships between electric double-layer formation, ionic redistribution, electrolyte-mediated carrier transport modulation, and experimentally measurable transport characteristics.

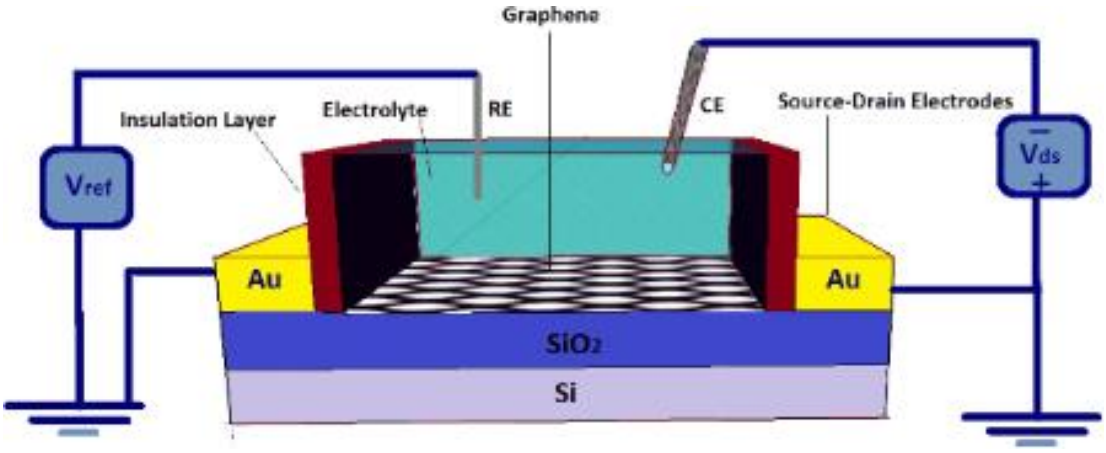

Figure 1.3: Framework illustrating the relationship between electrolyte-mediated interfacial interactions, graphene carrier modulation, and experimentally measurable sensing response[14]

Within this context, the present thesis investigates electrolyte-gated graphene field-effect transistors as coupled electrostatic and electronic transport systems rather than purely empirical sensing devices. Particular attention is directed toward understanding how electrolyte-mediated interfacial interactions influence graphene transport response under pH variation and biomolecular adsorption conditions. Continuum finite-element electrostatic modelling, atomistic considerations, and experimental electrical characterization are therefore combined to provide a physically consistent interpretation of graphene-based sensing mechanisms.

1.2.2 Research Objectives

The primary objective of this thesis is to investigate electrostatic modulation and sensing behaviour in electrolyte-gated graphene field-effect transistors operating under electrolyte conditions relevant to biosensing applications. The study aims to establish a clearer physical understanding of how ionic transport, interfacial electrostatics, and adsorption-mediated interactions influence measurable electrical transport characteristics in graphene-based sensing platforms.

The specific objectives of the thesis are summarized as follows:

- To analyze electric double-layer formation, ionic redistribution, and electrostatic potential modulation near the graphene electrolyte interface.
- To study the influence of electrolyte concentration and Debye screening on graphene carrier transport behaviour under electrolyte-gated conditions.

- To investigate mobility modulation, disorder-induced scattering, and transport degradation mechanisms associated with electrolyte interactions and biomolecular adsorption in graphene transistor platforms.
- To investigate the transport behaviour of electrolyte-gated graphene field-effect transistors through continuum finite-element modelling approaches.
- To investigate pH-dependent electrical transport characteristics of graphene transistors operating in phosphate-buffered saline solutions.
- To experimentally evaluate transfer characteristics, Dirac voltage evolution, mobility variation, hysteresis behaviour, and disorder-mediated transport response.
- To examine biomolecular adsorption effects and electrostatic disorder mechanisms associated with albumin sensing in graphene transistor platforms.
- To employ modelling-assisted interpretation combining continuum electrostatic analysis with experimentally relevant transport and adsorption considerations.
- To correlate continuum electrostatic modelling with experimentally observed transport response to obtain a more physically consistent interpretation of sensing behaviour.

1.2.3 Expected Contributions

The work presented in this thesis is expected to contribute toward a broader understanding of electrolyte-mediated sensing mechanisms in graphene-based transistor platforms. In particular, the thesis seeks to establish clearer relationships between interfacial electrostatics, ionic screening, biomolecular adsorption, and electrical transport modulation in electrolyte-gated graphene devices.

From a modelling perspective, the thesis contributes to the development of modelling-assisted electrostatic interpretation that describes electrostatic potential distribution, ionic transport behaviour, and electric double-layer formation in electrolyte-gated transistor architectures. These approaches provide insight into how electrolyte conditions influence graphene carrier modulation under realistic sensing environments[16].

From an experimental perspective, the thesis provides systematic electrical characterization of electrolyte-gated graphene transistors under varying pH and electrolyte conditions, including analysis of transfer characteristics, Dirac voltage evolution, hysteresis response, and transport

behaviour in phosphate-buffered saline solutions. This experimental analysis further provides insight into mobility modulation and disorder-mediated transport mechanisms during electrolyte-gated sensing.

The thesis further contributes toward bridging the gap between continuum electrostatic modelling and experimentally observed sensing response by integrating electrostatic analysis with atomistic considerations associated with biomolecular adsorption processes [17]. Such multiscale interpretation may support the future design of graphene-based biosensors with improved sensitivity, operational stability, and reliability in complex electrolyte environments.

Beyond sensing performance alone, the present work aims to provide a clearer physical interpretation of how electrolyte-mediated interfacial phenomena influence the electrical behaviour of graphene transistor sensors operating under physiologically relevant conditions.

1.3 Thesis Organization

The present thesis investigates electrolyte-gated graphene field-effect transistors through a combined modelling and experimental framework, with particular emphasis on understanding the electrostatic and transport mechanisms governing sensing behaviour in electrolyte environments. The work integrates fabrication, electrical characterization, continuum electrostatic modelling, and multiscale interpretation in order to examine how interfacial ionic interactions influence graphene-based biosensors operating under physiologically relevant conditions.

The thesis is organized into six chapters, each addressing a specific aspect of the research developed throughout this work.

Chapter 1 introduces the scientific background associated with graphene-based biosensing technologies and electrolyte-gated transistor platforms. The chapter presents the research motivation, objectives, and current state of the art related to graphene biosensors, electrolyte gating, and interfacial electrostatic phenomena.

Chapter 2 describes the materials, fabrication procedures, and experimental methodologies employed for the preparation and characterization of graphene devices. Particular attention is given

to graphene transfer procedures, nanofabrication processes, Raman spectroscopy, and electrical transport measurement configurations used throughout the thesis.

Chapter 3 presents the theoretical and computational modelling framework developed for electrolyte-gated graphene transistors. The chapter discusses electric double-layer formation, ionic transport, electrostatic modulation, and continuum finite-element modelling approaches relevant to graphene–electrolyte interfaces. Atomistic considerations associated with biomolecular adsorption processes are also introduced.

Chapter 4 investigates electrostatic modulation and pH sensing behaviour in electrolyte-gated graphene transistors through combined modelling and experimental analysis. The influence of ionic screening, electrolyte concentration, and pH variation on electrical transport response is systematically examined under phosphate-buffered saline conditions.

Chapter 5 focuses on albumin sensing and disorder-mediated transport behaviour in graphene transistor platforms. The chapter examines the relationship between biomolecular adsorption, electrostatic disorder, and experimentally observed transport characteristics, including mobility variation, disorder-mediated transport behaviour, and electrostatic modulation together with multiscale interpretation of sensing behaviour.

Chapter 6 summarizes the principal findings of the thesis and outlines potential future research directions associated with graphene-based biosensors, electrolyte-gated transistor platforms, and multiscale electrostatic modelling approaches.

The chapters are arranged to progressively connect the fabrication, modelling, and experimental aspects of electrolyte-gated graphene biosensors, allowing the electrostatic and transport mechanisms governing sensing behaviour to be examined across multiple p,hysical scales.

State of the Art

1.4 Background and State of the Art

1.4.1 Biosensing Technologies and Analytical Targets

Biosensors occupy an important position in modern analytical science because they provide a route for detecting biological and chemical species through direct conversion of a recognition event into a measurable signal. Their relevance extends across clinical diagnostics, environmental monitoring, food safety, and biochemical analysis, where rapid response, selectivity, and operation with small sample volumes are often required [1,2]. Compared with conventional laboratory techniques, biosensors offer the possibility of simpler measurement procedures and closer integration with portable or point-of-care platforms.

A biosensor typically combines two essential components: a recognition element and a transducer. The recognition element interacts selectively with the target analyte, while the transducer converts the resulting biochemical or physicochemical change into an electrical, optical, mechanical, or thermal signal [3]. Depending on the transduction principle, biosensors may be classified into electrochemical, optical, piezoelectric, thermal, and field-effect-based devices [4,5]. Among these, electrochemical and transistor-based sensors are particularly attractive when direct electrical readout, miniaturization, and compatibility with integrated electronics are required.

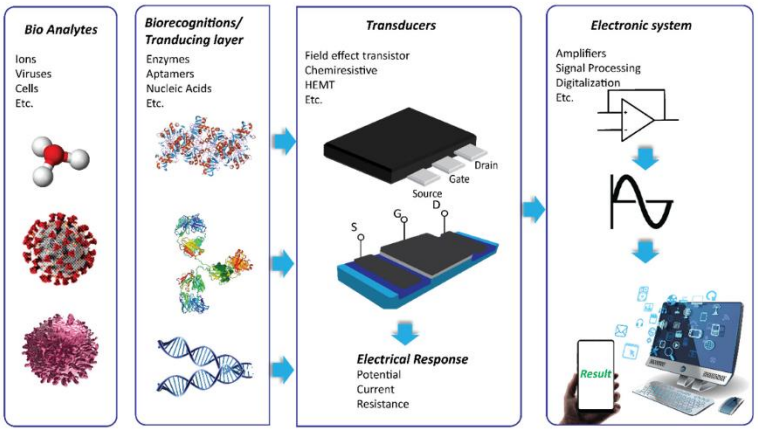

Figure 1.4: General workflow of biosensing systems showing analyte recognition, signal transduction, and electrical readout processes.Adapted from Ref.19

The choice of analytical target strongly influences the design and operation of a biosensor. In biomedical contexts, relevant targets include ions, small molecules, proteins, nucleic acids, hormones, metabolites, and pathogen-related biomarkers [17]. Each class of analyte introduces different sensing requirements. Small molecules may produce weak interfacial perturbations, proteins often exhibit complex charge distributions and adsorption behaviour, while ionic species such as protons directly influence local electrochemical conditions. For this reason, a sensing platform intended for biological applications must be evaluated not only by its sensitivity, but also by how reliably it operates in liquid and electrolyte environments.

pH sensing represents one of the simplest but most informative cases for studying interfacial electrochemical response. Variations in proton concentration modify surface charge conditions and local electrostatic potential, making pH a useful model system for investigating charge-sensitive transduction mechanisms [9]. Protein detection, on the other hand, introduces additional complexity because biomolecules interact with sensor surfaces through electrostatic forces, dipolar interactions, hydration effects, and adsorption geometry. These effects are particularly relevant for field-effect-based biosensors, where the measured signal depends on how interfacial charge variations influence carrier transport in the active channel.

As biosensing technologies continue to evolve, increasing attention has been directed toward electrically active sensing platforms capable of operating in electrolyte environments and complex biological media. This direction is especially relevant for label-free sensors, where molecular interactions are monitored directly without fluorescent, enzymatic, or radioactive labels [17,18]. The performance of such devices is therefore closely linked to the properties of the sensing interface, the transduction material, and the surrounding electrolyte medium. These considerations naturally motivate the use of nanostructured materials, whose large surface-to-volume ratio can enhance the coupling between molecular interactions and measurable device response.

1.4.2 Nanomaterials for Biosensing Applications

The introduction of nanostructured materials has significantly expanded the capabilities of electrically transduced biosensors by enhancing interfacial sensitivity and charge-coupling efficiency at the sensing interface [6,7]. Owing to their reduced dimensionality and large surface-to-volume ratio, nanomaterials enable stronger interaction between target analytes and the active

sensing region, allowing small biochemical perturbations to generate measurable electrical responses. These characteristics have motivated extensive research into nanoscale transducers for applications requiring rapid, label-free, and highly sensitive detection.

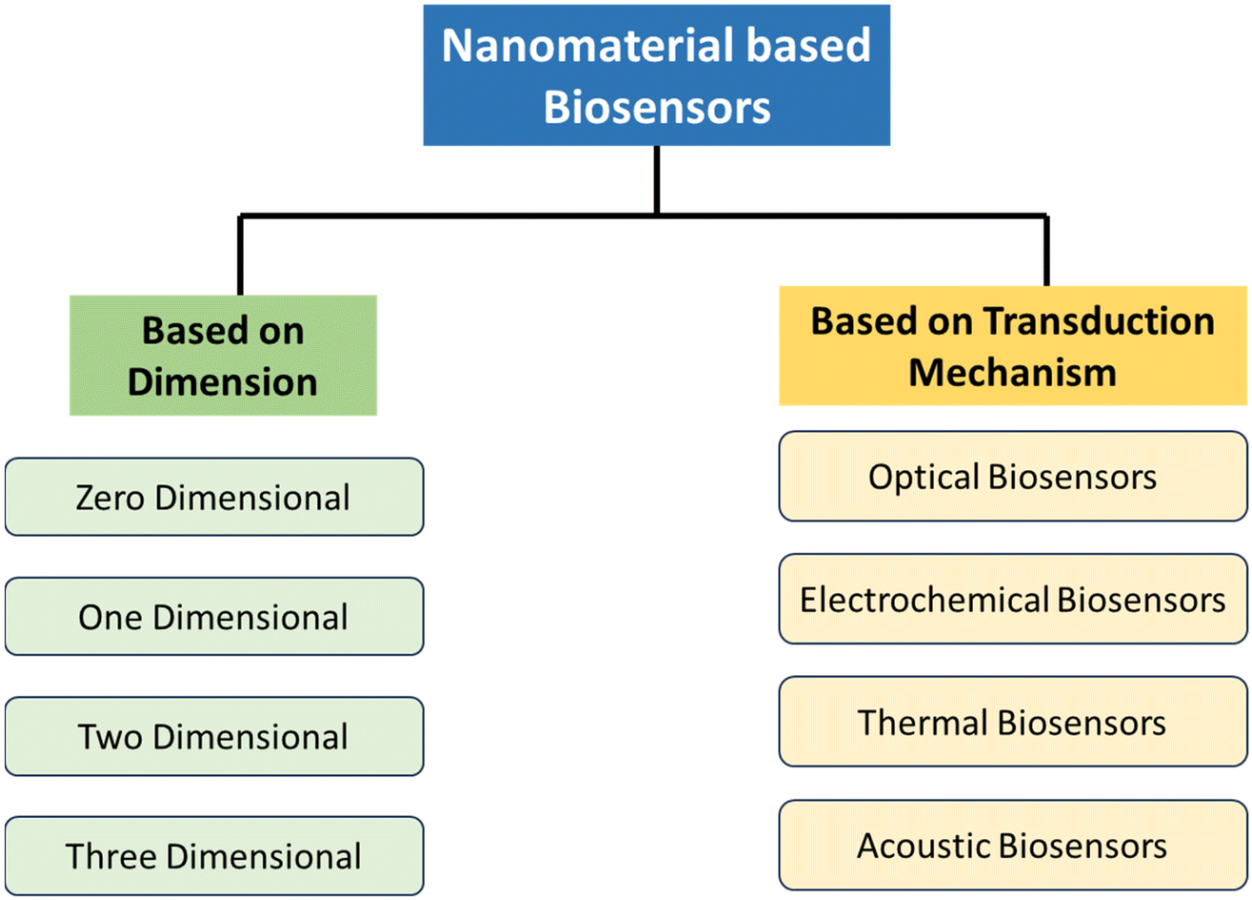

Figure 1.5: Representative nanomaterials employed in biosensing applications highlighting nanoscale transduction mechanisms and interfacial sensing architectures. Adapted from Singh et al. (2025) Ref.20

Among the different classes of nanomaterials investigated for biosensing applications, carbon-based nanostructures have attracted particular interest because of their favorable electrical transport properties and compatibility with miniaturized device architectures [10]. Carbon nanotubes were initially explored extensively for electronic sensing owing to their nanoscale geometry and strong sensitivity to local charge perturbations occurring near the device surface [11]. Their use demonstrated the potential of low-dimensional conductive materials for electrically transduced biosensing platforms operating under liquid-phase conditions.

Subsequent advances in two-dimensional materials research directed increasing attention toward graphene as a promising transducer material for next-generation biosensors [5,6]. In contrast to one-dimensional nanostructures, graphene provides a continuous electrically conductive surface directly exposed to the surrounding environment, enabling efficient coupling between interfacial charge redistribution and carrier transport within the material. This characteristic is particularly important for sensing platforms operating in electrolyte environments, where variations in ionic distribution and molecular adsorption strongly influence local electrostatic conditions.

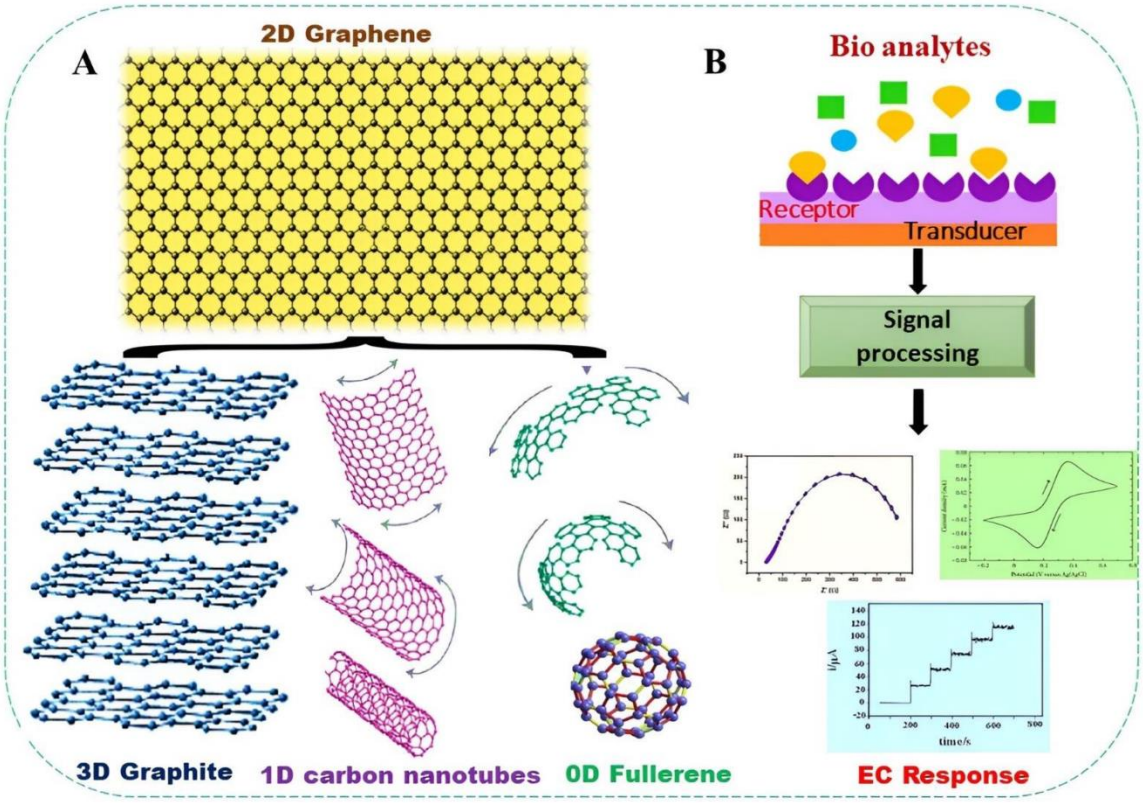

Figure 1.6: Graphene-based biosensing platforms for electrochemical and bioanalytical applications. Adapted from Ashraf et al. (2022) Ref. 21

Graphene-based sensing devices have therefore been extensively investigated for applications involving ion detection, pH sensing, protein adsorption monitoring, and biochemical recognition [122]. The atomically thin structure of graphene allows electrical transport properties to respond sensitively to perturbations occurring at the solid–liquid interface, while the planar geometry supports integration into field-effect transistor architectures suitable for electrolyte-gated operation. As a result, graphene has become one of the most widely studied materials for

electrically active biosensing platforms requiring direct electrostatic transduction under liquid-phase conditions.

In addition to pristine graphene, several graphene derivatives and hybrid structures have also been explored for biosensing applications, including graphene oxide, reduced graphene oxide, and graphene-based heterostructures combined with metallic nanoparticles or other two-dimensional materials [22]. These approaches are often employed to improve chemical functionalization capability, molecular selectivity, and interfacial stability in complex biological environments. Nevertheless, pristine graphene remains an important model material for investigating electrostatic transport modulation because of its strong sensitivity to interfacial charge redistribution and relatively well-understood electronic behaviour.

The growing interest in graphene-based sensing platforms has consequently stimulated extensive research into graphene field-effect transistor architectures and electrolyte-gated sensing configurations. Among these approaches, graphene transistor platforms have emerged as particularly attractive systems for investigating electrically transduced biosensing under electrolyte conditions.

1.4.3 Graphene and Graphene Field-Effect Transistors

Graphene has become one of the most intensively investigated materials for electrically transduced biosensing due to its strong sensitivity to interfacial charge perturbations and surface adsorption processes. Since charge transport in graphene occurs within a single atomic layer directly exposed to the surrounding environment, even small variations in local charge distribution can influence its electrical behaviour. This characteristic has positioned graphene among the most promising transducer materials for sensing platforms operating under liquid-phase and electrolyte conditions [6-8]

The electronic transport properties of graphene, combined with its planar geometry and electrostatic tunability, have motivated extensive research into graphene-based electronic devices for chemical and biological sensing applications. In particular, graphene field-effect transistors (GFETs) have emerged as attractive sensing platforms because the carrier concentration within the graphene channel can be efficiently modulated by electrostatic interactions occurring near the

surface. Molecular adsorption, ionic redistribution, and variations in interfacial charge environment may therefore produce measurable changes in electrical transport behaviour[11,14]

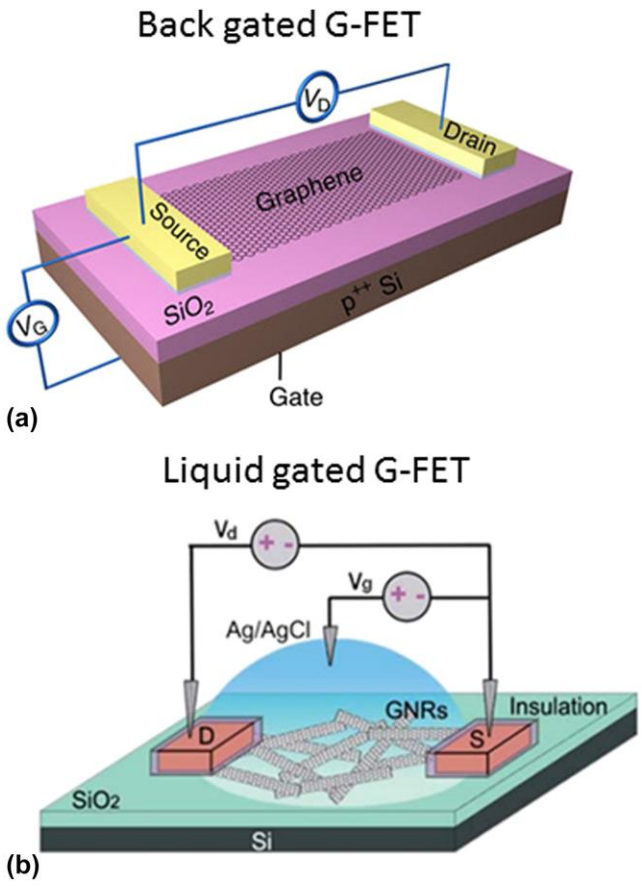

Figure 1.7: Schematic illustration of a back-gated and liquid-gated Graphene Field Effect Transistor. Adapted from Thakoor et al. (2024) Ref. 25

In a typical GFET architecture, graphene forms the conductive channel connecting source and drain electrodes, while an external gate electrode modulates carrier concentration through an applied electric field. Unlike conventional semiconductors, graphene exhibits ambipolar transport behaviour, where both electrons and holes can contribute to electrical conduction depending on the gate potential. The transition between electron- and hole-dominated conduction occurs near the charge neutrality point, commonly referred to as the Dirac point, which represents an important electrical characteristic in graphene transistor measurements [9-11]

The high sensitivity of graphene transistors to interfacial charge perturbations has motivated their investigation across a broad range of sensing applications, including gas sensing, ion detection,

pH monitoring, and biomolecular recognition [18,19]. In these systems, adsorption processes occurring near the graphene surface can modify carrier concentration, induce local electrostatic disorder, or influence scattering mechanisms within the conductive channel, thereby influencing mobility evolution and disorder-mediated transport response during sensing. As a result, electrical transport measurements provide indirect information regarding molecular and ionic interactions occurring at the sensing interface[9,10,24]

Compared with conventional bulk transducer materials, graphene provides direct electrostatic coupling between the surrounding environment and the conductive channel because every atom is exposed to the sensing interface. This property becomes particularly important under liquid-phase operation, where ionic redistribution and interfacial charge modulation strongly influence transistor behaviour. The planar structure of graphene additionally supports integration into scalable electronic architectures suitable for electrically transduced biosensing platforms.

Graphene transistor devices are frequently operated under electrolyte-gated conditions for sensing applications performed in liquid environments. Under these conditions, ions within the electrolyte participate directly in the gating process through interfacial charge redistribution near the graphene surface. Consequently, the electrical behaviour of graphene transistors becomes strongly influenced by electrolyte composition, ionic screening,and adsorption-mediated interactions occurring near the solid–liquid interface .These characteristics have established graphene transistor architectures as important platforms for investigating electrically transduced sensing phenomena under liquid-phase conditions. Understanding how interfacial ionic interactions influence graphene carrier dynamics, therefore, remains central to the interpretation and optimization of graphene-based biosensors.

1.4.4 Electrolyte Gating and Interfacial Electrostatics

Electrolyte-gated operation plays a central role in graphene transistor biosensors designed for liquid-phase sensing and biochemical detection under physiological conditions. Unlike conventional solid-state dielectric gating, electrolyte-gated devices employ an ionic medium positioned above the graphene surface, allowing gate modulation to occur through ionic redistribution within the liquid environment. This configuration enables strong coupling between the electrolyte and the graphene channel while operating at relatively low gate voltages [9.10].

When a gate potential is applied, mobile ions within the electrolyte rearrange near the solid–liquid interface, forming an electric double layer (EDL) at both the gate electrode-electrolyte and graphene-electrolyte interfaces [12,13]. Because the separation between oppositely charged ionic regions occurs over nanometric distances, the resulting interfacial capacitance becomes extremely large compared with conventional dielectric-gated systems. Consequently, small variations in gate bias can produce substantial modulation of graphene carrier concentration and transport behaviour.

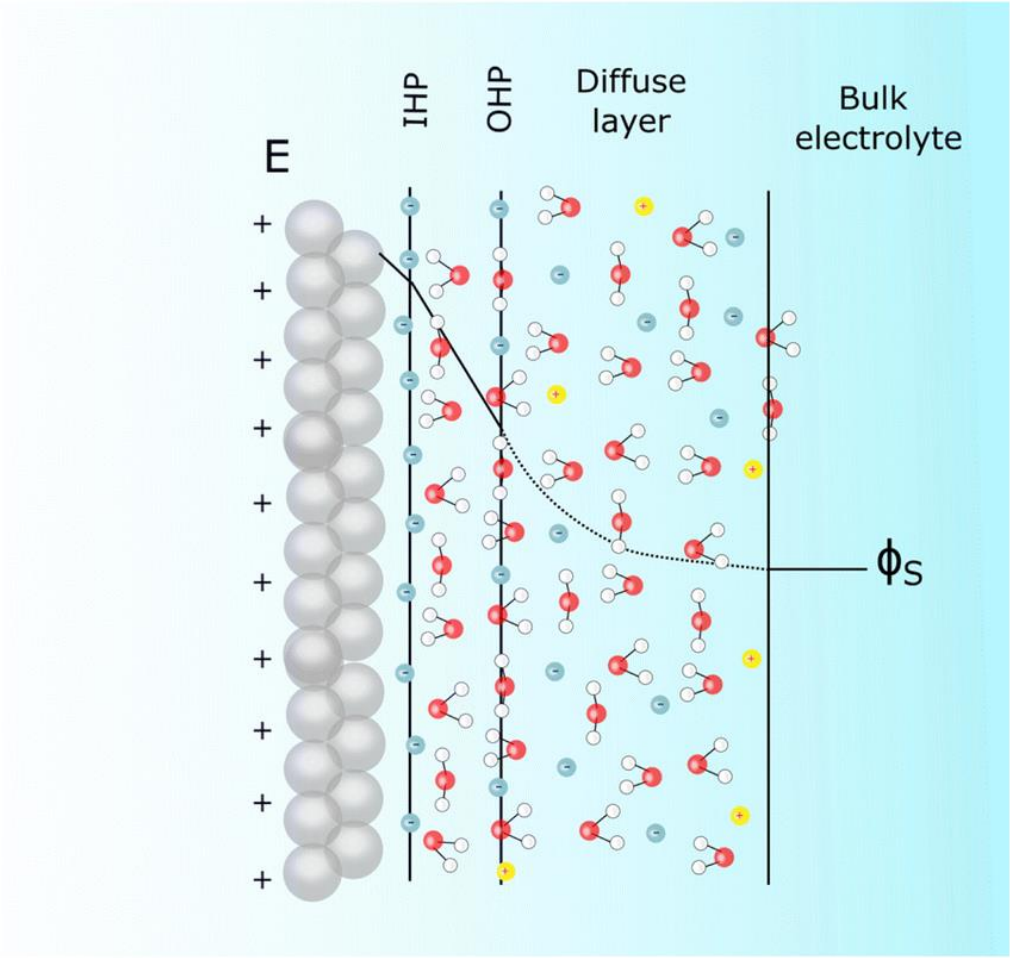

Figure 1.8: Interfacial charge distribution and electric double-layer behaviour at electrochemical interfaces relevant to electrolyte-gated graphene transistors. Adapted from Mohandas et al. (2024).Ref.26

The interfacial ionic structure in electrolyte-gated systems is commonly described using the Stern model, in which ions located close to the surface form a compact adsorption region surrounded by a diffuse ionic layer extending into the electrolyte. Near the graphene interface, these ionic regions strongly influence local potential distribution, charge screening behaviour, and field-induced

carrier modulation within the conductive channel. As a result, the electrical response of graphene transistor devices becomes highly sensitive to variations occurring at the electrolyte interface [12-14].

An important parameter governing ionic interactions in electrolyte environments is the Debye screening length, which defines the characteristic distance over which charge perturbations are screened within the electrolyte medium. Under physiological electrolyte concentrations, the Debye length is typically reduced to nanometric dimensions, meaning that charge-mediated interactions originating from biomolecules may be substantially attenuated before influencing the graphene surface. Consequently, electrolyte concentration and ionic composition strongly affect sensing sensitivity and transport response in graphene-based biosensors operating under liquid conditions[9,10,24].

In electrolyte-gated graphene transistors, the measured electrical characteristics are therefore influenced not only by intrinsic graphene transport properties, but also by interfacial ionic interactions involving pH variation, ion redistribution, molecular adsorption, and local surface charge modulation 14]. These coupled effects become particularly important for biosensing applications involving charged biomolecules and physiological buffer solutions, where the surrounding electrolyte environment directly influences the relationship between molecular adsorption and electrical signal generation.

The strong interaction between ionic redistribution and graphene carrier transport has motivated extensive theoretical and experimental investigation into graphene transistor behaviour under electrolyte conditions. For graphene biosensors operating in liquid environments, these interfacial ionic effects remain central to understanding carrier modulation and experimentally observed sensing response.

1.4.5 Current Progress in Graphene Biosensing

Electrolyte-gated graphene transistors have been extensively investigated for electrically transduced biosensing applications due to their compatibility with liquid-phase operation and strong sensitivity to interfacial charge perturbations [9,10]. Their ability to directly couple molecular interactions occurring at the solid–liquid interface with measurable electrical transport

response has established graphene transistor platforms among the most actively studied technologies for label-free biochemical detection.[24]

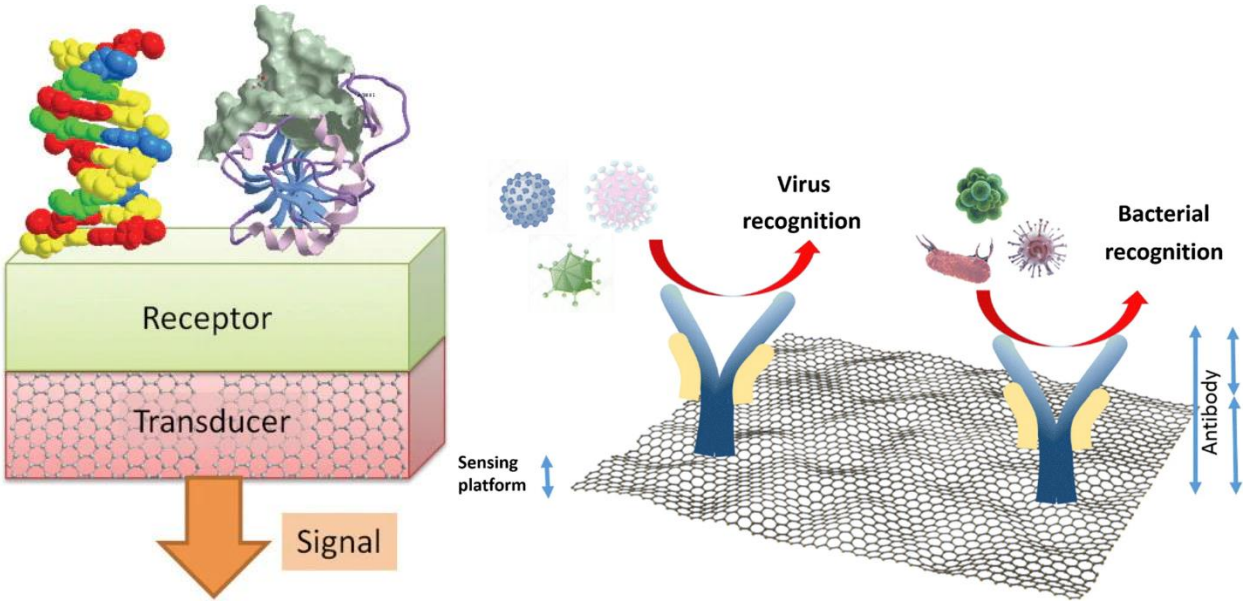

Figure 1.9: Representative graphene biosensing applications illustrating electrolyte-gated biochemical detection platforms. Adapted from Pumera (2011).Ref.27

Among the different sensing applications explored in recent years, pH sensing has become one of the most widely investigated functionalities in electrolyte-gated graphene devices. Variations in proton concentration modify local ionic conditions and surface charge distribution near the graphene channel, producing measurable changes in conductance and gate-dependent transport characteristics. Experimental studies have demonstrated reversible and stable pH-dependent electrical response in graphene transistors operating under physiological electrolyte environments, highlighting their suitability for liquid-phase sensing applications [9,10].

Protein sensing has also attracted substantial attention because biomolecular adsorption near the graphene surface can influence local charge distribution and carrier transport within the conductive channel. Depending on electrolyte conditions, molecular charge state, and adsorption configuration, protein interactions may induce variations in Dirac voltage, carrier mobility, hysteresis behaviour, and overall transport response. These effects have motivated extensive investigation into graphene transistor architectures for electrically transduced biomolecular detection under electrolyte-gated conditions[17,24]

Despite substantial experimental progress, several challenges continue to limit the interpretation and optimization of sensing behaviour in graphene transistor biosensors operating under physiological conditions. One of the principal limitations arises from ionic screening within concentrated electrolytes, where charge-mediated interactions become strongly attenuated over nanometric distances through Debye screening [12,13]. Under these conditions, electrical signals associated with biomolecular adsorption may become partially screened before significantly influencing graphene carrier transport. Most reported studies primarily analyze Dirac voltage shifts, while comparatively fewer investigations systematically examine transport degradation, mobility modulation, and disorder-related effects during sensing [11,16,18].

In addition, experimentally observed sensing response often reflects the combined influence of multiple coupled phenomena, including ion redistribution, interfacial charge modulation, adsorption-induced disorder, and carrier scattering processes occurring within the graphene channel [21,24]. As a consequence, isolating the dominant physical mechanisms responsible for electrical signal variation remains challenging, particularly in electrolyte environments where ionic interactions strongly affect transport behaviour.

Recent developments in graphene biosensing research have therefore increasingly focused not only on sensitivity enhancement, but also on improving the physical interpretation of sensing mechanisms under realistic electrolyte conditions. This aspect is particularly relevant for electrolyte-gated transistor platforms, where electrical response is closely connected to interfacial ionic interactions and charge-mediated transport modulation occurring near the graphene surface.

The interpretation of sensing behaviour in electrolyte-gated graphene transistors therefore remains closely connected to understanding how ionic environments and interfacial adsorption processes influence carrier transport within the device channel.

1.4.6 Research Gap and Thesis Positioning

Although electrolyte-gated graphene transistors have demonstrated strong potential for biochemical sensing applications, the physical interpretation of sensing response under electrolyte conditions remains incompletely understood. Numerous experimental studies have reported measurable electrical response associated with pH variation, ion concentration, and biomolecular

adsorption; however, the mechanisms governing transport modulation in electrolyte environments are often influenced by multiple coupled effects occurring simultaneously at the graphene-electrolyte interface [9,10].

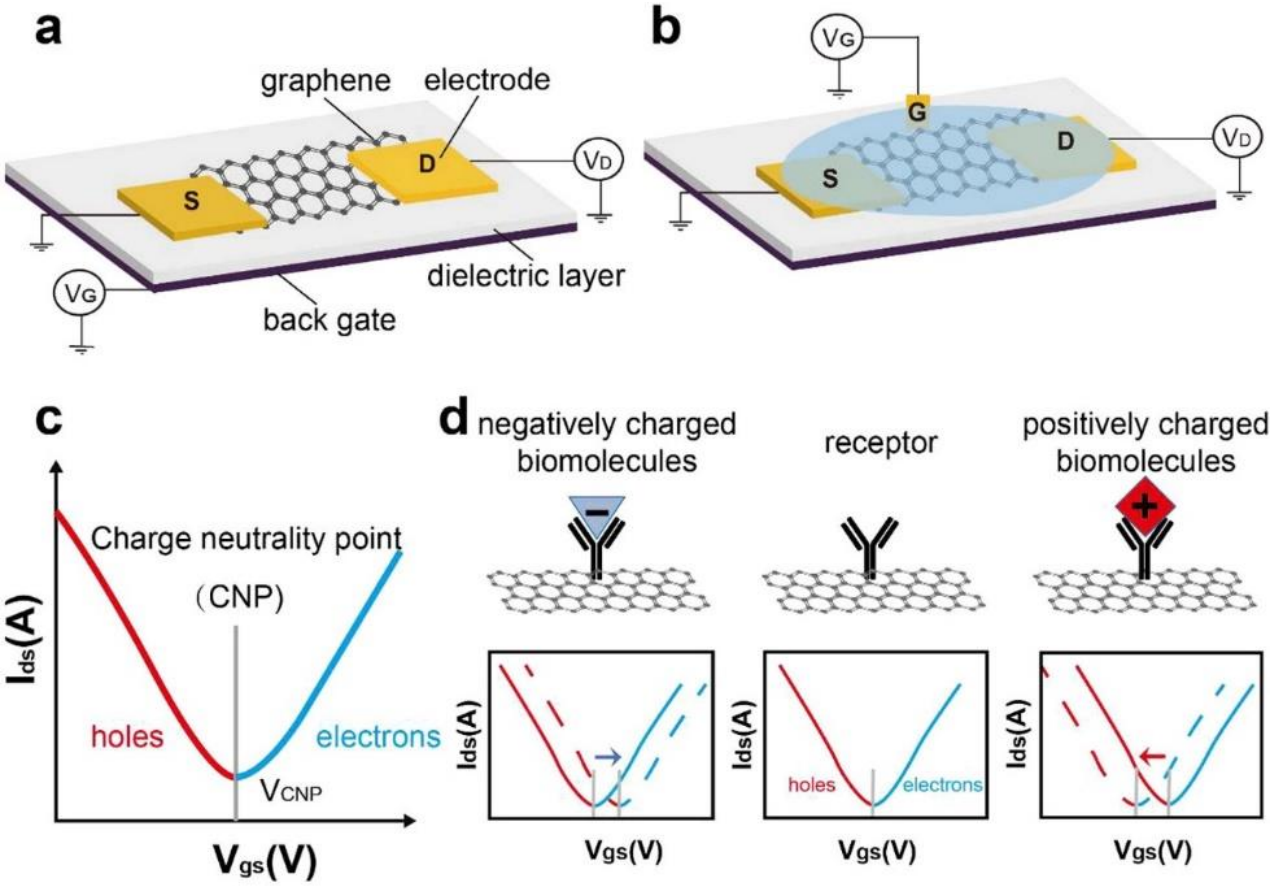

Figure 1.10: Conceptual framework illustrating coupled ionic, adsorption-induced, and transport-related phenomena governing sensing behaviour in graphene transistor biosensors. Adapted from. Zhao et.al. Ref. 18

One of the principal challenges in graphene biosensing arises from the role of the surrounding electrolyte medium in charge-coupled sensing processes. Under physiological conditions, high ionic concentrations strongly influence local charge interactions through Debye screening, reducing the effective distance over which biomolecular charges can modulate graphene carrier transport. Consequently, experimentally measured electrical signals frequently depend not only on biomolecular adsorption itself, but also on electrolyte composition, ionic redistribution, and surface-mediated charge interactions occurring near the graphene channel [12-14].

In addition, variations in conductance, Dirac voltage, mobility, and hysteresis behaviour observed in graphene transistor devices are often interpreted primarily through empirical electrical trends without fully correlating them to the underlying physical processes governing carrier modulation [11,24]. As a result, distinguishing the relative contributions of adsorption-induced charge transfer, electrolyte-mediated screening, carrier scattering, and local disorder formation remains challenging, particularly under liquid-phase operating conditions.

Another limitation in current graphene biosensing research is the partial separation between experimental characterization and physically consistent interpretation of electrolyte-mediated transport behaviour. Experimental studies commonly focus on device response and sensing performance, whereas theoretical investigations often examine isolated electrostatic or transport effects under simplified conditions. Establishing direct relationships between ionic interactions occurring at the graphene-electrolyte interface and experimentally measurable transport characteristics therefore remains an open challenge.

This aspect becomes particularly relevant for protein sensing applications, where biomolecular adsorption may simultaneously influence local charge distribution, carrier scattering behaviour, and electrolyte-dependent interfacial structure near the graphene surface[17]. Moreover, while Dirac voltage shifts are widely employed as the primary sensing metric in graphene biosensors, comparatively limited attention has been directed toward understanding mobility degradation, disorder-assisted transport modulation, and scattering-related phenomena arising from electrolyte-mediated interactions and biomolecular adsorption [16,18]. A more comprehensive transport-level interpretation is therefore required to establish physically consistent relationships between sensing response and graphene carrier dynamics. Consequently, understanding sensing response in graphene transistor biosensors requires consideration of coupled ionic, transport, and adsorption-related phenomena rather than isolated electrical measurements alone.

Within this context, the present thesis positions electrolyte-gated graphene transistors as coupled electrostatic and electronic transport systems rather than purely empirical sensing devices. The work combines experimental electrical characterization with continuum electrostatic analysis in order to investigate how electrolyte-mediated charge interactions influence graphene carrier modulation under pH variation and biomolecular adsorption conditions.

Particular emphasis is placed on understanding electric double-layer formation, ionic screening behaviour, adsorption-associated transport disorder, and electrolyte-dependent carrier modulation in graphene transistor platforms operating in physiological buffer environments. The investigations presented in the following chapters are therefore directed toward understanding how electrolyte-mediated charge interactions influence graphene transport behaviour across multiple physical scales.

1.5 Chapter Summary

This chapter established the scientific background and research context underlying electrolyte-gated graphene transistor biosensors. The discussion introduced the fundamental principles of biosensing technologies and progressively narrowed toward graphene-based sensing platforms, emphasizing the role of graphene field-effect transistors as electrically active interfaces for liquid-phase biochemical detection.

The chapter further examined the importance of electrolyte gating and interfacial ionic interactions in governing graphene transport behaviour under physiological conditions. Particular focus was directed toward electric double-layer formation, ionic screening, and charge-mediated carrier modulation at the graphene-electrolyte interface, highlighting how these effects influence experimentally observed sensing response in graphene transistor devices.

Review of the current literature demonstrated that, despite substantial advances in graphene biosensing, several challenges remain associated with interpreting transport behaviour in complex electrolyte environments. In particular, the coupled influence of ionic redistribution, adsorption-induced disorder, and electrolyte-mediated charge interactions continues to complicate the physical interpretation of sensing mechanisms in electrolyte-gated graphene transistors.

Together, these considerations position graphene transistor biosensors as coupled electrostatic and electronic transport systems rather than purely empirical sensing devices. The chapter therefore established the scientific foundation for the present thesis, which aims to investigate electrolyte-mediated carrier modulation and transport behaviour through combined experimental characterization and electrostatic interpretation.

Having established the scientific context and research positioning of electrolyte-gated graphene biosensors, the next chapter focuses on the materials, fabrication procedures, and experimental methodologies employed throughout this work.

1.6 References

1. Thévenot, D. R., Toth, K., Durst, R. A., & Wilson, G. S. (2001). Electrochemical biosensors: Recommended definitions and classification. Biosensors and Bioelectronics, 16(1–2), 121–131.
2. Wang, J. (2006). Electrochemical biosensors: Towards point-of-care cancer diagnostics. Biosensors and Bioelectronics, 21(10), 1887–1892.
3. Turner, A. P. F. (2013). Biosensors: Sense and sensibility. Chemical Society Reviews, 42(8), 3184–3196.
4. Lisdat, F., & Schäfer, D. (2008). The use of electrochemical impedance spectroscopy for biosensing. Analytical and Bioanalytical Chemistry, 391(5), 1555–1567.
5. Dash, G. N., Pattanaik, S. R., & Behera, S. (2014). Graphene for electron devices: The panorama of a decade. IEEE Journal of the Electron Devices Society, 2(5), 77–104.
6. Geim, A. K., & Novoselov, K. S. (2007). The rise of graphene. Nature Materials, 6(3), 183–191.
7. Novoselov, K. S., Geim, A. K., Morozov, S. V., et al. (2004). Electric field effect in atomically thin carbon films. Science, 306(5696), 666–669.
8. Schedin, F., Geim, A. K., Morozov, S. V., et al. (2007). Detection of individual gas molecules adsorbed on graphene. Nature Materials, 6(9), 652–655.
9. Ohno, S., Maehashi, K., & Matsumoto, K. (2009). Electrolyte-gated graphene field-effect transistors for detecting pH and protein adsorption. Nano Letters, 9(9), 3318–3322.
10. Dankerl, M., Hauf, M., Lippert, A., et al. (2010). Graphene solution-gated field-effect transistor array for sensing applications. Advanced Functional Materials, 20(18), 3117–3124.
11. Schwierz, F. (2010). Graphene transistors. Nature Nanotechnology, 5(7), 487–496.
12. Bazant, M. Z., Thornton, K., & Ajdari, A. (2004). Diffuse-charge dynamics in electrochemical systems. SIAM Review, 46(2), 261–311.
13. Israelachvili, J. N. (2011). Intermolecular and surface forces (3rd ed.). Academic Press.

14. Karimi, H., Rahmani, R., Mashayekhi, R., Ranjbari, L., Shirdel, A. H., Haghighian, N., et al. (2014). Analytical development and optimization of a graphene–solution interface capacitance model. Beilstein Journal of Nanotechnology, 5(1), 603–609.
15. Xu, Y., & Tian, C. S. (2023). A platform for exploring microscopic processes at electrode–electrolyte interfaces. Nature.
16. Brancolini, G., Calzolari, A., et al. (2024). Multiscale modelling approaches for graphene-based biosensing interfaces. Sensors, 24.
17. Peña-Bahamonde, J., Nguyen, H. N., Fanourakis, S. K., & Rodrigues, D. F. (2018). Recent advances in graphene-based biosensor technology with applications in life sciences. Journal of Nanobiotechnology, 16(1), 75.
18. Zhao, W., Zhang, W., Chen, J., Li, H., Han, L., Li, X., ... & Wang, L. (2024). Sensitivity-enhancing strategies of graphene field-effect transistor biosensors for biomarker detection. ACS sensors , 9 (6), 2705-2727.
19. Falina, S., Syamsul, M., Rhaffor, N. A., Sal Hamid, S., Mohamed Zain, K. A., Abd Manaf, A., & Kawarada, H. (2021). Ten Years Progress of Electrical Detection of Heavy Metal Ions (HMIs) Using Various Field-Effect Transistor (FET) Nanosensors: A Review. Biosensors, 11(12), 478. https://doi.org/10.3390/bios11120478.
20. Singh, N. B., Monjur, A., Kumar, B., Varshney, S., & Susan, M. A. B. H. (2025). Revolutionizing healthcare with nanosensor technology. RSC advances , 15 (46), 38774-38810.
21. Ashraf, G., Aziz, A., Iftikhar, T., Zhong, Z.-T., Asif, M., & Chen, W. (2022). The Roadmap of Graphene-Based Sensors: Electrochemical Methods for Bioanalytical Applications. *Biosensors*, *12*(12), 1183. https://doi.org/10.3390/bios12121183
22. Pumera, M. (2010). Graphene-based nanomaterials and their electrochemistry. Chemical Society Reviews, 39(11), 4146–4157.
23. Castro Neto, A. H., Guinea, F., Peres, N. M. R., et al. (2009). The electronic properties of graphene. Reviews of Modern Physics, 81(1), 109–162.
24. Hess, L., Seifert, M., & Garrido, J. A. (2013). Graphene transistors for bioelectronics. Proceedings of the IEEE, 101(7), 1780–1792.
25. Terse-Thakoor, T., Badhulika, S., & Mulchandani, A. (2017). Graphene based biosensors for healthcare. Journal of Materials Research , 32 (15), 2905-2929

26. Mohandas, N., Bawari, S., Shibuya, J. J., Ghosh, S., Mondal, J., Narayanan, T. N., & Cuesta, A.(2024). Understanding electrochemical interfaces through comparing experimental andcomputational charge density–potential curves. Chemical Science, 15(18, 6643-6660.
27. Pumera, M. (2011). Graphene in biosensing. Materials today, 14 (7-8), 308-315.

CHAPTER 2

Materials, Fabrication and Experimental Methods

2.1 Introduction to Materials and Device Fabrication

The realization of graphene-based electrolyte-gated field-effect transistor (EG-GFET) devices requires a systematic integration of material selection, nanofabrication techniques, and device architecture. While Chapter 1 established the fundamental principles governing graphene-based biosensing, the practical implementation of these concepts depends strongly on the quality of materials and the precision of fabrication processes.

Graphene serves as the active channel material in the devices investigated in this work due to its atomic thickness and pronounced sensitivity to variations in surface charge [1-3]. However, device performance is not governed solely by the intrinsic properties of graphene. It is also influenced by several external factors, including interactions with the underlying substrate, the configuration of electrodes, and imperfections introduced during fabrication. Careful control of these aspects is therefore necessary to achieve consistent and reproducible device behavior [2].

Nanofabrication defines the physical structure of the device and directly impacts its electrical characteristics. Among the available techniques, electron beam lithography (EBL) offers the resolution and flexibility required to pattern nanoscale features with high precision [4-5]. This capability is particularly important for electrolyte-gated systems, where the geometry and spatial arrangement of electrodes can affect electric field distribution, ion transport, and gating efficiency.

The operational environment also plays a key role in determining device response. Since the devices are intended for sensing in liquid media, the properties of the electrolyte and its interaction with the graphene surface must be considered. The formation of an electric double layer at the graphene–electrolyte interface enables efficient electrostatic modulation of the channel and provides the basis for sensing functionality [6,7].

This chapter describes the materials and fabrication processes used to realize the graphene-based devices studied in this thesis. It includes an overview of the materials used, followed by a detailed discussion of nanofabrication techniques, with an emphasis on electron-beam lithography. The

fabrication procedure, device architecture, and experimental setup used for electrical characterization and sensing measurements are then presented.

By linking material selection, fabrication methodology, and device operation, this chapter establishes the experimental framework for the investigations discussed in the subsequent chapters.

2.2 Materials and Substrate System

The performance of graphene-based electrolyte-gated devices is strongly influenced by the selection of materials and the quality of interfaces formed during fabrication. In particular, the electrical characteristics and sensing response of graphene field-effect transistors are governed by factors such as graphene quality, substrate properties, and the chemical environment in which the device operates. Careful control of these parameters is therefore essential to ensure reproducible device behavior and reliable sensing performance.

In electrolyte-gated configurations, the interaction between graphene and the surrounding medium plays a central role in determining device response. Variations in material quality, including defects, impurities, and structural inhomogeneities, can influence carrier transport, charge distribution, and sensitivity to surface interactions. Similarly, the substrate and electrode materials contribute to device performance through their impact on charge transfer, electrostatic coupling, and contact resistance. This section describes the materials used in this work, including graphene from different sources, commercially available graphene platforms, and supporting device components.

2.2.1 Graphene Materials

Graphene used in this work is obtained from multiple sources, including mechanically exfoliated graphene, chemical vapor deposition (CVD)-grown graphene, and commercially supplied graphene fabricated devices. The use of different graphene sources enables a comparative assessment of material quality and its influence on device performance, particularly in electrolyte-gated sensing applications.

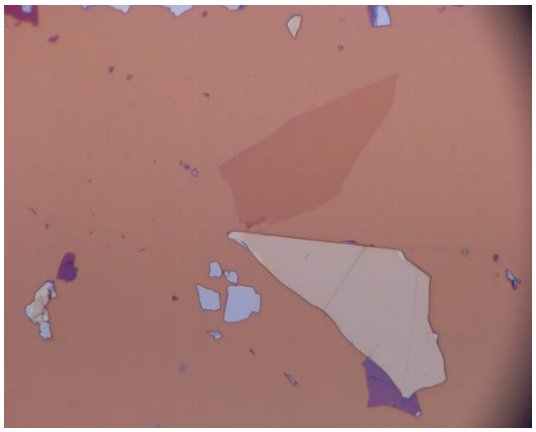

Figure 2.1: Mechanical Exfoliated Graphene on 285nm Silicon Substrate

Mechanical exfoliation is employed to obtain high-quality graphene flakes through the cleavage of bulk graphite. This method, first demonstrated by Novoselov et al., produces graphene with minimal structural defects and high carrier mobility, making it suitable for investigating intrinsic electronic properties [1]. Due to the absence of grain boundaries and low levels of disorder, exfoliated graphene often exhibits near-ideal transport behavior. However, the method is inherently limited by its lack of scalability and the difficulty in controlling flake size and spatial location, which restricts its use in reproducible device fabrication.

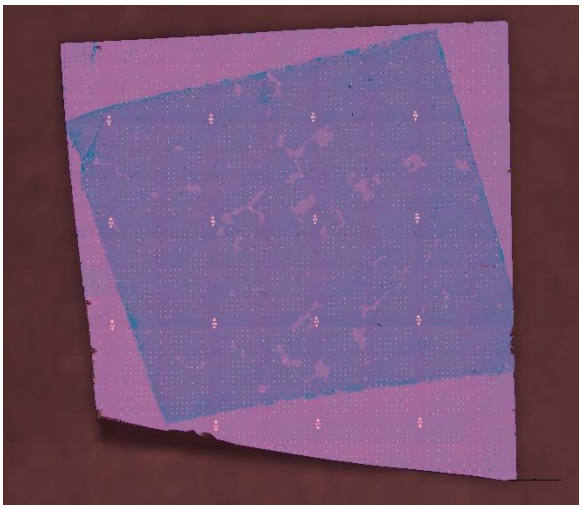

Figure 2.2: CVD Grown Graphene on Si/SiO2 Substrate

Chemical vapor deposition provides an alternative approach for producing large-area graphene suitable for device integration. In this method, graphene is grown on metal substrates, typically

copper, through the decomposition of hydrocarbon precursors at elevated temperatures, followed by transfer onto insulating substrates for electronic applications [8]. CVD graphene enables uniform coverage over relatively large areas, facilitating the fabrication of multiple devices with similar geometries. Nevertheless, the growth and transfer processes can introduce structural imperfections such as grain boundaries, wrinkles, and residual contamination, which act as scattering centers and influence carrier transport [2].

In addition to CVD graphene prepared through laboratory methods, commercially available graphene on Si/SiO_2 substrates obtained from suppliers such as Graphenea are also used in this work. These substrates consist of CVD-grown graphene transferred onto insulating wafers under controlled conditions, providing improved reproducibility and consistency compared to manual transfer processes. The use of commercial graphene allows for more standardized device fabrication and enables direct comparison between different fabrication approaches.

The structural and electronic quality of graphene plays a critical role in determining device characteristics. Defects, impurities, and grain boundaries can modify the local electronic structure, influence carrier mobility, and introduce charge trapping effects, particularly near the Dirac point. At the same time, these features may enhance sensitivity in sensing applications by providing additional sites for molecular adsorption. As a result, the relationship between graphene quality and sensing performance is not strictly monotonic and requires careful experimental evaluation.

By employing graphene from multiple sources, this work enables a systematic investigation of the interplay between material quality, fabrication processes, and sensing behavior in electrolyte-gated devices. This approach provides insight into the trade-offs between high electronic performance, scalability, and reproducibility.

2.2.2 Commercial Graphene-Based Devices

As earlier mentioned, in addition to lab-prepared graphene materials used for device fabrication, commercially fabricated graphene-based field-effect transistor (GFET) platforms, including S-20 and mGFET 4D devices, are also employed in this study. These devices consist of pre-patterned graphene channels integrated with metallic source and drain electrodes, and are designed for direct electrical characterization without the need for additional lithographic processing.

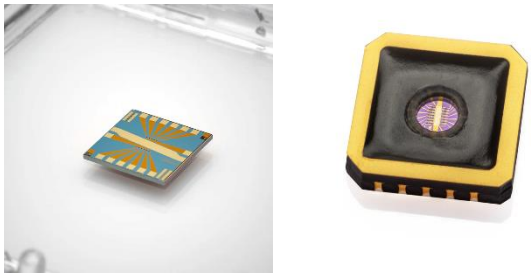

Figure 2.3: Commercial Devices including GFET S-20 and mGFET-4D for sensing

The S-20 devices typically feature well-defined graphene channels with integrated electrode geometries and contact pads suitable for probing or wire bonding. Similarly, the mGFET 4D platform incorporates multiple graphene channels and electrode configurations on a single chip, enabling parallel measurements and comparative analysis under controlled conditions. The predefined architecture of these devices ensures consistent channel dimensions and electrode spacing, which are essential for reproducible electrical measurements.

The use of commercially fabricated devices provides several advantages. First, it minimizes fabrication-induced variability, allowing a clearer assessment of intrinsic material properties and device response. Second, it enables benchmarking against devices fabricated in-house using electron-beam lithography, particularly for electrical characteristics and sensing performance. Third, these platforms facilitate rapid experimental testing by eliminating several fabrication steps.

However, it is important to note that the fabrication processes underlying commercial devices are not directly controlled within this work. As a result, variations in graphene quality, contact resistance, and surface condition may influence device behavior. These factors are considered during analysis and comparison with fabricated devices in Modena for our experiments.

By combining laboratory-fabricated devices with commercially available platforms, this study provides a comprehensive evaluation of graphene-based electrolyte-gated devices, accounting for both fabrication-controlled and standardized device architectures.

2.2.3 Substrate

Graphene devices investigated in this work are fabricated on silicon substrates with a thermally grown silicon dioxide (SiO_2) layer. The Si/SiO_2 platform is widely used in graphene-based electronics due to its mechanical stability, compatibility with standard microfabrication processes, and well-defined dielectric properties.

The SiO_2 layer serves as an insulating surface that supports the graphene channel and electrically isolates it from the underlying silicon. In addition, the dielectric properties of SiO2 influence the electrostatic environment of graphene, particularly in field-effect configurations. Although electrolyte gating is employed in this work, substrate-induced effects remain relevant, as charge impurities, surface roughness, and trapped charges at the SiO_2 interface can affect carrier transport and local doping in graphene [7].

Interactions between graphene and the substrate can introduce scattering centers that influence carrier mobility, especially near the Dirac point where the density of states is low. These interactions may also lead to unintentional doping, shifting the charge neutrality point, and modifying the baseline electrical characteristics of the device. As a result, the quality and cleanliness of the substrate surface are important factors in achieving consistent and reproducible device performance.

Before graphene integration and lithographic processing, the substrates are cleaned to remove organic contaminants and particulate residues. This is typically achieved through solvent cleaning using acetone and isopropanol, followed by drying with a nitrogen gun. Such cleaning procedures help to improve graphene adhesion and reduce variability in device fabrication.

In the context of electrolyte-gated devices, the substrate also plays an indirect role by influencing the overall device stability and measurement reliability. While the electric double layer formed at the graphene–electrolyte interface dominates the gating behavior, substrate-induced effects can contribute to long-term drift and variability in electrical response [6-7]. Careful control of substrate preparation and processing is therefore essential to ensure reliable experimental outcomes.

2.2.4 Electrolytes

The electrolyte plays a central role in the operation of graphene-based electrolyte-gated field-effect transistors, as it enables electrostatic modulation of the graphene channel through ionic charge redistribution. In contrast to conventional solid-state gating, the use of an electrolyte allows efficient coupling between the gate electrode and the graphene surface at relatively low operating voltages.

In this work, electrolyte solutions such as phosphate-buffered saline (PBS) and aqueous solutions containing target analytes were used as the gating medium. PBS is widely employed in biosensing applications due to its well-defined ionic strength and stable pH, which provide a controlled electrochemical environment for reliable measurements. The use of such electrolytes ensures reproducible formation of the electric double layer and stable electrical characteristics during device operation.

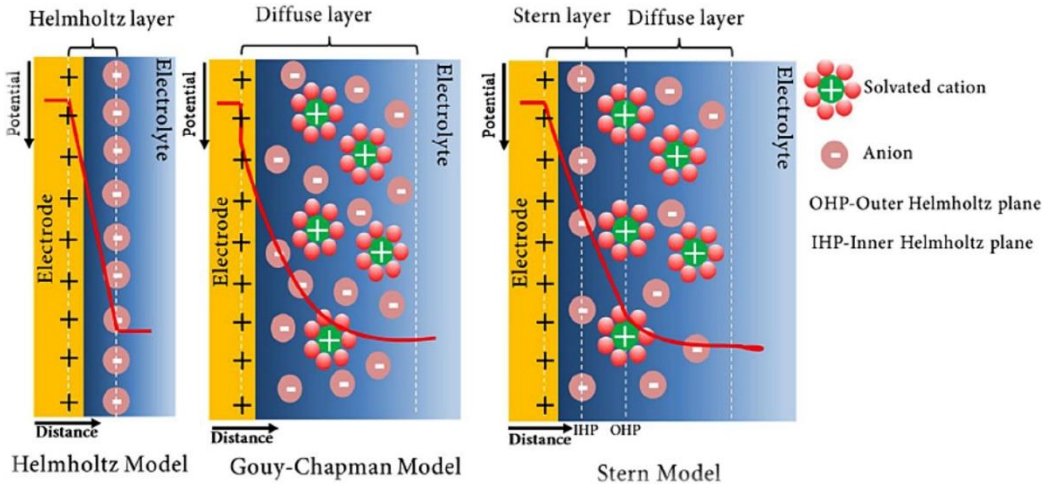

Figure 2.4: Models expalining Electric Dobule Formation at Graphene-Electrolyte Interface

When a gate voltage is applied through the electrolyte, mobile ions in the solution redistribute in response to the electric field, forming an electric double layer at the graphene–electrolyte interface. This interfacial structure consists of a compact layer of specifically adsorbed ions (Stern layer) and a diffusion layer extending into the bulk electrolyte. Together, these layers behave as a nanoscale capacitor with a high capacitance per unit area, enabling effective modulation of carrier density in graphene [6].

The high capacitance associated with the electric double layer arises from its extremely small effective thickness, typically in the order of nanometers [9]. As a result, significant changes in carrier concentration can be achieved with relatively small applied gate voltages. This characteristic is particularly advantageous for sensing applications, where low-voltage operation is desirable for compatibility with biological systems.

The properties of the electrolyte, including ionic strength, pH, and composition, influence the structure of the electric double layer and consequently affect device behavior. In particular, the ionic strength determines the extent of electrostatic screening in the solution, which can limit the effective interaction distance between charged analytes and the graphene surface. This effect becomes especially important in biosensing applications involving large biomolecules, where ionic screening can reduce the measurable electrical response.

In addition to enabling electrostatic gating, the electrolyte also provides the medium in which sensing interactions occur. Variations in ion concentration, pH, or the presence of target biomolecules can alter the local electrostatic environment at the graphene surface, leading to measurable changes in device conductance [9]. Careful selection and control of the electrolyte are therefore essential to ensure reliable and reproducible sensing performance.

2.3 Graphene Preparation and Characterization

The performance of graphene-based devices depends not only on the fabrication process but also on the quality and integrity of the graphene material after transfer and processing. Therefore, appropriate preparation and characterization steps are essential to ensure that the graphene maintains its structural and electronic properties throughout device fabrication.

2.3.1 Graphene Preparation and Transfer

Graphene samples used in this work were prepared using both mechanical exfoliation and chemical vapor deposition (CVD) techniques, as described in Section 2.2. Mechanically exfoliated graphene was directly transferred onto Si/SiO_2 substrates, while CVD-grown graphene was transferred from metal growth substrates onto insulating substrates for device fabrication.

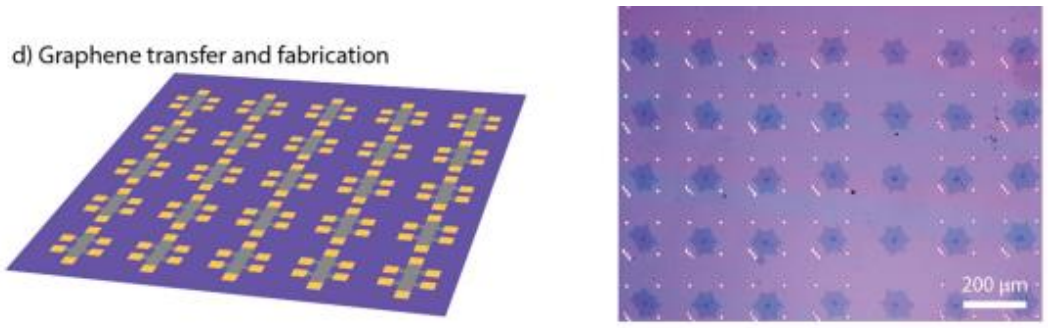

Figure 2. 5: Scalable CVD synthesis of single crystal graphene

The transfer of CVD graphene typically involves the use of a polymer support layer, such as poly(methyl methacrylate) (PMMA), followed by chemical etching of the metal substrate and subsequent transfer onto the target substrate [8,10]. After transfer, the polymer layer is removed using appropriate solvents, leaving the graphene film on the substrate. Although this method enables large-area graphene integration, it can introduce residues, wrinkles, and structural inhomogeneities that may affect device performance.

Careful handling during transfer and cleaning steps is therefore necessary to minimize contamination and preserve the electrical properties of graphene.

2.3.2 Scanning Electron Microscopy (SEM)

Scanning electron microscopy (SEM) imaging is based on the interaction of a focused electron beam with the sample surface, generating signals that provide information about surface morphology and structure. SEM is used to examine the surface morphology and structural features of the fabricated devices. SEM imaging provides information on the continuity of graphene films, the quality of lithographically defined patterns, and the alignment of metal electrodes with respect to the graphene channel.

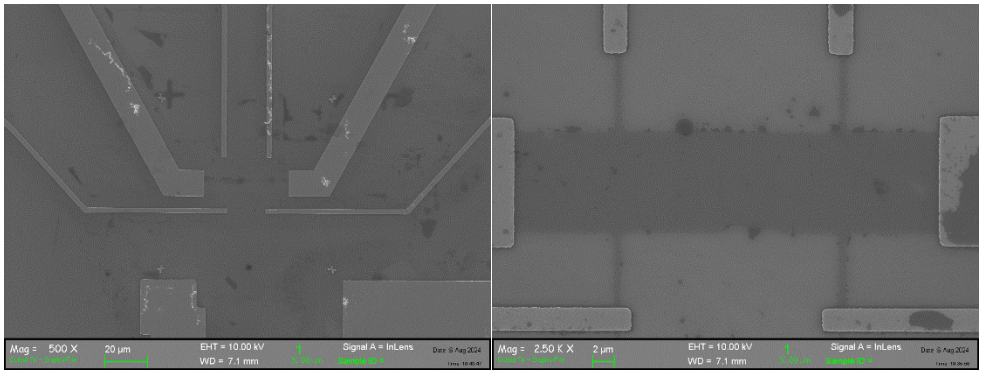

Figure 2.6: SEM images showing Graphene Channel of fabricated device for counter electrode geometry

In particular, SEM is employed to verify the integrity of graphene after transfer, identify defects such as cracks or discontinuities, and assess the quality of device fabrication steps, including pattern definition and metal deposition. The technique is also useful for visualizing electrode geometries and ensuring proper connectivity between device components.

The structural information obtained from SEM imaging is directly relevant to device performance, as discontinuities in the graphene channel or poor electrode alignment can lead to increased contact resistance and reduced measurement reliability.

2.3.3 Raman Spectroscopy of Graphene

Figure 2.7: LABRAM Horiba Raman Spectroscopy Setup - CIGS UNIMORE

Raman spectroscopy is employed as a non-destructive technique to assess the structural quality and layer characteristics of graphene. Raman spectroscopy is based on inelastic scattering of light, where the energy shift of scattered photons provides information about vibrational modes in the material. In this work, Raman measurements are used to evaluate defect density, number of layers, and overall material quality following transfer and processing.

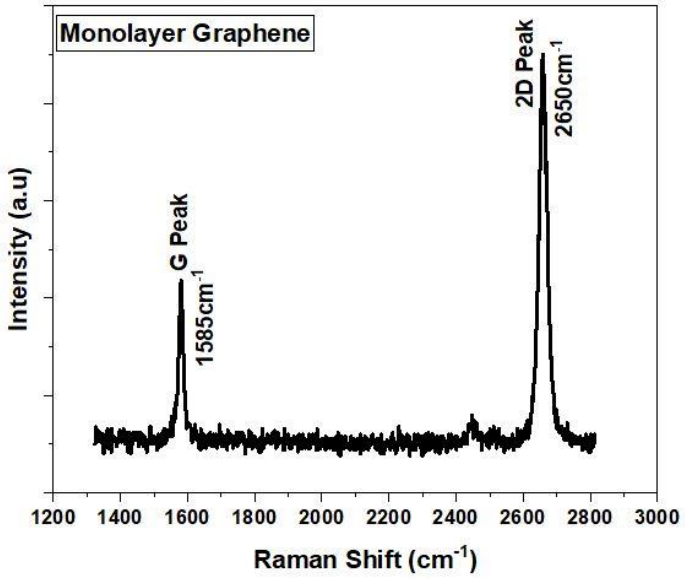

Figure 2.8: Raman Spectrum of Graphene

The Raman spectrum of graphene is characterized by prominent features, including the G peak (~1580 cm^{-1}), the 2D peak (~2700 cm^{-1}), and the D peak (~1350 cm^{-1}). The intensity and shape of these peaks provide information about the structural properties of graphene. In particular, the ratio of the D peak to G peak intensities (I_D/I_G) is commonly used as an indicator of defect density, while the shape and intensity of the 2D peak provide insight into the number of graphene layers [11].

In the context of this work, Raman spectroscopy is used to confirm the presence of graphene after transfer and to assess any changes in material quality resulting from fabrication processes. Variations in peak intensity and position are also indicative of strain, doping, and interaction with the substrate.

These measurements are particularly important in the context of electrolyte-gated devices, where defects and doping can significantly influence the position of the Dirac point and the sensitivity to surface charge variations.

By combining Raman spectroscopy and SEM imaging, a comprehensive assessment of graphene quality and device integrity is achieved. These characterization techniques provide essential

validation of the fabrication process and support the interpretation of electrical measurements presented in later chapters.

2.4 Nanofabrication Strategy

The fabrication of graphene-based electrolyte-gated field-effect transistor devices requires precise control over device geometry, electrode configuration, and material interfaces. Given the nanoscale dimensions of the graphene channel and the sensitivity of the device to structural variations, the choice of fabrication methodology plays a critical role in determining device performance and reproducibility

2.4.1 Top-Down Nanofabrication Approach

Nanofabrication techniques can be broadly categorized into bottom-up and top-down approaches. Bottom-up methods involve the assembly of materials from atomic or molecular precursors and are commonly used in material synthesis processes such as chemical vapor deposition. While these approaches are effective for producing high-quality materials, they provide limited control over the spatial definition of device features.

In contrast, top-down fabrication techniques rely on the selective patterning and removal of material to define structures with well-controlled geometry. This approach is widely employed in micro- and nanoelectronics, where precise alignment, reproducibility, and scalability are essential [4,5]. For graphene-based devices, top-down fabrication enables the definition of electrodes, channels, and contact regions with high spatial accuracy.

In the present work, a top-down fabrication strategy is adopted to ensure consistent device realization and to enable systematic variation of device parameters.

2.4.2 Design Considerations for Graphene Devices

The performance of electrolyte-gated graphene devices is influenced not only by material properties but also by device architecture. Parameters such as channel dimensions, electrode spacing, and contact geometry play a significant role in determining the distribution of the electric field and the efficiency of electrostatic gating.

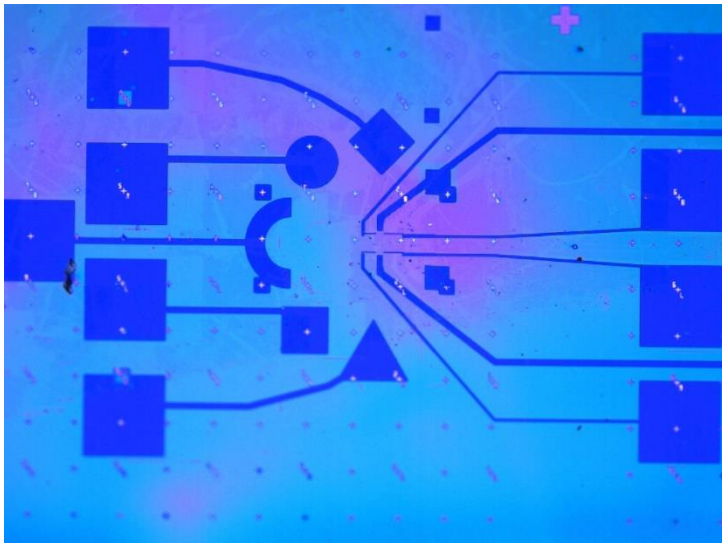

Figure 2.9: Different shapes and geometry of counter electrode

In particular, the configuration of the counter electrode in electrolyte-gated systems can influence ion distribution and the resulting electric double layer formation at the graphene–electrolyte interface. Variations in electrode geometry, including shape, size, and relative positioning, may therefore affect gating efficiency and overall sensing response.

In this work, device design is approached in a systematic manner, with careful consideration given to electrode configuration and geometry. This enables the investigation of how structural parameters influence electrical characteristics and sensing behavior.

2.4.3 Selection of Electron Beam Lithography

Among the nanofabrication techniques, Electron Beam Lithography (EBL) is selected as the primary method for device patterning. EBL offers high spatial resolution and flexibility in pattern design, allowing the fabrication of nanoscale features without the need for physical masks. This is particularly advantageous for graphene devices, where precise definition of electrode geometry and channel dimensions is required [4-5].

The use of EBL also enables the fabrication of multiple device configurations on the same substrate, facilitating comparative studies of device geometry. This capability is central to the objectives of the present work, which include the investigation of electrode-related effects on electrolyte-gated device behavior

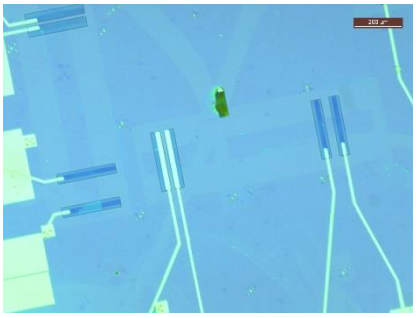

Figure 2.10: Multiple Fabricated Devices on single CVD graphene substrate by Electron Beam Lithography

In addition to electron beam lithography, conventional optical lithography is employed in selected fabrication steps where high-resolution patterning is not required. Optical lithography provides a rapid and efficient method for defining larger features such as contact pads and alignment structures. While its resolution is limited compared to EBL, it offers advantages in terms of processing speed and simplicity. In the present work, optical lithography is used as a complementary technique, whereas electron beam lithography remains the primary method for defining nanoscale device features.

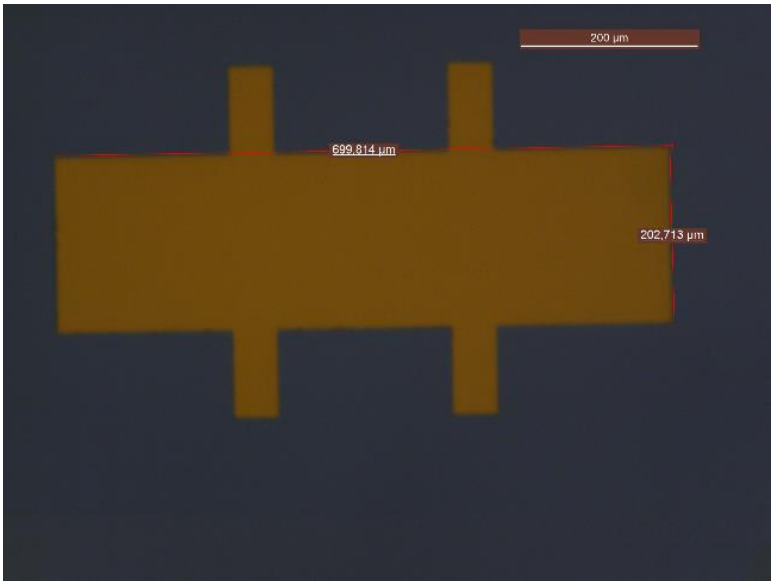

Figure 2.11: Hall Bar Geometry for sensing by Optical Lithography

2.5 Electron Beam Lithography

Electron beam lithography (EBL) is employed in this work as the primary nanofabrication technique for defining graphene-based device structures. As discussed in the previous section, precise control over electrode geometry and channel dimensions is essential for investigating the electrical and sensing behavior of electrolyte-gated graphene devices. EBL provides the spatial resolution and design flexibility required to achieve this level of control.

Figure 2.12: ZEISS Electron Beam Lithography Setup -Nanofabrication Facility -Physics Department-UNIMORE

In addition to its high-resolution capability, the maskless nature of EBL allows rapid modification of device layouts, enabling systematic variation of structural parameters such as electrode spacing

and configuration. This is particularly important in the present study, where the influence of device geometry, including counter electrode design, is investigated. The use of EBL, therefore forms the foundation for the fabrication strategy adopted in this work.

The following subsections describe the fundamental principles of electron beam lithography, the physical mechanisms governing electron–matter interactions, and the process parameters relevant to the fabrication of graphene-based devices.

2.5.1 Fundamentals of Electron Beam Lithography

Electron beam lithography (EBL) is employed in this work as the primary technique for nanoscale patterning of graphene devices. The method enables direct writing of electrode geometries and channel structures with high spatial resolution, which is essential for controlling device characteristics in electrolyte-gated configurations. In comparison with optical lithography, EBL provides superior patterning precision and design flexibility, making it particularly suitable for research-scale fabrication where multiple device architectures are investigated [4-5,12].

Electron beam lithography is based on the use of a focused beam of high-energy electrons that is scanned over a resist-coated substrate according to a predefined pattern. Unlike conventional optical lithography, which relies on light and photomasks for pattern transfer, EBL is a maskless, direct-write technique. This enables the fabrication of structures with dimensions well below the diffraction limits of optical methods, allowing accurate definition of nanoscale features.

The high resolution of EBL arises from the short effective wavelength of accelerated electrons, which significantly reduces diffraction effects. In practice, the electron beam induces localized chemical modification within a radiation-sensitive resist, typically a polymer such as poly(methyl methacrylate) (PMMA). In positive resists, electron exposure leads to chain scission, reducing the molecular weight of the polymer and increasing its solubility in a developer solution. The exposed regions are subsequently removed during development, leaving behind a patterned resist structure that defines the device geometry.

A key advantage of EBL is its ability to provide precise control over critical device dimensions, including channel length, electrode spacing, and contact geometry. This level of control is particularly important for graphene-based field-effect transistor devices, where small variations in geometry can significantly influence carrier transport, electric field distribution, and sensing response. Furthermore, the maskless nature of EBL allows rapid modification of pattern designs, enabling systematic investigation of device architecture within a single fabrication workflow.

Despite these advantages, EBL is inherently a serial writing technique, in which patterns are generated point-by-point or line-by-line. This results in relatively low throughput compared to parallel techniques such as optical lithography. However, for research applications, where flexibility and resolution are prioritized over fabrication speed, EBL remains one of the most powerful and widely used nanofabrication methods.

In the context of the present work, EBL provides a robust platform for the fabrication of graphene devices with controlled geometry. Its ability to accurately define nanoscale features enables systematic exploration of electrode configuration effects, including variations in counter electrode geometry, which are central to the investigation of electrolyte-gated transport and sensing behavior.

2.5.2 Electron–Matter Interaction

The resolution and fidelity of patterns generated by electron beam lithography are fundamentally governed by the interaction between the incident electron beam and the resist–substrate system. When high-energy electrons impinge on a resist-coated substrate, they undergo a series of scattering processes that determine the spatial distribution of deposited energy. This energy distribution directly influences the extent of resist exposure and, consequently, the accuracy of the patterned structures [4,5].

Electron–matter interactions can be broadly classified into elastic and inelastic scattering. In elastic scattering, electrons are deflected by the electrostatic potential of atomic nuclei without significant energy loss. This process alters the trajectory of the electrons and contributes to the lateral spreading of the beam as it propagates through the resist. In contrast, inelastic scattering involves

energy transfer from the incident electrons to the material, leading to the generation of secondary electrons and other excitations.

Secondary electrons play a critical role in the lithographic process, as they are primarily responsible for inducing chemical modification in the resist. Due to their relatively low energy, secondary electrons deposit energy locally within the resist, enabling the chain scission mechanism that defines exposed regions in positive resists such as PMMA. However, their spatial distribution extends beyond the primary beam diameter, contributing to the broadening of the effective exposure region.

In addition to secondary electrons, backscattered electrons are generated through large-angle scattering events within the substrate. These electrons retain a significant fraction of their initial energy and can travel relatively long lateral distances before re-emerging into the resist layer. As a result, they contribute to exposure in regions away from the intended beam location, further modifying the exposure profile.

The combined influence of forward scattering within the resist and backscattering from the substrate leads to a non-uniform spatial distribution of deposited energy. This distribution is often described by a point spread function (PSF), which characterizes the radial spread of exposure around the beam impact point. The PSF typically consists of a narrow central component associated with forward scattering and a broader tail resulting from backscattered electrons.

Understanding these interaction mechanisms is essential for optimizing lithographic parameters and achieving accurate pattern definition. In the context of graphene device fabrication, where nanoscale variations in electrode geometry can significantly affect electrical characteristics, control of electron scattering effects is particularly important. Careful selection of exposure conditions and resist parameters is therefore required to minimize unintended exposure and ensure reproducible fabrication outcomes.

2.5.3 Proximity Effect and Resolution Limits

The resolution and accuracy of patterns defined by electron beam lithography are limited not only by the intrinsic beam diameter but also by the spatial distribution of energy deposited within the

resist during exposure. As discussed in the previous section, electron scattering processes give rise to exposure beyond the intended beam location. This phenomenon, known as the proximity effect, represents one of the primary challenges in achieving high-fidelity nanoscale patterning [12,13].

The proximity effect arises from the cumulative contribution of scattered electrons to regions adjacent to the target pattern. As a result, areas near the intended exposure may receive additional dose, leading to feature broadening, reduced edge definition, and deviations from the designed geometry. These effects are particularly significant for closely spaced features or dense pattern regions, where overlapping exposure can substantially alter the final structure.

In graphene-based device fabrication, the proximity effect is of particular importance because small deviations in electrode spacing or channel dimensions can directly influence electrical characteristics. Variations in feature size may affect carrier transport, electric field distribution, and the efficiency of electrostatic gating in electrolyte-gated configurations. Consequently, precise control of pattern dimensions is essential for ensuring reproducible device performance.

The extent of the proximity effect depends on several process parameters, including beam energy, resist thickness, substrate properties, and pattern density. Higher acceleration voltages generally improve local resolution by reducing forward scattering within the resist, although they may also enhance backscattering contributions from the substrate. Similarly, thicker resist layers can increase lateral energy spread, while high-density patterns are more susceptible to cumulative exposure effects.

To mitigate proximity-induced distortions, exposure parameters must be carefully optimized. This includes selecting appropriate exposure doses, controlling resist thickness, and adjusting pattern layouts to minimize unintended overlap of exposure regions. In some cases, proximity effect correction (PEC) techniques may be employed to compensate for variations in local dose distribution.

In the present work, careful optimization of exposure conditions is carried out to ensure accurate pattern transfer and to maintain consistency across devices with different geometries. This is particularly important for isolating the influence of intentional design variations, such as changes in electrode configuration, from fabrication-induced deviations. By minimizing proximity effects,

it is possible to achieve reliable nanoscale patterning suitable for systematic investigation of graphene-based device behavior.

2.5.4 EBL System and Process Parameters

Electron beam lithography systems are typically based on modified scanning electron microscope (SEM) platforms, equipped with beam control and pattern generation capabilities. These systems enable precise focusing and scanning of a high-energy electron beam over a resist-coated substrate under high-vacuum conditions, ensuring stable beam propagation and minimizing scattering by ambient molecules [4, 13, 14].

A typical EBL system consists of an electron source, an electron optics column, a beam deflection system, and a motorized sample stage. The electron source generates a focused beam that is accelerated to a specified energy, while the optics column controls beam focusing and spot size. The beam deflection system enables controlled scanning of the beam across the substrate according to the predefined pattern, and the sample stage allows accurate positioning and alignment during fabrication.

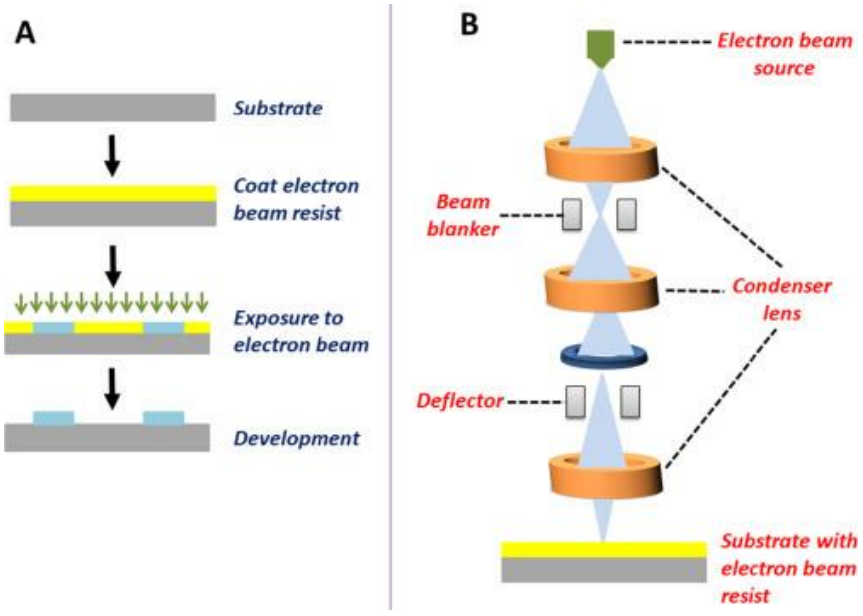

Figure 2.13: Working Principle of Electron Beam Lithography [Reproduced from Book [15]

The quality of the lithographic pattern is determined by several process parameters, which must be carefully optimized to achieve accurate and reproducible device structures. Among the most critical parameters is the **acceleration voltage**, which determines the energy of the incident electrons. Higher acceleration voltages generally reduce forward scattering within the resist, improving resolution, but may increase penetration depth and backscattering from the substrate.

The **beam current** is another important parameter, influencing both the exposure dose and the writing speed. Higher beam currents allow faster patterning but may lead to increased beam diameter and reduced resolution. Conversely, lower beam currents provide improved resolution at the cost of longer exposure times. The selection of beam current, therefore, involves a trade-off between throughput and pattern fidelity.

Exposure dose, defined as the charge delivered per unit area, plays a central role in determining the extent of resist modification. For positive resists such as PMMA, the dose must be sufficient to induce complete chain scission in the exposed regions while avoiding excessive exposure that can lead to feature broadening. The optimal dose depends on resist thickness, molecular weight, and development conditions, and is typically determined through calibration.

Additional parameters, including **step size and dwell time**, influence the spatial distribution of exposure. The step size defines the spacing between successive beam positions, while the dwell time determines the duration of exposure at each point. Together, these parameters control the uniformity of dose distribution and must be selected to ensure consistent pattern formation.

In the context of this work, process parameters are optimized to achieve reliable patterning of graphene devices with well-defined electrode geometry and channel dimensions. Maintaining consistent exposure conditions across different device designs is particularly important, as it enables meaningful comparison of electrical characteristics and sensing performance. Careful control of these parameters ensures that variations in device behavior can be attributed to intentional design differences rather than fabrication-induced variability.

2.5.5 Resist System and PMMA Exposure Mechanism

The resist material plays a central role in electron beam lithography, as it serves as the medium through which the electron beam pattern is initially defined. In this work, poly(methyl methacrylate) (PMMA) is used as the electron beam resist due to its high resolution capability, well-established processing characteristics, and compatibility with graphene device fabrication [14,16].

PMMA is a positive-tone resist, meaning that the regions exposed to the electron beam become more soluble in the developer solution. This behavior arises from the interaction of high-energy electrons with the polymer structure, which induces chain scission along the polymer backbone. As a result, the molecular weight of the exposed regions is reduced, increasing their solubility and enabling selective removal during development. This process allows the transfer of the designed pattern into the resist layer with high spatial precision.

The exposure behavior of PMMA is influenced by the spatial distribution of deposited energy within the resist, which is governed by electron scattering processes discussed in previous sections. In particular, secondary electrons generated during exposure contribute significantly to the effective exposure region, extending beyond the primary beam diameter. This effect must be considered when defining nanoscale features, as it influences the resolution and accuracy of pattern transfer.

The performance of PMMA as a resist depends on parameters such as molecular weight, film thickness, and exposure conditions. Thinner resist films generally provide higher resolution due to reduced electron scattering, whereas thicker films offer greater mechanical stability during subsequent processing steps such as metal deposition and lift-off. In practice, the resist thickness is selected to balance resolution requirements with process robustness.

In addition to its role in pattern formation, PMMA is widely used in lift-off processes for defining metal electrodes. After exposure and development, metal is deposited onto the patterned resist, and the remaining resist is subsequently removed to leave metal only in the desired regions. The quality of this process depends on the resist profile and adhesion characteristics, which must be controlled to ensure clean pattern transfer.

One of the key challenges associated with PMMA-based processing is the potential for residual contamination on the graphene surface. Due to the high sensitivity of graphene to surface adsorbates, residual resist can introduce unintended doping, increase scattering, and degrade device performance. This is particularly critical for electrolyte-gated sensing applications, where the device response depends strongly on the surface condition of the graphene channel. Careful process control and cleaning steps are therefore required to minimize contamination and preserve the intrinsic properties of graphene.

In the present work, PMMA is employed as the primary resist for electron beam lithography, and its processing conditions are optimized to achieve consistent pattern definition across devices. This ensures reliable fabrication of graphene structures and supports systematic investigation of the influence of device geometry on electrical and sensing behavior.

2.5.6 Pattern Design and Exposure Optimization

The successful implementation of electron beam lithography depends not only on the underlying physical processes but also on careful pattern design and optimization of exposure conditions. In graphene-based device fabrication, where structural parameters directly influence electrical performance, precise control over pattern geometry is essential.

Pattern design begins with the generation of a layout that defines the geometry of the device, including the graphene channel, source and drain electrodes, and associated contact structures. Computer-aided design (CAD) (i.e. k-layout) tools are used to create these layouts, allowing flexibility in defining complex geometries and enabling systematic variation of structural parameters. In the present work, particular emphasis is placed on the design of electrode configurations, including variations in shape, size, and spacing, in order to investigate their influence on device behavior.

The geometry of the electrodes plays a significant role in determining the electrical characteristics of electrolyte-gated graphene devices. Variations in electrode spacing and channel dimensions can affect carrier transport, local electric field distribution, and the efficiency of electrostatic coupling through the electrolyte. In addition, the configuration of the counter electrode influences ion distribution and the formation of the electric double layer at the graphene–electrolyte interface. As

a result, precise definition of these geometrical parameters is critical for achieving reproducible and interpretable device responses.

The translation of the designed pattern into a physical structure requires careful optimization of exposure parameters, particularly the exposure dose. The dose determines the amount of energy delivered to the resist and must be sufficient to ensure complete development of the intended pattern without causing excessive feature broadening due to proximity effects. Establishing an optimal dose window is therefore essential for maintaining accurate feature dimensions.

In addition to the global exposure dose, local variations in pattern density can influence the effective dose distribution across the resist. Dense regions may receive additional exposure from scattered electrons, while isolated features may experience reduced effective dose. This spatial variation must be considered during pattern design to ensure uniform feature definition across the device.

Other exposure parameters, including beam current, step size, dwell time, and acceleration voltage, also influence pattern fidelity. These parameters are selected to ensure uniform energy deposition and consistent pattern formation across devices. In particular, maintaining consistent exposure conditions is essential when comparing devices with different geometries, as it allows the influence of design variations to be distinguished from fabrication-induced effects.

In the present work, pattern design and exposure conditions are systematically optimized to achieve reproducible fabrication of graphene devices with well-defined electrode geometries. This controlled approach enables reliable investigation of the relationship between device architecture and electrical performance, which forms a central objective of this study.

2.5.7 Development and Pattern Transfer

Following electron beam exposure, the latent pattern formed in the resist is converted into a physical structure through the development process. For positive-tone resists such as PMMA, the regions exposed to the electron beam undergo polymer chain scission and become more soluble in the developer solution. During development, these exposed regions are selectively removed, leaving behind a patterned resist layer that defines the geometry of the device [4, 5, 13, 14].

The development process is typically carried out using a solution of methyl isobutyl ketone (MIBK) diluted in isopropyl alcohol (IPA), which selectively dissolves the exposed PMMA. The quality of pattern transfer depends critically on development conditions, including developer composition, development time, and temperature. Insufficient development may result in incomplete removal of exposed regions, while excessive development can erode unexposed areas, leading to loss of feature definition. Careful optimization of these parameters is therefore required to achieve sharp and well-defined patterns [17].

After development, the patterned resist serves as a mask for subsequent material deposition. In this work, metallic electrodes are deposited onto the substrate to define the source and drain contacts of the graphene devices. The deposition process is followed by a lift-off step, in which the remaining resist is removed, along with any metal deposited on top of it, leaving metal only in the desired patterned regions.

The success of the lift-off process depends on the resist profile and adhesion characteristics. A well-defined resist profile facilitates clean separation of unwanted material, ensuring accurate transfer of the intended pattern. Inadequate resist profile or excessive metal coverage can lead to incomplete lift-off, resulting in residual metal structures or bridging between features.

For graphene-based devices, the development and pattern transfer steps are particularly critical due to the sensitivity of graphene to surface contamination. Residual resist or metallic particles remaining on the graphene surface can introduce unintended doping, increase carrier scattering, and degrade device performance. This is especially important in electrolyte-gated sensing applications, where the electrical response is strongly influenced by surface interactions at the graphene–electrolyte interface.

In the present work, development and lift-off processes are carefully controlled to ensure clean pattern transfer and minimal contamination of the graphene surface. This is essential for achieving reproducible device characteristics and for enabling reliable interpretation of electrical measurements. The completion of these steps marks the transition from pattern definition to fully fabricated device structures, which are described in detail in the following section.

2.6 Device Fabrication Process

The fabrication of graphene-based electrolyte-gated field-effect transistor devices involves a sequence of carefully controlled processing steps, including substrate preparation, graphene integration, lithographic patterning, and metal contact formation. Each stage plays a critical role in determining the structural integrity and electrical performance of the final device. In the present work, a combination of electron beam lithography and, where appropriate, optical lithography is employed to define device features with varying spatial scales.

2.6.1 Substrate Preparation

The fabrication process begins with the preparation of the substrate, typically consisting of a silicon wafer with a thermally grown silicon dioxide (SiO_2) layer. Prior to device fabrication, the substrate is cleaned to remove organic contaminants and particulate matter that may interfere with graphene adhesion and lithographic patterning.

Cleaning is generally performed using sequential rinsing in organic solvents such as acetone and isopropanol (IPA), followed by rinsing with deionized water. The substrate is then dried using a nitrogen gun. This cleaning procedure ensures a relatively uniform and contamination-free surface, which is essential for achieving consistent graphene transfer and resist coating.

2.6.2 Graphene Integration

Graphene is incorporated onto the prepared substrate using different approaches depending on the source material. For CVD-grown graphene, a transfer process is employed to move the graphene film from the growth substrate onto the target Si/SiO_2 substrate. This typically involves the use of a polymer support layer, such as PMMA, followed by etching of the metal growth substrate and subsequent transfer of the graphene onto the desired surface.

In the case of mechanically exfoliated graphene, flakes are directly deposited onto the substrate through mechanical cleavage of bulk graphite. This method provides high-quality graphene but with limited control over flake size and position. Commercially supplied graphene samples, which are typically CVD-grown and pre-transferred, are also used to facilitate device fabrication with improved reproducibility.

The quality of graphene after integration is influenced by factors such as transfer-induced contamination, wrinkles, and defects. These features can affect both the electrical properties and sensing performance of the devices and are therefore considered in subsequent analysis.

2.6.3 Lithographic Patterning

The definition of device geometry, including electrodes and contact structures, is achieved through lithographic patterning. Electron beam lithography is used as the primary technique for defining nanoscale features, such as the graphene channel region and closely spaced electrodes. The high resolution of EBL enables precise control over feature dimensions and allows systematic variation of device geometry.

In addition to EBL, optical lithography is employed in selected steps where high resolution is not required, such as the definition of larger contact pads and alignment markers. For having multiple devices on a substrate, EBL takes too long to pattern the pre-design structure; in this case, the best possible solution is to make the larger contact pad with optical lithography, which is quite fast. This strategy has been adopted while fabricating devices at the Nanotechnology Group, Univeristy of Salamanca.The use of optical lithography in these cases improves fabrication efficiency while maintaining sufficient accuracy for macroscopic features.

During lithographic processing, a resist layer (PMMA for EBL) is deposited onto the substrate, exposed according to the desired pattern, and developed to create a patterned resist mask. This mask defines the regions where material deposition or removal will occur in subsequent steps.

2.6.4 Development and Metal Contact Deposition

Following resist patterning, the pattern was then develped by immersing the fabricated device in a developer solution named AR-56 for 1 minute and 30 seconds in IPA.Then metal contacts are deposited to form the source and drain electrodes of the device. Metal deposition is typically carried out using thermal evaporation (at FIM UNIMORE) and electron beam evaporation (Nanotechnology Group, University of Salamanca, which allows controlled deposition of thin metallic films onto the substrate.

Commonly used metal combinations include adhesion layers such as chromium or Platinum, followed by a conductive layer such as gold. The choice of metals is guided by considerations of adhesion, electrical conductivity, and compatibility with graphene. The deposited metal conforms to the patterned resist structure, covering both the exposed substrate regions and the remaining resist.

2.6.5 Lift-Off Process

After metal deposition, the lift-off process is used to remove the resist along with the metal deposited on top of it, leaving behind metal only in the regions defined by the developed pattern. This step is typically performed by immersing the sample in a solvent such as acetone for 15 minutes, which dissolves the resist and releases the unwanted metal

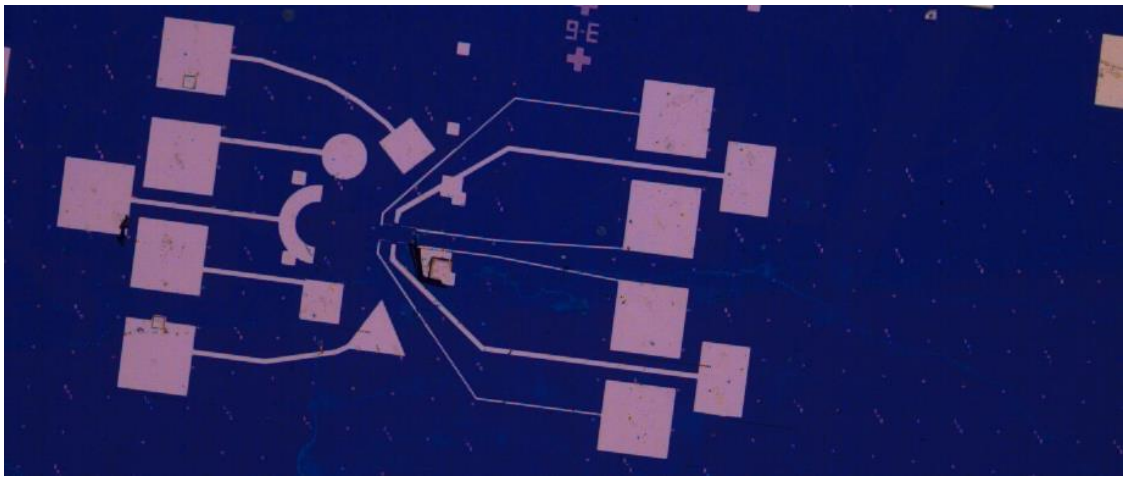

Figure 2.14: Optical Image after lit-off

The success of the lift-off process depends on the quality of the resist pattern and the thickness of the deposited metal. Proper lift-off results in well-defined metal electrodes with minimal residual material. Any remaining residues can affect the electrical performance of the device and are therefore minimized through careful processing and cleaning.

2.6.6 Device Geometry and Design Variations

The fabricated devices are designed with controlled variations in geometry to investigate their influence on electrical and sensing behavior. Parameters such as channel length, electrode spacing, and counter electrode configuration are systematically varied across different devices.

In particular, the geometry of the counter electrode is considered as a key design parameter in electrolyte-gated systems. Variations in electrode shape, size, and positioning can influence the distribution of the electric field and the formation of the electric double layer at the graphene–electrolyte interface. By incorporating these variations into the fabrication process, the study aims to examine their impact on device performance in a controlled and reproducible manner.

2.7 Device Architecture and Electrolyte Configuration

The fabricated graphene devices are configured as electrolyte-gated field-effect transistors, where the electrical behavior of the graphene channel is modulated through an ionic medium rather than a conventional solid dielectric. This configuration enables strong electrostatic coupling between the gate electrode and the graphene channel, making it particularly suitable for sensing applications in liquid environments.

The device architecture consists of a graphene channel connected to metallic source and drain electrodes, which define the conduction path for charge carriers. The channel is exposed to an electrolyte solution, which serves as the gating medium. A gate voltage is applied through an external electrode immersed in the electrolyte, commonly referred to as the counter or reference electrode. This arrangement allows the gate potential to be transmitted through the ionic solution to the graphene surface

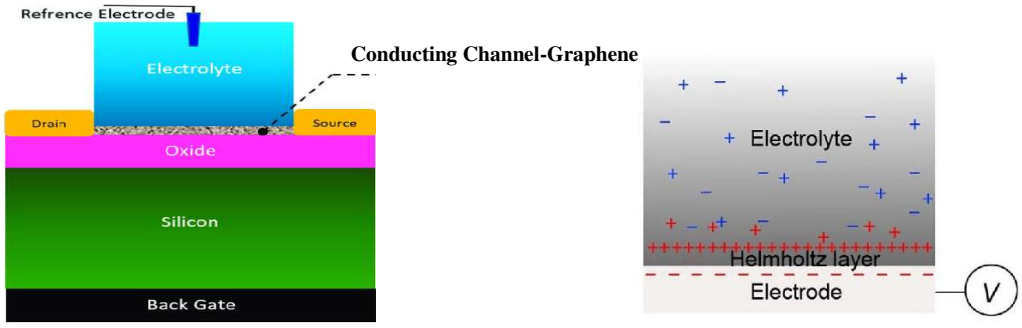

Figure 2.15: Schematic of Electrolyte Gated Graphene Field Effect Transistor and Formation of Electric Double Layer at Graphene-Electrolyte Interface

When a gate voltage is applied, ions in the electrolyte redistribute near the graphene surface, leading to the formation of an electric double layer at the graphene–electrolyte interface [6,7]. This electric double layer acts as a nanoscale capacitor with high capacitance, enabling efficient modulation of carrier density in the graphene channel at relatively low applied voltages. As a result, small variations in surface charge or local electrostatic potential can induce measurable changes in the electrical conductance of the device.

The configuration of the gate electrode plays an important role in determining the distribution of the electric field within the electrolyte. In contrast to conventional field-effect devices, where the gate geometry is fixed by a solid dielectric structure, electrolyte-gated systems allow flexibility in electrode design. Parameters such as electrode shape, size, and distance from the graphene channel can influence ion distribution and the resulting electrostatic coupling.

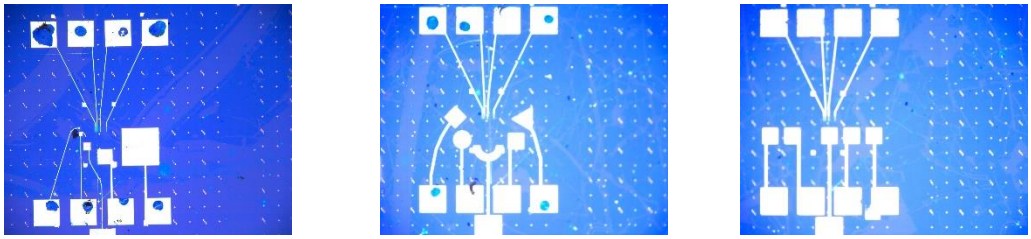

Figure 2.16: Counter Electrode Fabricated Deived with differnt sizes, shapes and distance

In the present work, particular attention is given to the role of counter electrode geometry in modulating device behavior. By varying the physical configuration of the gate electrode, it is possible to explore how geometric factors influence the formation of the electric double layer and

the efficiency of electrostatic gating. This provides an opportunity to examine device performance beyond intrinsic material properties and to identify design parameters that can enhance sensitivity and reproducibility.

The electrolyte used in the measurements serves both as a gating medium and as the environment in which analyte interactions occur. Changes in electrolyte composition, pH, or the presence of biomolecules can alter the local electrostatic conditions at the graphene surface. These changes are reflected in the electrical characteristics of the device, typically observed as shifts in the Dirac point or variations in conductance.

The open configuration of the graphene channel, in direct contact with the electrolyte, allows for real-time interaction with chemical and biological species. While this enhances sensitivity, it also introduces challenges related to environmental stability and contamination. Variations in ionic strength, temperature, and surface adsorption can influence device response and must be considered during experimental measurements.

The device architecture and electrolyte configuration described in this section provide the foundation for the electrical characterization and sensing experiments presented in the following sections. By combining precise device fabrication with controlled electrolyte gating, the system enables systematic investigation of graphene-based sensing mechanisms under realistic operating conditions.

2.8 Electrical Measurement Setup

The electrical characterization of the fabricated graphene devices is performed to evaluate their transport properties and response under electrolyte gating conditions. These measurements provide the basis for analyzing device behavior, including carrier modulation, Dirac point shifts, and sensitivity to external perturbations.

2.8.1 Measurement Configuration

The graphene devices are operated in a field-effect configuration, where the current flowing through the graphene channel is measured as a function of the applied gate voltage. The graphene

channel is contacted by metallic source and drain electrodes, and a bias voltage is applied between these electrodes to drive current through the device.

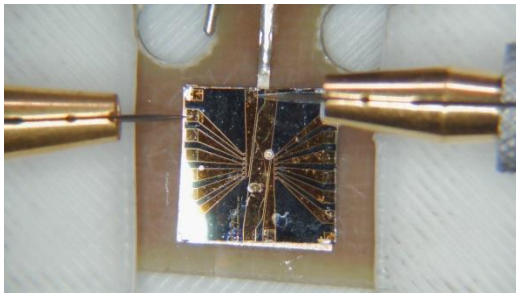

Figure 2.17: Probe contacts showing the measuring mechanism of Graphene Field Effect Transistor

A gate voltage is applied through the on-chip gate counter electrode, the electrode should cover the graphene channel under investigation, and the gate counter electrode enables electrostatic modulation of the carrier concentration in the graphene channel. This electrolyte-gated configuration allows efficient control of the channel conductance due to the high capacitance of the electric double layer formed at the graphene-electrolyte interface.

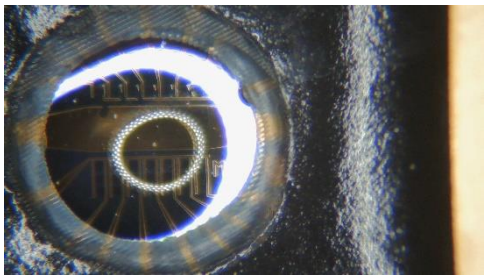

Figure 2.18: Electrolyte covering the graphene channel and the counter electrode

The primary measurement involves recording the drain current as a function of gate voltage, commonly referred to as the transfer characteristic. This measurement provides information about the ambipolar transport behavior of graphene, including the position of the Dirac point, which corresponds to the minimum conductance condition.

2.8.2 Instrumentation

Electrical measurements are carried out using a source-meter, which is capable of simultaneously applying voltage and measuring current with high precision.

The DC source meter is used to apply the source–drain bias voltage and to measure the resulting current through the graphene channel.

The gate voltage is also controlled through the measurement system which can be increased upto 200V, depending on the experimental setup.In our case we measure at low bias voltage likes 20, 50mV by sweeping gate voltage in between -40V to +40V. The use of precision instrumentation ensures accurate measurement of low currents and small changes in electrical response, which are critical for detecting subtle variations induced by analyte interactions.

The devices are typically measured using probe contacts and also using the Graphenea card for the case of package commercial devices which are wire bonded Care is taken to ensure stable electrical contact during measurements to avoid fluctuations or noise in the recorded data.

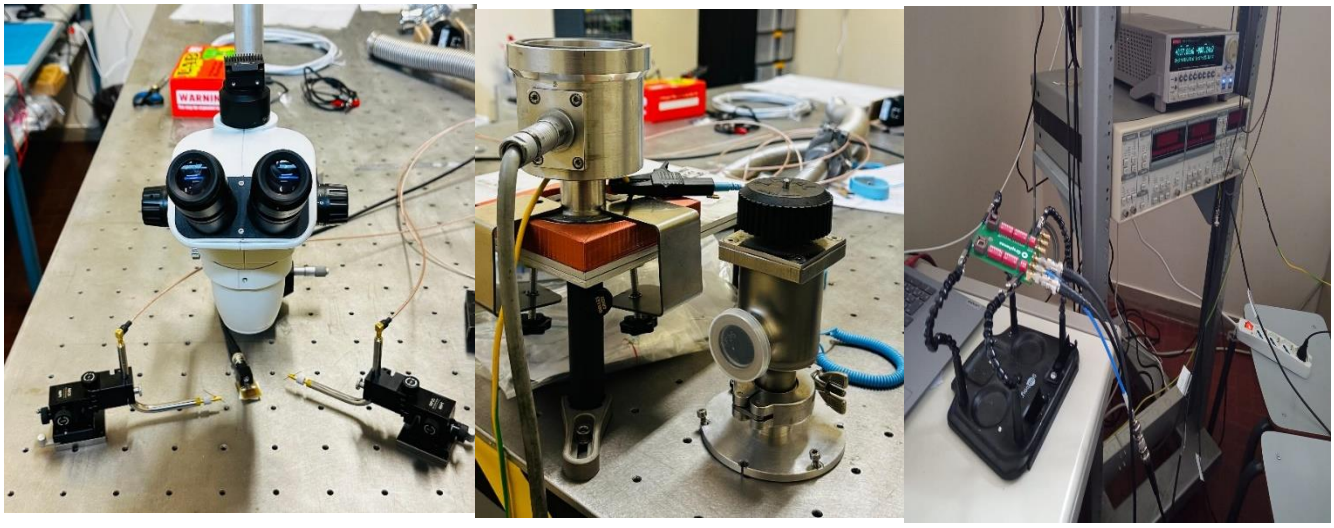

Figure 2.19: Electrical Transport Measurement setup under ambient conditions, vacuum and for the packaged device with Graphenea Card

2.8.3 Measurement Procedure

The electrical characterization begins with baseline measurements of the graphene device in the absence of analytes, typically in a controlled electrolyte environment. A constant source–drain voltage is applied, and the gate voltage is swept over a defined range to obtain the transfer characteristics of the device.

From these measurements, key parameters such as the Dirac point voltage is extracted. The position of the Dirac point provides information about the charge neutrality condition in graphene and is sensitive to changes in the local electrostatic environment.

Subsequent measurements are performed under varying experimental conditions, such as changes in electrolyte composition, pH, or the introduction of biomolecules. The measurement protocol is maintained consistently across different conditions to ensure comparability of results. Parameters such as sweep rate, voltage range, and stabilization time are controlled to minimize measurement variability.

2.9 Sensing Experimental Methodology

The sensing performance of the fabricated graphene devices is evaluated through controlled experiments involving variations in electrolyte conditions and the introduction of target analytes. The electrolyte-gated configuration enables direct interaction between the graphene surface and the surrounding environment, allowing changes in chemical composition to be transduced into measurable electrical signals. In this work, sensing experiments are primarily focused on pH variation and protein detection using human serum albumin (HSA), with additional consideration given to the broader applicability of the device platform.

2.9.1 pH Sensing Measurements

pH sensing is employed as a model system to investigate the response of graphene devices to changes in ionic concentration and surface charge. Variations in pH alter the protonation state of species present at the graphene-electrolyte interface, leading to changes in surface potential and electrostatic conditions. These changes are reflected in the electrical characteristics of the device, particularly in the position of the Dirac point.

For pH measurements, the device is exposed to electrolyte solutions with different pH values prepared in Phosphate Buffer Saline (PBS) solution. The graphene channel remains in direct contact with the electrolyte, while the gate voltage is applied through on chip gate electrode.

The measurement procedure involves recording the transfer characteristics of the device at each pH value. A constant source-drain bias is maintained, and the gate voltage is swept over a defined range. The experiments are repeated for the bias voltages 20mV, 50mV, 100mV and 200mV with a gate sweeping in between 0 to 1 volt with a step size of 400. Changes in the Dirac point voltage are used as a primary indicator of pH response, as shifts in this parameter reflect variations in the local electrostatic environment.

Care is taken to ensure that measurements are performed under stable conditions, with sufficient time allowed for the system to reach equilibrium after each change in pH. This helps to minimize transient effects and ensures that the recorded response accurately represents the steady-state behavior of the device.

2.9.2 Protein Detection: Human Serum Albumin (HSA)

The detection of protein biomarkers is investigated using human serum albumin (HSA), a widely studied protein with clinical relevance in the assessment of kidney function and overall physiological status. The relatively large size and complex structure of proteins introduce additional challenges in electrolyte-gated sensing, particularly due to ionic screening effects.

HSA solutions of varying concentrations (0.01, 0.05, 0.1, 0.5,1,5,10 and 30mg/ml) are prepared in an ultrapure electrolyte environment. The graphene device is exposed to these solutions, allowing the protein molecules to interact with the graphene surface either through direct adsorption or through electrostatic interactions. These interactions can induce changes in local charge distribution and surface potential, which in turn affect the electrical response of the device [18,19]

Electrical measurements are performed following the same protocol used for baseline characterization, with transfer characteristics recorded for each concentration of HSA. The baseline characterization is done with the Deionized Water. Based on IV and Transfer response measurements, the changes in the Dirac point voltage and conductance are analyzed to evaluate

the sensing response. Due to the influence of Debye screening in electrolyte environments, the effective interaction between the protein and the graphene channel is limited to regions close to the surface. As a result, the observed response may depend strongly on electrolyte conditions and device configuration.

The detection of HSA in this work serves as a representative example of protein sensing using graphene-based devices and provides insight into the challenges associated with detecting large biomolecules in electrolyte-gated systems.

2.10 Data Processing and Analysis

The data obtained from the transport measurements has been analysed using Origin pro 2023 software. The measurements data obtained from graphene devices are analyzed to extract key parameters that describe their transport behavior and sensing response. Given the sensitivity of graphene to changes in its electrostatic environment, careful processing and interpretation of the data are essential for obtaining reliable and meaningful results.

A primary feature of interest in graphene field-effect measurements is the transfer characteristic, which represents the variation of drain current as a function of gate voltage. From this curve, the position of the Dirac point is identified as the gate voltage corresponding to minimum conductance. This point reflects the charge neutrality condition in graphene and serves as a key parameter for analyzing changes in the local electrostatic environment.

Shifts in the Dirac point voltage are used as a primary indicator of sensing response [9]. Variations in pH, ionic concentration, or the presence of biomolecules can alter the surface potential at the graphene–electrolyte interface, leading to a shift in the Dirac point. By comparing the Dirac point position under different experimental conditions, it is possible to quantify the response of the device to external perturbations.

In addition to Dirac point analysis, changes in the overall conductance profile are also considered. Variations in conductance can arise from modifications in carrier concentration, scattering mechanisms, or contact effects. While the Dirac point provides a convenient reference for

electrostatic changes, conductance variations can offer complementary information regarding transport behavior and interaction mechanisms.

For quantitative analysis, the sensitivity of the device is evaluated by relating the change in electrical response to the variation in analyte concentration or pH. In the case of pH sensing, sensitivity is commonly expressed as the change in Dirac point voltage per unit change in pH. For protein detection, the response may be analyzed as a function of analyte concentration, with emphasis on trends rather than absolute calibration, given the influence of ionic screening and surface interactions.

To ensure consistency in data analysis, all measurements are processed using a uniform methodology. Parameters such as the voltage sweep range and identification of the Dirac point are handled in a consistent manner across different datasets. This approach minimizes subjective variation in parameter extraction and enables meaningful comparison between devices and experimental conditions.

It is also important to consider sources of variability in the data. Fluctuations in measurement conditions, device-to-device differences, and material-related factors can all contribute to variations in the observed response. By combining multiple measurements and comparing trends across devices, it is possible to distinguish systematic behavior from random variations.

The analysis framework described in this section provides a structured approach for interpreting the electrical response of graphene-based devices under electrolyte gating. This approach is applied consistently in the subsequent chapters to evaluate sensing performance and to examine the influence of device geometry and material properties.

2.11 Summary of Chapter

This chapter has presented the materials, fabrication methodology, and experimental framework used for the realization of graphene-based electrolyte-gated field-effect transistor devices. The selection of graphene from multiple sources, along with the use of silicon-based substrates and controlled processing materials, provides a foundation for investigating the influence of material properties on device behavior.

A top-down nanofabrication approach has been employed, with electron beam lithography serving as the primary technique for defining nanoscale device features. The principles of electron–matter interaction, resist behavior, and exposure optimization have been discussed to establish the basis for reliable patterning. The fabrication process, including substrate preparation, graphene integration, lithographic patterning, metal deposition, and lift-off, enables the realization of devices with controlled geometry.

The device architecture has been configured for electrolyte gating, allowing efficient modulation of the graphene channel through the formation of an electric double layer at the graphene–electrolyte interface. The flexibility of this configuration facilitates the investigation of electrode geometry and its influence on device performance.

Electrical characterization and sensing methodologies have been outlined, including measurements of transfer characteristics and analysis of Dirac point shifts in response to variations in pH and protein concentration. A consistent data processing approach has been established to ensure reliable interpretation of experimental results.

The combination of controlled fabrication, well-defined device architecture, and systematic measurement protocols provides a robust platform for analyzing graphene-based sensing behavior. These experimental foundations support the investigations presented in the subsequent chapters, where the electrical characteristics and sensing performance of the fabricated devices are examined in detail. \

2.12 References

1. Novoselov, K. S., Geim, A. K., Morozov, S. V., Jiang, D., Zhang, Y., Dubonos, S. V., Grigorieva, I. V., & Firsov, A. A. (2004). Electric field effect in atomically thin carbon films. Science, 306(5696), 666–669.
2. Geim, A. K., & Novoselov, K. S. (2007). The rise of graphene. Nature Materials, 6, 183–191.
3. Castro Neto, A. H., Guinea, F., Peres, N. M. R., Novoselov, K. S., & Geim, A. K. (2009). The electronic properties of graphene. Reviews of Modern Physics, 81, 109–162.
4. Madou, M. J. (2011). Fundamentals of microfabrication (2nd ed.). CRC Press.

5. Papadopoulos, C. (2016). Nanofabrication: principles and applications. Cham: Springer.
6. Bard, A. J., & Faulkner, L. R. (2000). Electrochemical methods: Fundamentals and applications (2nd ed.). Wiley.
7. Israelachvili, J. N. (2011). Intermolecular and surface forces (3rd ed.). Academic Press.
8. Li, X., Cai, W., An, J., Kim, S., Nah, J., Yang, D., Piner, R., Velamakanni, A., Jung, I., Tutuc, E., Banerjee, S. K., Colombo, L., & Ruoff, R. S. (2009). Large-area synthesis of high-quality and uniform graphene films on copper foils. Science, 324, 1312–1314.
9. Ohno, Y., Maehashi, K., Yamashiro, Y., & Matsumoto, K. (2009). Electrolyte-gated graphene field-effect transistors for detecting pH and protein adsorption. Nano Letters, 9, 3318–3322.
10. Reina, A., Jia, X., Ho, J., Nezich, D., Son, H., Bulović, V., Dresselhaus, M. S., & Kong, J. (2009). Large area, few-layer graphene films on arbitrary substrates by chemical vapor deposition. Nano Letters, 9, 30–35.
11. Ferrari, A. C., Meyer, J. C., Scardaci, V., Casiraghi, C., Lazzeri, M., Mauri, F., Piscanec, S., Jiang, D., Novoselov, K. S., Roth, S., & Geim, A. K. (2006). Raman spectrum of graphene and graphene layers. Physical Review Letters, 97, 187401.
12. Vieu, C., Carcenac, F., Pepin, A., Chen, Y., Mejias, M., Lebib, A., Manin-Ferlazzo, L., Couraud, L., & Launois, H. (2000). Electron beam lithography: Resolution limits and applications. Applied Surface Science, 164, 111–117.
13. Rius, G. (2008). Electron beam lithography for nanofabrication (Doctoral dissertation). Universitat Autònoma de Barcelona.
14. Zhou, J. (2019). Electron beam lithography for nanofabrication (Doctoral dissertation).
15. Pandya, A., & Singh, V. (2022). Micro/nanofluidics and lab-on-chip based emerging technologies for biomedical and translational research applications—Part B.
16. Chen, W., Ahmed, H., & Cui, Z. (1993). Fabrication of high resolution PMMA resist structures by electron beam lithography. *Journal of Vacuum Science & Technology B, 11*(6), 2519–2523.
17. Tseng, A. A. (2004). Nanofabrication: Fundamentals and applications. Small, 1, 924–939.
18. Heller, I., Kong, J., Heering, H. A., Williams, K. A., Lemay, S. G., & Dekker, C. (2008). Influence of electrolyte composition on liquid-gated carbon nanotube and graphene transistors. Journal of the American Chemical Society, 130, 12212–12213.

19. Peña-Bahamonde, J., Nguyen, H. N., Fanourakis, S. K., & Rodrigues, D. F. (2018). Recent advances in graphene-based biosensors for the detection of pathogens. Journal of Nanobiotechnology, 16.

CHAPTER 3

Theoretical Framework and Computational Modelling of GFET Biosensors

3.1 Introduction

Graphene-based electrolyte-gated field-effect transistors (GFETs) have emerged as highly promising platforms for chemical and biological sensing because of their exceptional electrical properties, large surface-to-volume ratio, and strong sensitivity to interfacial electrostatic perturbations. In electrolyte-gated configurations, the electrical response of graphene is governed not only by charge transport within the graphene channel but also by ionic processes occurring at the graphene-electrolyte interface. Consequently, understanding the sensing behaviour of electrolyte-gated GFETs requires a modelling framework capable of resolving coupled electrostatic, ionic, and molecular-scale interactions across multiple spatial and temporal scales.

At the device level, the modulation of graphene conductivity is governed by electrostatic coupling through the formation of an electric double layer (EDL) at the graphene-electrolyte interface. The resulting interfacial capacitance enables efficient carrier modulation at relatively low gate voltages and provides high sensitivity to changes in the local electrochemical environment. Continuum modelling approaches based on coupled electrostatic and ionic transport equations therefore provide an effective framework for analysing electric potential distributions, ion transport behaviour, and carrier modulation within electrolyte-gated graphene devices [1–3].

However, continuum descriptions alone are insufficient to fully capture microscopic interfacial interactions occurring near the graphene surface. In biosensing systems, processes such as biomolecular adsorption, ion organization, hydration-layer formation, and orientation-dependent electrostatic interactions occur at molecular length scales and strongly influence device behaviour. Atomistic simulation approaches, including Brownian Dynamics and molecular dynamics methods, therefore provide complementary insight into adsorption behaviour and interfacial charge distributions that cannot be resolved using continuum formulations alone [4,5].

To address these challenges, a multiscale modelling strategy is adopted in this thesis. Continuum-level finite element simulations are implemented using COMSOL Multiphysics to investigate electrostatic modulation and ionic transport within electrolyte-gated GFET structures. In parallel,

atomistic adsorption modelling is employed to investigate biomolecular interactions occurring near the graphene interface. The combined use of continuum and atomistic approaches provides a physically consistent framework for linking microscopic interfacial interactions with experimentally observed electrical sensing behaviour.

The objective of this chapter is to establish the theoretical and computational framework used throughout this thesis. The fundamental principles governing graphene transistor operation are first introduced, followed by description of the electrolyte-gated device configuration and the electrostatic mechanisms governing electric double-layer formation. The governing continuum equations used for electrostatic and ionic transport modelling are then presented together with their implementation in a finite element framework. Subsequently, atomistic modelling approaches relevant to graphene biosensing systems are introduced, followed by discussion of the multiscale integration strategy used to connect continuum and molecular-level descriptions.

The modelling framework developed in this chapter forms the basis for the simulation studies presented in the following chapters, where computational analysis is combined with experimental characterization to investigate the sensing behaviour of electrolyte-gated graphene biosensors.

3.2 Fundamentals of GFET Operation

Graphene-based field-effect transistors differ fundamentally from conventional semiconductor transistors because graphene possesses a unique two-dimensional electronic structure characterized by a zero bandgap and linear energy dispersion near the Dirac points [6,7,8]. Graphene consists of a single atomic layer of sp^2-bonded carbon atoms arranged in a hexagonal honeycomb lattice, producing electronic states in which the conduction and valence bands meet at the charge neutrality point without formation of an energy gap.

Near the Dirac point, charge carriers in graphene behave as massless Dirac fermions, resulting in exceptionally high carrier mobility and ambipolar transport behaviour. Unlike conventional semiconductors, where electrical conduction is dominated by either electrons or holes, graphene supports both electron and hole conduction depending on the applied gate voltage. This ambipolar transport behaviour is one of the defining characteristics of GFET operation and plays an important role in sensing applications.

The electrical conductivity of graphene is governed by the carrier density within the graphene channel. In a field-effect transistor configuration, an applied gate voltage modulates the carrier density through capacitive electrostatic coupling between the gate electrode and graphene. The induced carrier density can be expressed as:

$$n = \frac{C_g}{e}\left(V_g - V_D\right) - - - - - - - - (Eq.1)$$

where 'Cg' is the gate capacitance per unit area, 'Vg' is the applied gate voltage, 'V_D' is the Dirac voltage corresponding to the charge neutrality point, and 'e' is the elementary charge [9]. Variations in the Dirac voltage provide information regarding changes in the electrostatic environment surrounding the graphene channel and are therefore commonly used in sensing applications.

Under low-field conditions, charge transport in graphene can be described using a drift-diffusion approximation in which the drain current is expressed as:

$$I_D = W.\mu.N.\frac{V_{DS}}{L} \ldots\ldots\ldots\ldots\ldots\ldots (Eq.2)$$

where 'W' and 'L' are the channel width and channel length, respectively, 'μ' is the carrier mobility, and 'V_{DS}' is the applied drain–source voltage [10]. In practical graphene devices, the conductivity is additionally influenced by carrier scattering arising from impurities, substrate interactions, lattice defects, phonons, and adsorbed species.

A characteristic feature of graphene is the existence of finite minimum conductivity near the Dirac point despite the absence of induced charge carriers. This behaviour originates from residual carrier inhomogeneity and charge fluctuations within the graphene channel. Although the absence of a bandgap limits the achievable on/off ratio compared with conventional semiconductor devices, it enables continuous electrostatic modulation of conductivity over a broad gate-voltage range, which is advantageous for sensing applications.

The transfer characteristics of GFETs are typically represented by the drain current as a function of gate voltage and exhibit a characteristic V-shaped profile centred near the Dirac point. Shifts in the transfer curve and variations in carrier mobility or transconductance provide important information regarding changes in the local electrostatic environment and adsorption processes occurring near the graphene surface.

In electrolyte-gated configurations, electrostatic carrier modulation occurs through ionic coupling at the graphene-electrolyte interface, requiring explicit consideration of electric double-layer formation and electrolyte transport phenomena. These electrochemical mechanisms governing electrolyte-gated operation are discussed in the following sections.

3.3 Device Geometry and Electrolyte-Gated Configuration

The electrolyte-gated graphene field-effect transistor investigated in this work consists of a graphene conducting channel interfaced directly with an electrolyte medium and controlled through an external gate electrode. Unlike conventional silicon-based field-effect transistors, where electrostatic modulation occurs through a solid dielectric layer, electrolyte-gated GFETs operate through ionic coupling at the graphene–electrolyte interface. This configuration enables extremely high interfacial capacitance and efficient carrier modulation at relatively low operating voltages.

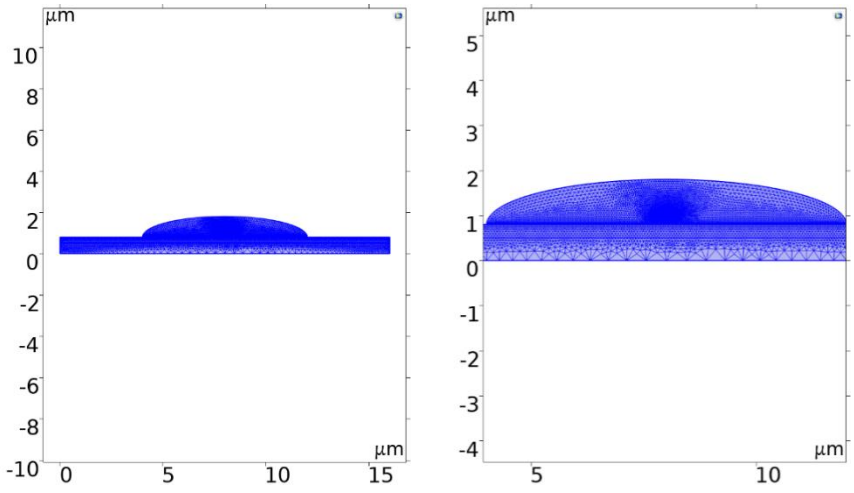

Figure 3.1: Schematic representation of the electrolyte-gated graphene field-effect transistor geometry used for continuum finite element modelling, showing the graphene channel, source and drain electrodes, electrolyte domain, and gate electrode.

The device geometry employed in the present modelling framework comprises a graphene channel connected to metallic source and drain electrodes and exposed to an electrolyte domain acting as the gate dielectric. A gate electrode positioned within the electrolyte applies the external bias required for electrostatic modulation of the graphene channel. Figure 3.2 illustrates the representative device geometry and computational configuration implemented in this work.

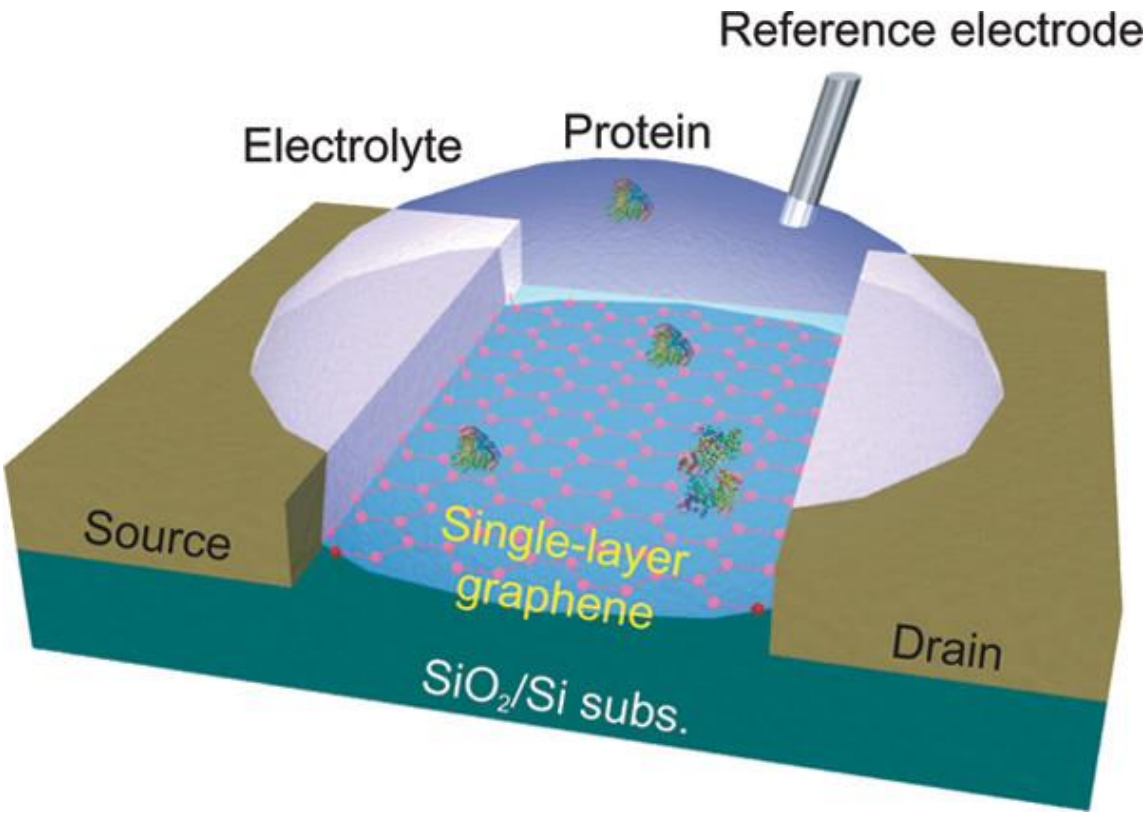

Figure 3.2: Conceptual illustration of electrostatic gating in electrolyte-gated graphene field-effect transistors showing ion redistribution and electric double-layer formation near the graphene–electrolyte interface (Taken from Ref.[11])

The graphene channel is represented as a conductive layer located at the interface between the substrate and electrolyte domains. The source and drain electrodes define the carrier transport direction along the graphene sheet, while the electrolyte region above the graphene surface enables ionic gating through formation of an electric double layer. The dimensions of the computational domain are selected to remain consistent with the experimental device configuration while maintaining numerical stability and computational efficiency.

In electrolyte-gated configurations, the electrostatic interaction between the electrolyte and graphene channel is governed by ion redistribution near the graphene surface under an applied electric field. This process results in formation of electric double layers at the electrode–electrolyte interfaces and produces strong electrostatic coupling between the ionic medium and graphene channel. Consequently, understanding the electrochemical behaviour of electrolyte-gated GFETs requires explicit consideration of electric double-layer formation and ionic screening phenomena.

The electrolyte-gated geometry provides several important advantages for sensing applications. The nanometre-scale electric double layer produces capacitance values significantly larger than those achievable using conventional oxide dielectrics, thereby enhancing carrier modulation efficiency and sensitivity to local electrochemical perturbations. Furthermore, direct exposure of the graphene surface to the electrolyte enables strong interaction between adsorbed biomolecules and the graphene channel, making electrolyte-gated GFETs particularly attractive for label-free biosensing applications.

The electrostatic mechanisms governing electric double-layer formation and ionic screening behaviour within electrolyte-gated graphene systems are discussed in the following section.

3.4 Electrolyte-Gated Electrostatics and Electric Double-Layer Physics

The operation of electrolyte-gated graphene field-effect transistors is governed by electrostatic coupling between the graphene channel and the surrounding electrolyte medium. When an external gate voltage is applied through an electrode immersed within the electrolyte, mobile ions redistribute in response to the applied electric field, leading to formation of electric double layers at the electrode–electrolyte interfaces. These interfacial charge layers control the electrostatic modulation of the graphene channel and therefore play a central role in device operation.

At the graphene–electrolyte interface, oppositely charged ions accumulate near the graphene surface, forming a nanometre-scale electric double layer that behaves as an effective capacitor with exceptionally high capacitance per unit area [1–3]. Because the separation distance between ionic and electronic charges is extremely small, electrolyte-gated devices achieve efficient carrier modulation at relatively low gate voltages.

The structure of the electric double layer is commonly described using the Stern model, which combines a compact layer of specifically adsorbed ions near the surface with a diffuse ionic region extending into the bulk electrolyte. Figure 3.3 illustrates the electric double-layer structure formed at the graphene–electrolyte interface.

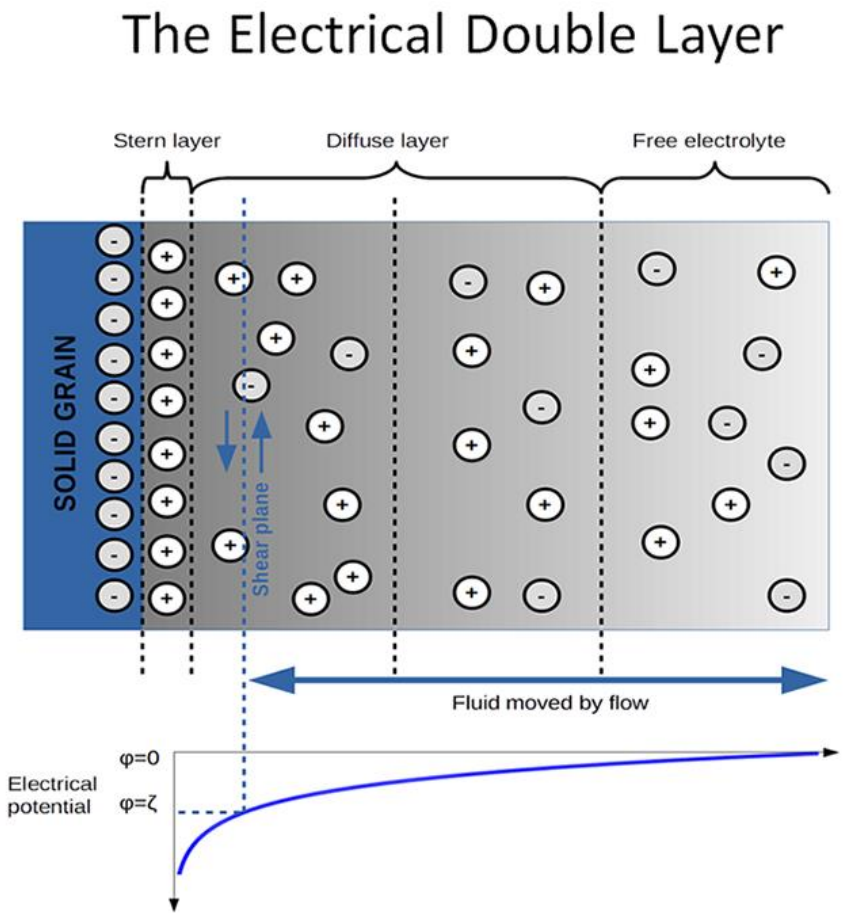

Figure 3.3: Schematic illustration of electric double-layer formation at the graphene-electrolyte interface based on the Stern model, showing compact and diffuse ionic regions. (Adapted rom Ref.12)

A key parameter governing electrostatic screening within the electrolyte is the Debye length, which defines the characteristic distance over which electric fields are screened by mobile ions. In physiological electrolytes, the Debye length is typically limited to only a few nanometres, meaning that electrostatic interactions arising from adsorbed biomolecules are strongly screened beyond this characteristic distance. Consequently, only charges located sufficiently close to the graphene surface effectively contribute to electrostatic modulation of the graphene channel.

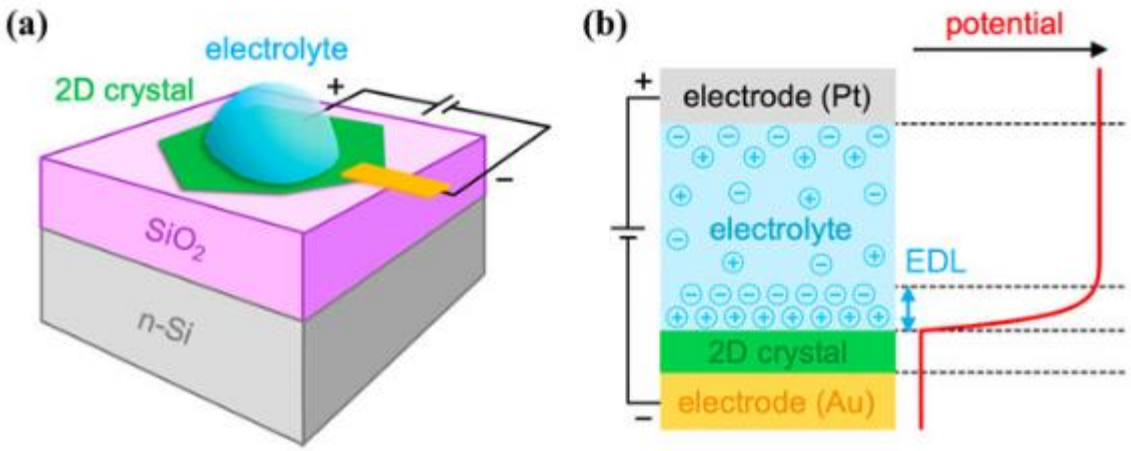

Figure 3.4: Schematic representation of electrolyte-gated electrostatic screening near a two-dimensional conducting channel illustrating electric double-layer formation and Debye-length-limited electrostatic modulation under electrolyte-gated sensing conditions. (Adapted from Chen and Bashir Ref. 13).

In physiological electrolytes, the Debye length is typically limited to only a few nanometres.The induced carrier density within graphene is directly related to the electrostatic potential drop across the electric double layer. Small perturbations in the local ionic environment, such as changes in ion concentration, pH, or biomolecular adsorption, therefore produce measurable changes in graphene conductivity. This strong electrostatic sensitivity forms the basis of electrolyte-gated graphene biosensing.

In practical sensing systems, the electrostatic environment is additionally influenced by ion adsorption, hydration-layer formation, surface contamination, and biomolecular interactions occurring near the graphene interface. These processes can modify the local electric potential and induce shifts in the Dirac voltage observed experimentally in GFET transfer characteristics.

Because electrolyte-gated graphene devices involve coupled electrostatic and ionic transport phenomena, quantitative modelling of device behaviour requires a continuum framework capable of simultaneously describing electric potential distributions, ion transport, and charge-carrier

modulation within graphene. The governing equations used to describe these coupled processes are presented in the following section.

3.5 Governing Equations and Continuum Modelling

To quantitatively describe the electrostatic and ionic processes discussed in Section 3.4, a continuum modelling framework based on coupled electrostatic and transport equations is required. Electrolyte-gated graphene transistors involve simultaneous interaction between electric potential distributions, ionic transport within the electrolyte, and electrostatic modulation of charge carriers in the graphene channel. These coupled processes can be described using a set of continuum equations forming the basis of device-level finite element simulations.

3.5.1 Electrostatics: Poisson Equation

The electrostatic potential distribution within the device is governed by Poisson's equation, which relates the local electric potential to the spatial charge distribution. Within the electrolyte domain, the charge density arises from the distribution of mobile ionic species and determines the resulting electric potential distribution near the graphene interface. The governing electrostatic equation is expressed as:

$$\nabla.(\varepsilon\nabla\emptyset) = -\rho \ldots\ldots\ldots\ldots\ldots.(Eq.3)$$

where ε is the dielectric permittivity of the medium, $\emptyset$ is the electric potential, and ρ is the local space-charge density arising from ionic charge distributions within the electrolyte. This equation provides continuum-level description of electrostatic potential variation throughout the electrolyte-gated device structure.

3.5.2 Ion Transport: Nernst-Planck Equation

Transport of ionic species within the electrolyte is described using the Nernst–Planck equation, which accounts for diffusion and electromigration under an applied electric field. This formulation enables description of ionic redistribution within the electrolyte under electrolyte-gated operating

conditions and provides a continuum representation of the electrostatic screening behaviour discussed previously in Section 3.4.The ionic flux of species (i) is expressed as:

$$J_i = -D_i \nabla c_i - z_i \mu_i c_i \nabla \emptyset$$

where 'Ji' is the ionic flux, 'Di' is the diffusion coefficient, 'ci' is the ionic concentration, 'zi' is the ionic valence, (F) is Faraday's constant, (R) is the universal gas constant, (T) is the absolute temperature, and (\phi) is the electrostatic potential. The first term describes concentration-driven diffusion, while the second term represents electric-field-driven ionic migration.

Conservation of ionic species within the electrolyte is additionally described using the continuity equation:

$$\frac{\partial c_i}{\partial t} + \nabla . J_i = 0 \ldots\ldots\ldots\ldots\ldots (Eq.)$$

Under steady-state conditions employed in the present work, the temporal term approaches zero.

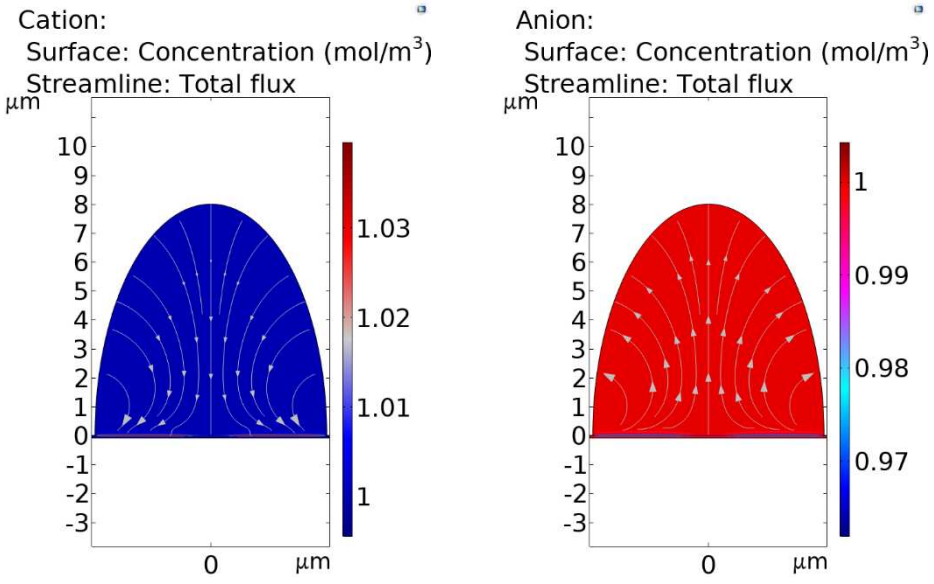

Figure 3.5: Finite element simulation of ionic concentration distributions and transport streamlines within the electrolyte domain under electrolyte-gated conditions showing (a) cation transport and (b) anion transport behaviour.

3.5.3 Charge Transport in Graphene

Charge transport within the graphene channel is described using a drift-diffusion framework in which the current density depends on carrier concentration and electric-field-driven carrier motion. Because graphene exhibits ambipolar transport behaviour, both electron and hole contributions influence the conductivity near the Dirac point. Variations in electrostatic potential at the graphene–electrolyte interface therefore directly influence carrier density and conductivity within the graphene channel.

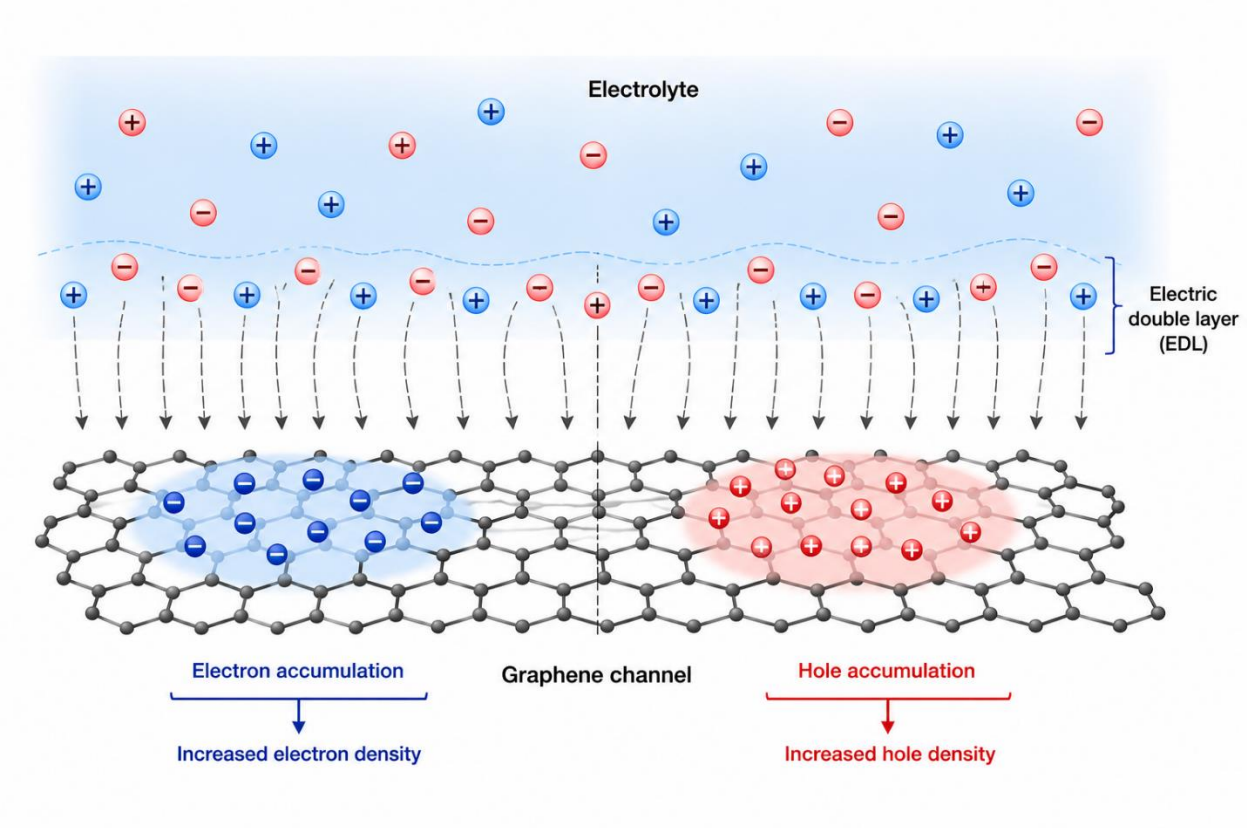

Figure 3.6: Conceptual illustration of electrostatic carrier modulation within the graphene channel arising from electrolyte-gated operation and interfacial ionic coupling

The graphene current density may be expressed in simplified form as:

$$J = qn\mu E \ldots\ldots\ldots\ldots\ldots\ldots (Eq.$$

here (J) is the current density, (q) is the elementary charge, (n) is the carrier concentration, 'μ' is the carrier mobility, and (E) is the applied electric field. Electrostatic perturbations arising from ionic redistribution and biomolecular adsorption therefore modulate graphene conductivity through changes in local carrier density and carrier transport behaviour.

3.5.4 Coupled Multiphysics Framework

The governing equations described above are intrinsically coupled. The electric potential obtained from Poisson's equation influences ionic transport through the migration term in the Nernst–Planck equation, while the resulting ion distribution simultaneously modifies the electrostatic charge density within the electrolyte. The electrostatic potential at the graphene interface additionally governs carrier density modulation within the graphene channel.

At the graphene-electrolyte boundary, the continuum framework represents electrostatic coupling through effective interfacial boundary conditions linking ionic charge accumulation in the electrolyte to induced electronic charge within graphene. The resulting system therefore constitutes a nonlinear coupled multiphysics problem requiring numerical solution through finite element discretization.

The coupled governing equations described in this section were implemented numerically within a finite element framework using COMSOL Multiphysics, as discussed in the following section.

3.6 COMSOL Finite Element Modelling Framework

The coupled governing equations described in the previous section were implemented numerically using COMSOL Multiphysics, a finite element simulation platform capable of solving strongly coupled multiphysics problems within complex geometries. The continuum framework developed in this work was used to investigate electrostatic potential distributions, ionic transport behaviour, and electrostatic carrier modulation within electrolyte-gated graphene devices.

3.6.1 Physics Modules and Computational Framework

The finite element model combines multiple physics interfaces to represent the coupled electrostatic and ionic transport processes governing electrolyte-gated GFET operation. The

Electrostatics module was employed to solve Poisson's equation and obtain electric potential distributions throughout the electrolyte and surrounding device domains. The Transport of Diluted Species module was additionally used to implement ionic diffusion and electromigration within the electrolyte.

Coupling between these modules enables self-consistent interaction between ionic charge distributions and electrostatic potential throughout the computational domain. This coupled framework provides continuum-level description of electrostatic modulation and ionic transport behaviour under electrolyte-gated operating conditions.

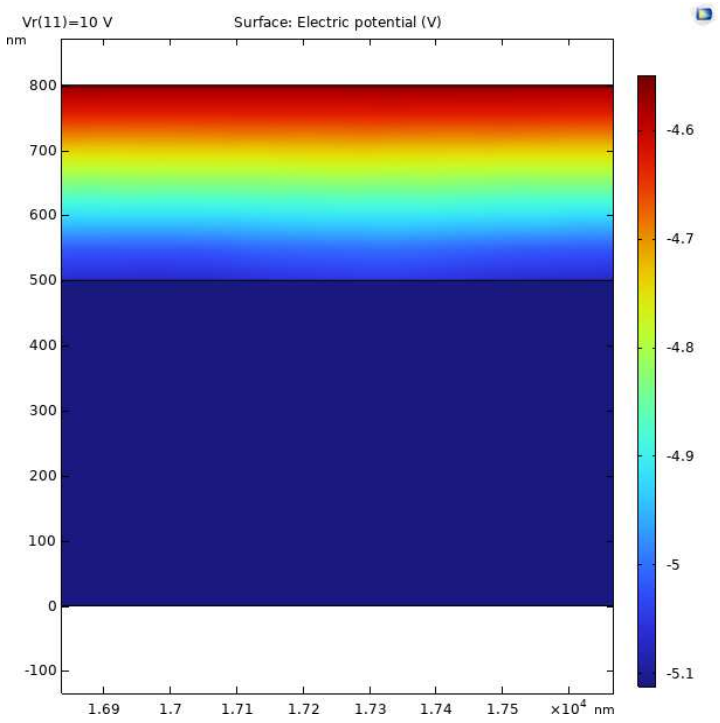

Figure 3.7: Simulated electric potential distribution within the electrolyte-gated graphene field-effect transistor under applied gate bias illustrating electrostatic modulation near the graphene–electrolyte interface.

3.6.2 Boundary Conditions and Interfaces

Appropriate boundary conditions were defined to reproduce the operating configuration of the electrolyte-gated graphene transistor. A fixed electric potential corresponding to the externally

applied gate voltage was imposed at the gate electrode boundary, while source and drain contacts defined the carrier transport direction along the graphene channel.

Bulk electrolyte boundaries were assigned fixed ionic concentrations corresponding to experimental electrolyte conditions. At the graphene–electrolyte interface, electrostatic coupling between ionic charge accumulation and induced graphene carrier density was represented through effective interfacial boundary conditions.

Name	Expression	Value	Description
C1	12E-5[F/m^2]	1.2E-4 F/m²	
Ceq	(C1+Ci_st)	0.0046512 F/m²	
Vdirac	50.3[V]	50.3 V	
NA	abs(sqrt(N0^2+(C1*(Vr-Vdirac)/e_const)^2)/thick)	1.1429E26 1/m³	
N0	1.75e11[cm^-2]	1.75E15 1/m²	
thick	.33[nm]	3.3E-10 m	
C_helm	epsilon0_const*eps_H2O/xS	0.48605 F/m²	
C_equ	Ci_st*C_helm/Ci_st+C_helm	0.9721 F/m²	
C_quantom	.01141[F/m^2]	0.01141 F/m²	
C_overal	C_equ*C_quantom/C_equ+C_quantom	0.02282 F/m²	
zX	-2	-2	Anion charge
cX_bulk	c0+cH_bulk	0.1001 mol/m³	Bulk anion concentration
cA_bulk	0	0	Bulk cation concentration
cH_bulk	10^-pHb[M]	1E-4 mol/m³	Bulk H+ concentration
Istr_bulk	0.5*(zA^2*cA_bulk+zX^2*cX_bulk+cOH_bulk+cH_bulk)	0.2003 mol/m³	Bulk ionic strength

Name	Expression	Value	Description
cH_bulk	10^-pHb[M]	1E-4 mol/m³	Bulk H+ concentration
Istr_bulk	0.5*(zA^2*cA_bulk+zX^2*cX_bulk+cOH_bulk+cH_bulk)	0.2003 mol/m³	Bulk ionic strength
cOH_bulk	10^-14[M^2]/cH_bulk	1E-4 mol/m³	Bulk OH- concentration
zA	+1	1	Cation charge
c0	.0001[M]	0.1 mol/m³	Concentration parameter
xD	sqrt(epsilon0_const*eps_H2O*V_therm/(2*F_const*Istr_bulk))	2.1494E-8 m	Debye length
DX	DA	1.33E-9 m²/s	Diffusion coefficient, anio
DA	1.33e-9[m^2/s]	1.33E-9 m²/s	Diffusion coefficient, cati..
DH	36.3e-4[cm^2/V/s]*V_therm	9.3264E-9 m²/s	Diffusion coefficient, H+
DOH	20.5e-4[cm^2/V/s]*V_therm	5.267E-9 m²/s	Diffusion coefficient, OH-
Vr	0[V]	0 V	down gate
Ka	10^-6[M]	0.001 mol/m³	Equilibrium constant
Kb	100[M]	1E5 mol/m³	Equilibrium constant
Vga	0[V]	0 V	Gate voltage (applied)
Ns	5e14[1/cm^2]	5E18 1/m²	Oxide surface binding sit..

Figure 3.8: Boundary conditions and electrostatic interfaces employed in the finite element modelling framework for electrolyte-gated graphene transistor simulations.

3.6.3 Meshing and Numerical Solution Strategy

Accurate resolution of electrostatic and ionic gradients near the graphene–electrolyte interface requires fine spatial discretization within regions of strong field variation. A non-uniform mesh was therefore employed, with refined finite elements positioned near the graphene interface and coarser elements used within bulk electrolyte regions to maintain computational efficiency.

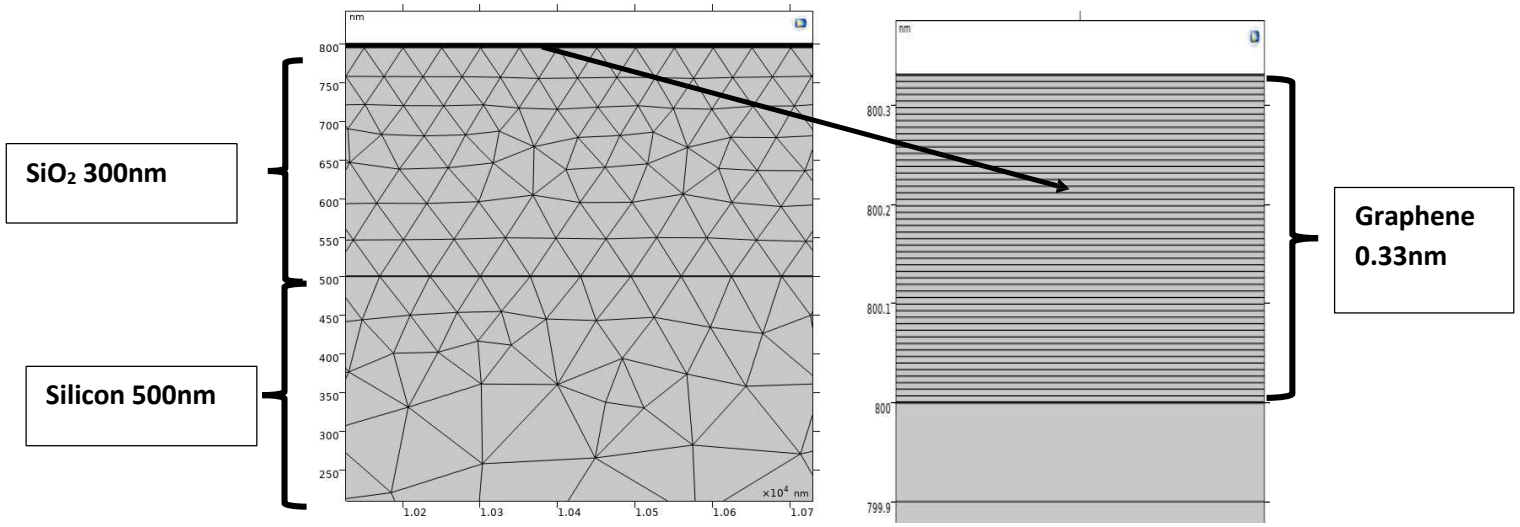

Figure 3.9: Finite element mesh employed for electrolyte-gated graphene transistor simulations showing refined spatial discretization near the graphene–electrolyte interface within the computational domain.

The coupled nonlinear system of equations was solved under steady-state conditions using finite element methods. Stationary solvers were employed to investigate equilibrium electrostatic behaviour and ionic distributions under applied gate voltages. Numerical convergence was verified through mesh refinement and consistency checks to ensure stability and physical reliability of the simulation framework.

Although continuum simulations effectively describe macroscopic electrostatic and ionic behaviour, they do not explicitly resolve molecular-scale interactions occurring near the graphene–electrolyte interface. Atomistic modelling approaches relevant to graphene biosensing systems are therefore discussed in the following section.

3.7 Atomistic Modelling Framework

Although continuum simulations provide important insight into macroscopic electrostatic and ionic behavior, they do not explicitly resolve molecular-scale interactions occurring near the graphene–electrolyte interface. In graphene biosensing systems, processes such as biomolecular adsorption, orientation-dependent interactions, and local charge redistribution occur at nanometer length scales and can significantly influence the electrostatic environment surrounding the graphene channel. Atomistic modelling approaches therefore provide complementary information regarding interfacial molecular behavior relevant to electrolyte-gated sensing.

Atomistic simulations describe the motion and interaction of individual atoms or molecules using classical mechanics and empirical interaction potentials. In molecular dynamics simulations, atomic motion is governed by Newton's equations of motion, while intermolecular interactions are represented through force fields describing bonded and non-bonded interactions [4]. Brownian Dynamics approaches additionally provide efficient description of diffusive molecular motion in implicit solvent environments and are particularly useful for investigating adsorption behaviour near surfaces.

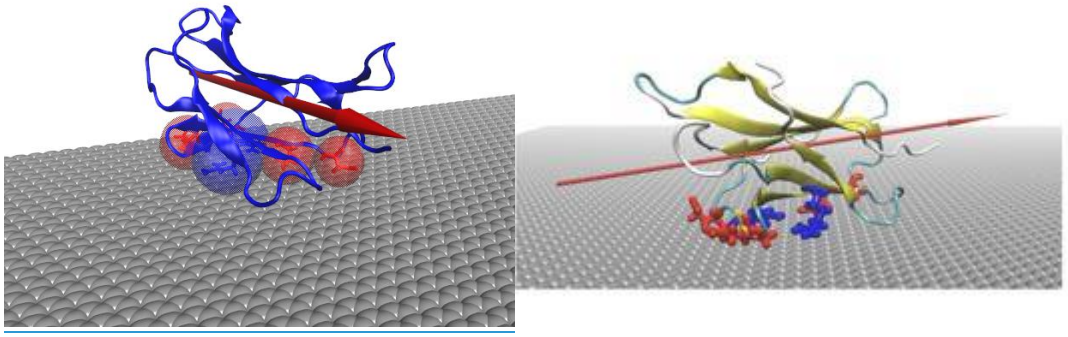

Figure 3.10: Representative atomistic adsorption configurations of biomolecules near graphene surfaces illustrating orientation-dependent interfacial interactions relevant to graphene-based biosensing (Adapted from 14,15)

In the context of graphene biosensors, atomistic approaches are primarily employed to investigate biomolecular adsorption configurations, orientation-dependent electrostatic interactions, and interfacial charge distributions near graphene surfaces. These molecular-level processes influence the local electrostatic environment experienced by the graphene channel and therefore contribute to experimentally observed sensing behavior.

In this work, atomistic adsorption analysis is used primarily to support interpretation of adsorption behavior and electrostatic perturbations occurring near the graphene interface rather than to provide exhaustive molecular-scale thermodynamic analysis. The atomistic framework therefore serves as a complementary component within the broader multiscale modelling strategy developed in this thesis.

Atomistic simulation approaches additionally provide insight into biomolecular interactions and adsorption-mediated electrostatic perturbations relevant to graphene biosensing systems, as discussed in the following section.

3.8 Applications of Atomistic Simulations in GFET Biosensors

Atomistic simulation approaches have been widely applied to investigate biomolecular interactions occurring near graphene surfaces in biosensing systems. These methods provide insight into adsorption configurations, interfacial electrostatic interactions, molecular orientation behaviour, and charge redistribution processes that influence sensing response in graphene-based devices.

In electrolyte-gated GFET biosensors, adsorption of biomolecules near the graphene surface modifies the local electrostatic environment through redistribution of ionic and molecular charges within the effective screening region of the electrolyte. The resulting perturbation of the interfacial electric field influences carrier density modulation within the graphene channel and contributes to experimentally observable changes in conductivity, transconductance, and Dirac voltage.

Atomistic adsorption analysis is particularly important because biomolecular orientation strongly influences the spatial distribution of electrostatic charge near the graphene surface. Different adsorption configurations can therefore produce significantly different electrostatic perturbations even for identical biomolecular species.

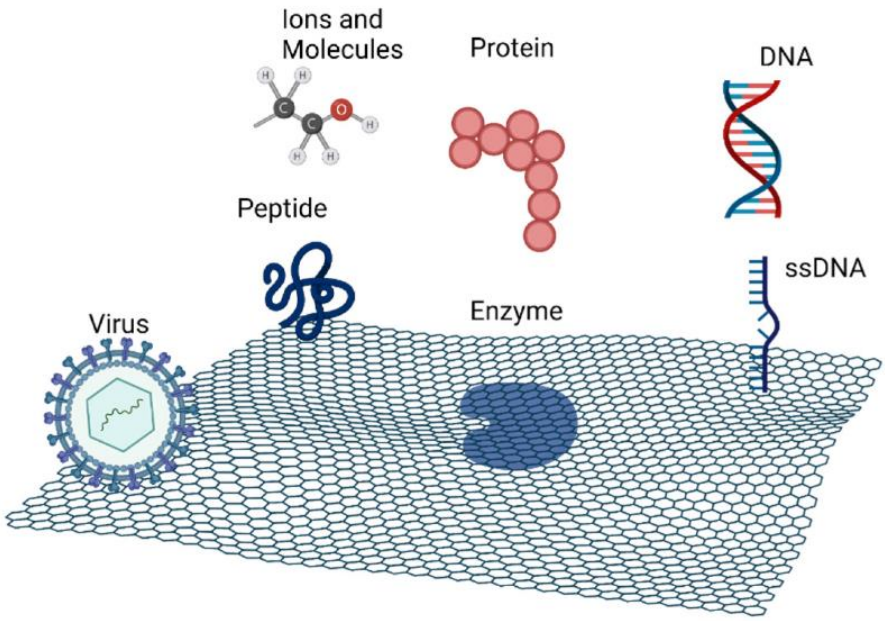

Figure 3.11: Representative bio-molecular systems interacting with graphene surfaces, illustrating adsorption-mediated interfacial interactions relevant to graphene-based biosensing applications. (Adapted from Ref.16)

In addition to adsorption orientation, atomistic simulations provide information regarding interfacial hydration structure, local ion organization, and heterogeneous surface interactions occurring near graphene interfaces. Such molecular-scale processes are difficult to resolve using continuum-level descriptions alone but may contribute significantly to sensing behaviour under electrolyte-gated conditions.

In the present work, atomistic adsorption analysis is employed primarily to support interpretation of electrostatic perturbations associated with biomolecular adsorption near the graphene interface. These molecular-level observations complement the continuum electrostatic simulations described previously and provide additional physical insight into the sensing mechanisms investigated experimentally in later chapters.

The complementary strengths of continuum and atomistic modelling approaches therefore motivate development of a multiscale framework capable of linking molecular-scale interactions with macroscopic device behaviour.

3.9 Multiscale Modelling Strategy

Electrolyte-gated graphene biosensors involve coupled physical phenomena occurring across multiple spatial scales. Continuum electrostatic models effectively describe macroscopic ionic transport, electric potential distributions, and carrier modulation within the device structure, whereas atomistic simulations provide molecular-level insight into adsorption behaviour and interfacial interactions occurring near the graphene surface. A multiscale modelling strategy is therefore required to connect these complementary physical descriptions.

In the framework developed in this work, continuum finite element simulations are employed to investigate electrostatic potential distributions and ionic transport behaviour within the electrolyte-gated GFET geometry. Atomistic adsorption analysis is additionally used to examine biomolecular interactions occurring near the graphene interface and to evaluate orientation-dependent electrostatic perturbations associated with adsorption processes.

The relationship between continuum and atomistic descriptions is illustrated schematically in Figure 3.12.

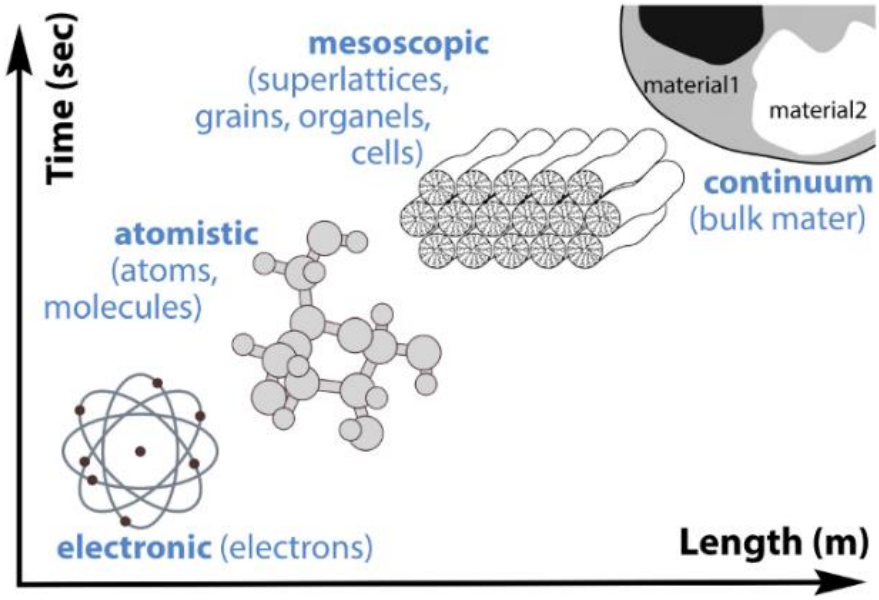

Figure 3.12: Multiscale modelling strategy integrating continuum electrostatic simulations with atomistic adsorption analysis for interpretation of electrolyte-gated graphene biosensing behaviour. (Taken from Ref.5)

Within this framework, continuum simulations provide macroscopic description of electrostatic modulation and electrolyte behaviour throughout the device domain, while atomistic simulations provide localized information regarding adsorption configurations and interfacial charge distributions near the graphene surface. Together, these approaches provide complementary physical interpretation of sensing mechanisms occurring within electrolyte-gated graphene biosensors.

The present multiscale framework does not involve fully self-consistent coupling between atomistic and continuum simulations. Instead, atomistic adsorption analysis is employed qualitatively to support interpretation of electrostatic perturbations and interfacial interactions observed experimentally and within continuum simulations. This approach significantly reduces computational complexity while maintaining physically meaningful interpretation of multiscale sensing behaviour.

The resulting modelling strategy therefore provides a physically consistent basis for interpretation of the experimental sensing behaviour investigated in the following chapters.

3.10 Model Parameters, Assumptions, and Limitations

Implementation of the multiscale modelling framework requires selection of appropriate physical parameters together with several simplifying assumptions necessary for computational feasibility. These assumptions influence the interpretation and applicability of the simulation results and should therefore be considered when analysing the modelling framework developed in this work.

Within the continuum framework, the electrolyte was treated as a homogeneous ionic medium with constant dielectric properties and isotropic ionic diffusion coefficients. Electrostatic and ionic transport behaviour were analysed under steady-state conditions, while fluid flow and transient electrochemical effects were neglected. The graphene channel was additionally represented using effective continuum electrostatic boundary conditions without explicit atomistic representation of the graphene lattice.

The atomistic adsorption analysis employed rigid-body representations of biomolecular structures and graphene surfaces, thereby neglecting large-scale conformational changes and explicit solvent

dynamics. Interfacial interactions were therefore interpreted primarily in terms of adsorption orientation and electrostatic perturbation behaviour rather than detailed molecular thermodynamics.

Furthermore, the multiscale framework developed in this work does not involve direct self-consistent coupling between atomistic and continuum simulations. Instead, continuum electrostatic simulations and atomistic adsorption analysis were used as complementary modelling approaches to provide physically consistent interpretation of experimentally observed sensing behaviour.

Despite these limitations, the combined continuum and atomistic framework provides important insight into electrostatic modulation, adsorption-induced perturbations, and multiscale sensing mechanisms governing electrolyte-gated graphene biosensors.

3.11 Summary of Chapter

This chapter established the theoretical and computational framework used throughout this thesis for investigation of electrolyte-gated graphene biosensors. Fundamental principles governing graphene transistor operation, electrolyte gating, and electric double-layer electrostatics were first introduced, followed by presentation of the governing continuum equations describing coupled electrostatic and ionic transport behaviour.

A finite element modelling framework implemented in COMSOL Multiphysics was subsequently presented for simulation of electrostatic potential distributions and ionic transport processes within electrolyte-gated GFET structures. Atomistic modelling approaches relevant to biomolecular adsorption and interfacial interactions near graphene surfaces were additionally discussed together with their application to graphene biosensing systems.

Finally, a multiscale modelling strategy integrating continuum electrostatic simulations with atomistic adsorption analysis was presented to provide physically consistent interpretation of electrolyte-gated graphene biosensing behaviour. The modelling framework developed in this chapter forms the basis for the simulation and experimental studies presented in the following chapters.

3.12 References

1. Bard, A. J., Faulkner, L. R., & White, H. S. (2022). *Electrochemical Methods: Fundamentals and Applications*. John Wiley & Sons.
2. Newman, J., & Thomas-Alyea, K. E. (2004). *Electrochemical Systems* (3rd ed.). Wiley.
3. Israelachvili, J. N. (2011). *Intermolecular and Surface Forces* (3rd ed.). Academic Press.
4. Frenkel, D., & Smit, B. (2002). *Understanding Molecular Simulation: From Algorithms to Applications* (2nd ed.). Academic Press.
5. Verkhovtsev, A. V., Solov'yov, I. A., & Solov'yov, A. V. (2021). Advances in multiscale modeling for novel and emerging technologies. *The European Physical Journal D, 75*(7), 207.
6. Castro Neto, A. H., Guinea, F., Peres, N. M. R., Novoselov, K. S., & Geim, A. K. (2009). The electronic properties of graphene. *Reviews of Modern Physics, 81*(1), 109–162.
7. Geim, A. K., & Novoselov, K. S. (2007). The rise of graphene. *Nature Materials, 6*(3), 183–191.
8. Schwierz, F. (2010). Graphene transistors. *Nature Nanotechnology, 5*(7), 487–496.
9. Das Sarma, S., Adam, S., Hwang, E. H., & Rossi, E. (2011). Electronic transport in two-dimensional graphene. *Reviews of Modern Physics, 83*(2), 407–470.
10. Novoselov, K. S., Geim, A. K., Morozov, S. V., Jiang, D., Zhang, Y., Dubonos, S. V., Grigorieva, I. V., & Firsov, A. A. (2004). Electric field effect in atomically thin carbon films. *Science, 306*(5696), 666–669.
11. Ohno, Y., Maehashi, K., Yamashiro, Y., & Matsumoto, K. (2009). Electrolyte-gated graphene field-effect transistors for detecting pH and protein adsorption. *Nano Letters, 9*(9), 3318–3322.
12. Revil, A., Jardani, A., Sava, P., & Haas, A. (2015). The seismoelectric method.
13. Chen, S., & Bashir, R. (2023). Advances in field-effect biosensors towards point-of-use. Nanotechnology, 34(49), 492002.
14. Baridi, G., Liaquat, A., Martini, L., Rapuzzi, F., Clericò, V., Amado, M., Diez, E., Abidi, E. H., Maschio, M. C., Corni, S., Meziani, Y. M., Brancolini, G., Rossella, F., & Rovati, L. (2026). Computational Simulation of a Surface Plasmonic Resonance Biosensor for β2-

Microglobulin Based on Electrolyte-Gated Graphene. *Sensors*, *26*(9), 2815. https://doi.org/10.3390/s26092815

15. Baridi, G., Liaquat, A., Martini, L., Rapuzzi, F., Clericò, V., Amado, M., Diez, E., Abidi, E. H., Maschio, M. C., Corni, S., Meziani, Y. M., Brancolini, G., Rossella, F., & Rovati, L. (2026). Multiscale Molecular Dynamics and Quantum–Electrostatic Modelling of Graphene Electric Double-Layer Transistors for β2-Microglobulin Biosensing, Electronics (Under Review)
16. Machado, M., Oliveira, A. M. L., Silva, G. A., Bitoque, D. B., Tavares Ferreira, J., Pinto, L. A., & Ferreira, Q. (2022). Graphene Biosensors—A Molecular Approach. *Nanomaterials*, *12*(10), 1624. https://doi.org/10.3390/nano12101624

Chapter 4

Electrolyte-Gated Graphene Transistors for pH Sensing: Modelling and Experimental Validation

4.1 Introduction

Electrolyte-gated graphene field-effect transistors (GFETs) provide a highly sensitive platform for probing interfacial electrostatic phenomena in aqueous environments, owing to the combination of graphene's high carrier mobility and efficient electrostatic coupling through the electric double layer (EDL) [1,2]. In these devices, the gate voltage is applied through an electrolyte, and the resulting redistribution of ions at the graphene-electrolyte interface leads to strong modulation of the carrier density in the graphene channel. This mechanism enables low-voltage operation, making GFETs particularly suitable for chemical and biological sensing applications [3]

Among various sensing modalities, pH sensing serves as a well-defined model system for investigating the response of electrolyte-gated devices. Variations in pH alter the concentration of protons (H^+) in solution, which influences the surface charge environment at the graphene interface through protonation and deprotonation. These changes modify the local electrostatic potential and are reflected in the device's electrical characteristics, typically observed as a shift in the Dirac point in transfer measurements [4].Due to its direct connection to interfacial charge regulation, pH sensing provides a controlled framework for analyzing electrostatic modulation mechanisms in GFETs.

In practical implementations, pH measurements are commonly performed in buffered electrolytes such as phosphate buffered saline (PBS), which contain a significant concentration of mobile ions, predominantly sodium (Na^+) and chloride (Cl^-). While pH determines the chemical state of the interface, the ionic strength of the electrolyte governs the extent of electrostatic screening through the Debye length [5]. As a result, the observed device response arises from the interplay between pH-induced surface charge modulation and electrostatic screening governed by the ionic environment [5,6]. This coupling is critical for interpreting sensing behaviour, particularly under conditions where high ionic strength can suppress sensitivity by reducing the effective gating field.

To describe these effects quantitatively, a continuum modelling framework based on electrostatics and ion transport is employed. As part of this study, a finite-element-based approach is developed to model electrolyte-gated GFETs by solving the coupled Poisson and Nernst-Planck equations, enabling the analysis of ion redistribution, electric potential profiles, and their influence on device characteristics [6]. This framework captures key features of the EDL and provides insight into how ionic concentration affects charge modulation in the graphene channel. The modelling component provides a theoretical basis for interpreting the experimental observations presented in this chapter.

In the present chapter, this modeling framework is first used to analyze electrolyte-induced modulation in GFETs, with particular emphasis on ion distributions and electrostatic potentials. The model is then extended to pH-dependent conditions by considering variations in the effective ionic environment. Subsequently, experimental measurements performed in PBS solutions are presented, and the resulting device characteristics are examined against the modeling predictions.

4.2 Modelling Framework

A quantitative understanding of electrolyte-gated graphene field-effect transistors requires a self consistent description of electrostatic potential and ionic transport in the electrolyte. In this work, a continuum modelling framework is employed to capture the interaction between mobile ions in the electrolyte and charge carriers in the graphene channel. The approach is based on the coupled solution of Poisson's equation and the Nernst-Planck equation, enabling the analysis of electric double layer formation and its influence on device characteristics [6-8]

A finite element-based modeling approach is utilized in this study to simulate electrolyte-gated GFET behavior under varying ionic conditions. The model considers a graphene channel in contact with an aqueous electrolyte containing monovalent ions, and describes the spatial distribution of electric potential and ion concentration in response to an applied gate bias [6]. This framework provides a physically consistent method for linking ion redistribution at the interface to measurable electrical responses of the device.

4.2.1 Device Geometry and Physical Representation

The simulated structure consists of a graphene channel interfaced with an electrolyte domain and contacted by source and drain electrodes. A gate electrode is introduced within the electrolyte to apply an external potential, establishing an electric field across the graphene-electrolyte interface. The graphene layer is treated as a two-dimensional conductive sheet, while the electrolyte is modelled as a continuous medium containing mobile ionic species.

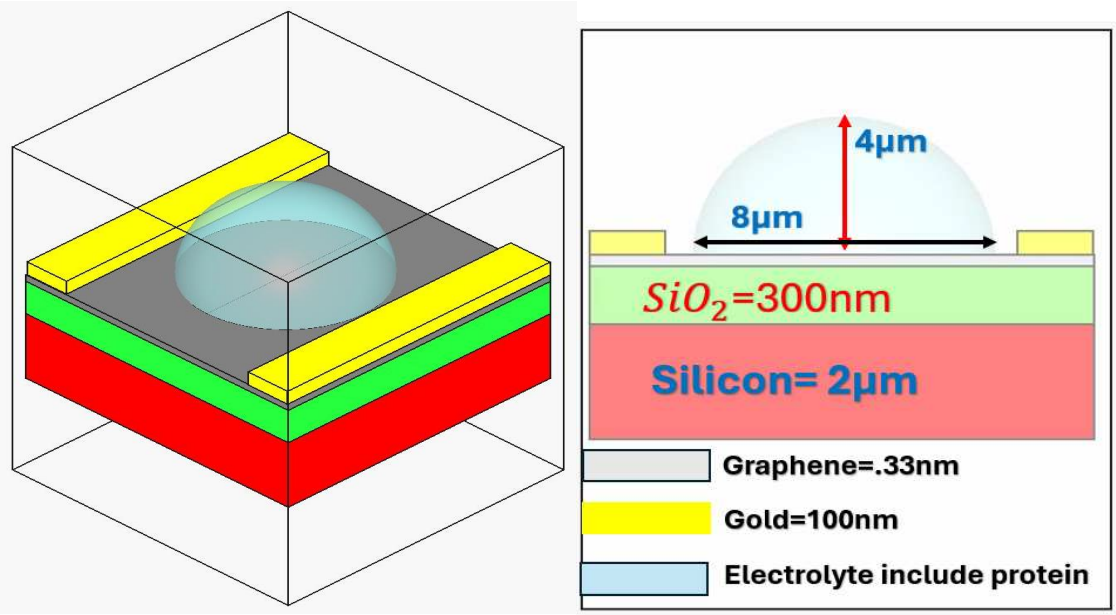

Figure 4.1: Two-dimensional and three-dimensional schematic representation of the electrolyte-gated graphene field-effect transistor geometry used in the modelling framework.

As illustrated in Figure 4.1, the computational domain is defined to capture both the interfacial region, where strong electric field gradients exist, and the bulk electrolyte, where ion concentrations approach equilibrium values. The thickness of the electrolyte region is selected to ensure that bulk behaviour is recovered away from the interface, while maintaining sufficient resolution of the electric double layer.

4.2.2 Governing Equations

The electrostatic potential within the system is described by Poisson's equation:

$$\nabla\cdot(\varepsilon\nabla\phi)=-\rho$$

Where ε is the dielectric permittivity, ϕ is the electric potential, and ρ is the local charge density arising from mobile ions in the electrolyte [7,8].

The transport of ionic species is governed by the Nernst-Planck equation, which accounts for both diffusion and electromigration:

$$J_i = -D_i \nabla c_i - \mu_i z_i c_i \nabla \phi$$

Where Ji is the flux of species i, Di is the diffusion coefficient, ci is the concentration, zi is the ionic valence, and μ_i is the mobility of the ion [7].

The coupling between these equations enables a self-consistent description of ion redistribution and electric field formation near the graphene surface, which is essential for modelling the electric double layer.

4.2.3 Boundary Conditions and Electrostatic Coupling

Appropriate boundary conditions are applied to represent device operation under electrolyte gating. A fixed potential is imposed at the gate electrode, while the source and drain contacts define the electrical bias across the graphene channel. At the outer boundaries of the electrolyte, bulk ion concentrations are specified to maintain equilibrium conditions.

At the graphene-electrolyte interface, the electrostatic coupling between the ionic charge in the electrolyte and the charge carriers in graphene is represented through a surface boundary condition. The accumulation of counter-ions near the graphene surface leads to the formation of the electric double layer, which acts as an effective gate dielectric with high capacitance [5,7,9].

4.2.4 Finite Element Implementation

The coupled system of equations is solved numerically using the finite element method. The model is implemented in a multiphysics simulation environment, where electrostatics and ion transport are solved simultaneously in a self-consistent manner. Spatial discretization is performed using a non-uniform mesh, with refined elements near the graphene-electrolyte interface to capture steep gradients in potential and ion concentration.

A stationary solver is employed to obtain steady state solutions corresponding to equilibrium ion distributions under applied bias conditions. The numerical implementation allows for systematic variation of parameters such as ion concentration, applied voltage, and electrolyte properties, providing insight into their impact on device behaviour [8].

4.2.5 Modelling Assumptions and Scope

To ensure computational tractability, several simplifying assumptions are adopted. The electrolyte is treated as an ideal solution containing monovalent ions, and ion–ion interactions beyond electrostatic effects are neglected. The system is assumed to be isothermal, and fluid flow within the electrolyte is not considered. Additionally, specific adsorption of ions and molecular-scale interactions at the graphene surface are not explicitly included.

Despite these simplifications, the model captures the dominant electrostatic mechanisms governing electrolyte gating and provides a reliable framework for interpreting experimental observations. The approach is particularly suitable for analyzing the influence of ionic strength and electric double layer formation on the electrical response of GFET devices. This modeling framework provides qualitative and quantitative insights into the electrostatic processes governing device operation and supports the interpretation of experimental results.

4.3 Electric Double Layer and Ion Transport

The electrical response of electrolyte-gated graphene transistors is governed by the redistribution of ions at the graphene–electrolyte interface, leading to the formation of the electric double layer (EDL). When a gate potential is applied through the electrolyte, mobile ions migrate under the influence of the electric field, resulting in a non-uniform charge distribution near the graphene surface. This interfacial charge accumulation establishes a strong local electric field that modulates the carrier density within the graphene channel [6,7].

4.3.1 Ion Distribution near the Graphene Interface

Under electrolyte gating conditions, positively charged ions (e.g., Na^+ in PBS) are attracted toward the graphene surface when a negative potential is applied, while negatively charged ions (e.g., Cl^-) are repelled. This selective accumulation of counter-ions and depletion of co-ions leads to the

formation of a charge layer adjacent to the graphene surface. The resulting ion distribution is not uniform but decays gradually into the bulk electrolyte, reflecting the balance between electrostatic forces and thermal motion [7,9]

Within the modelling framework employed in this study, this behaviour is captured through the coupled solution of the Poisson and Nernst–Planck equations, which describe the spatial variation of ion concentration in response to the applied potential [6]. The resulting ion profiles provide direct insight into the structure of the electric double layer and its dependence on electrolyte properties.

4.3.2 Structure of the Electric Double Layer

The electric double layer formed at the graphene-electrolyte interface consists of two distinct regions: a compact layer near the surface, often referred to as the Stern layer, and a diffuse region extending into the electrolyte, where ion concentration gradually approaches bulk values. The Stern layer accounts for ions that are strongly bound or specifically adsorbed near the surface, while the diffuse layer arises from thermally distributed ions governed by electrostatic interactions [9,10].

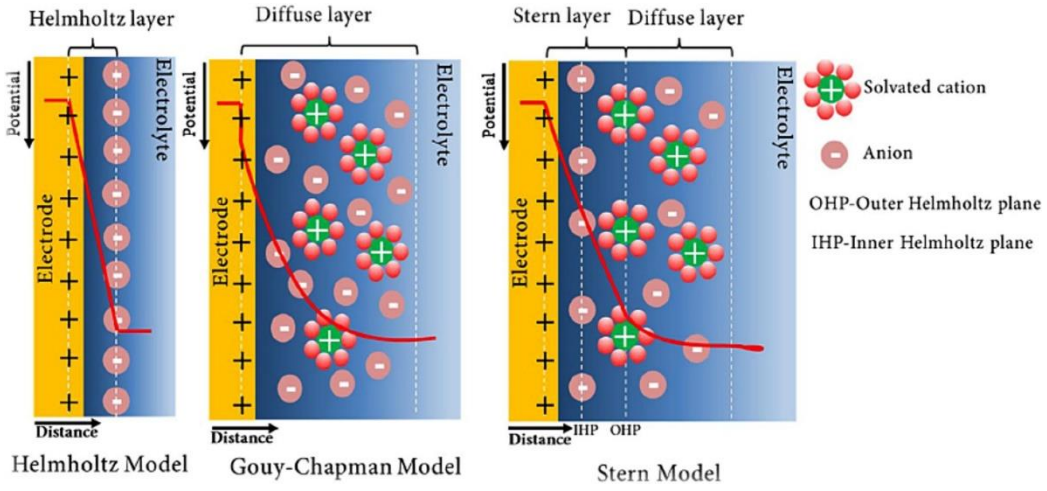

Figure 4.2: Schematic illustration of electric double-layer formation at the graphene–electrolyte interface based on compact and diffuse layer models.

The effective capacitance associated with the electric double layer is significantly higher than that of conventional solid dielectrics, enabling strong electrostatic coupling between the electrolyte and

the graphene channel. This high capacitance plays a central role in determining the sensitivity of electrolyte-gated devices, as small changes in interfacial charge can lead to substantial modulation of carrier density.

4.3.3 Influence of Ionic Strength and Debye Screening

The extent of ion redistribution in the electrolyte is governed by the Debye screening length, which defines the characteristic distance over which electric fields are screened by mobile ions. In electrolytes with high ionic strength, such as PBS, the Debye length is relatively short, leading to strong screening of the electric field. As a result, the electric double layer is confined to a narrow region near the graphene surface.

This screening effect has important implications for device performance. While a high ionic concentration enhances the capacitance of the electric double layer, it also reduces the effective range over which electrostatic modulation can occur. Consequently, the sensitivity of the device to changes in surface charge, such as those induced by pH variation, may be reduced under high ionic strength conditions [5,6].

4.3.4 Implications for GFET Operation

The formation of the electric double layer directly influences the electrical characteristics of the graphene transistor. The accumulation of counter-ions near the graphene surface induces an equal and opposite charge in the graphene channel, leading to modulation of the Fermi level and a shift in the Dirac point. The magnitude and direction of this shift depend on the applied gate potential, ion concentration, and surface charge conditions.

In the context of pH sensing, variations in proton concentration modify the interfacial charge environment, which in turn alters the structure of the electric double layer. This results in measurable changes in the transfer characteristics of the device. The combined influence of pH-induced surface charge and electrolyte screening therefore determines the overall sensing response, providing a direct link between interfacial electrochemistry and device-level electrical behaviour.

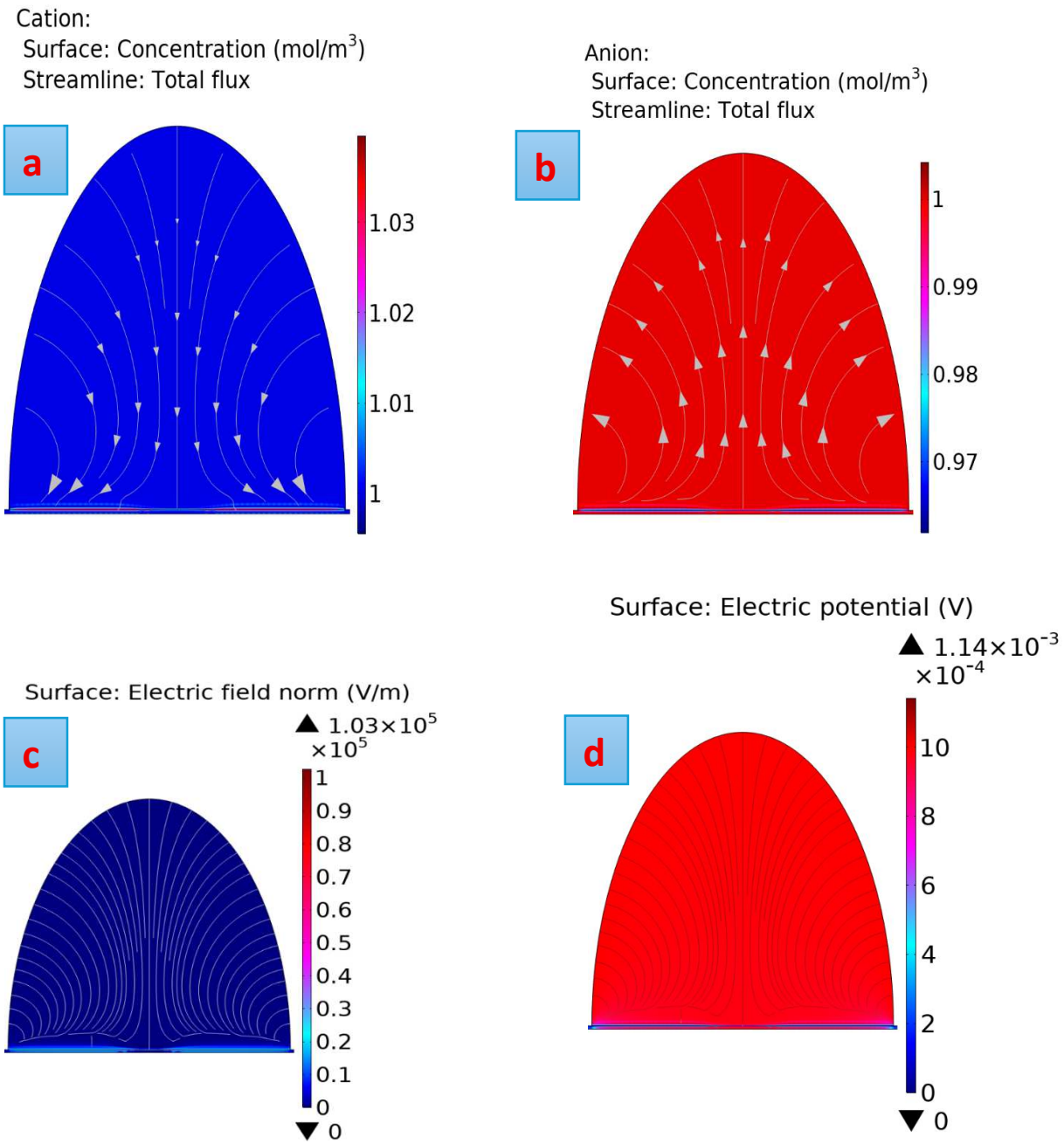

Figure 4.3: Simulated electric field and electrostatic potential distributions near the graphene–electrolyte interface during electric double-layer formation.

4.4 Modelling Results: Electrolyte Effects

The modelling framework described in the previous section is used to investigate the influence of electrolyte properties on the electrical behavior of graphene field-effect transistors, providing insight into the underlying electrostatic mechanisms. In particular, the spatial distribution of electric potential, ion concentration, and their impact on device characteristics are examined under

varying ionic conditions. The results provide insight into how electrolyte-induced charge redistribution governs the electrostatic modulation of the graphene channel.

4.4.1 Electrostatic Potential Distribution

The application of a gate potential through the electrolyte leads to the formation of a non-uniform electric potential profile across the graphene-electrolyte interface. As ions redistribute in response to the applied field, a strong potential gradient develops within the electric double layer region, while the potential remains nearly constant in the bulk electrolyte.

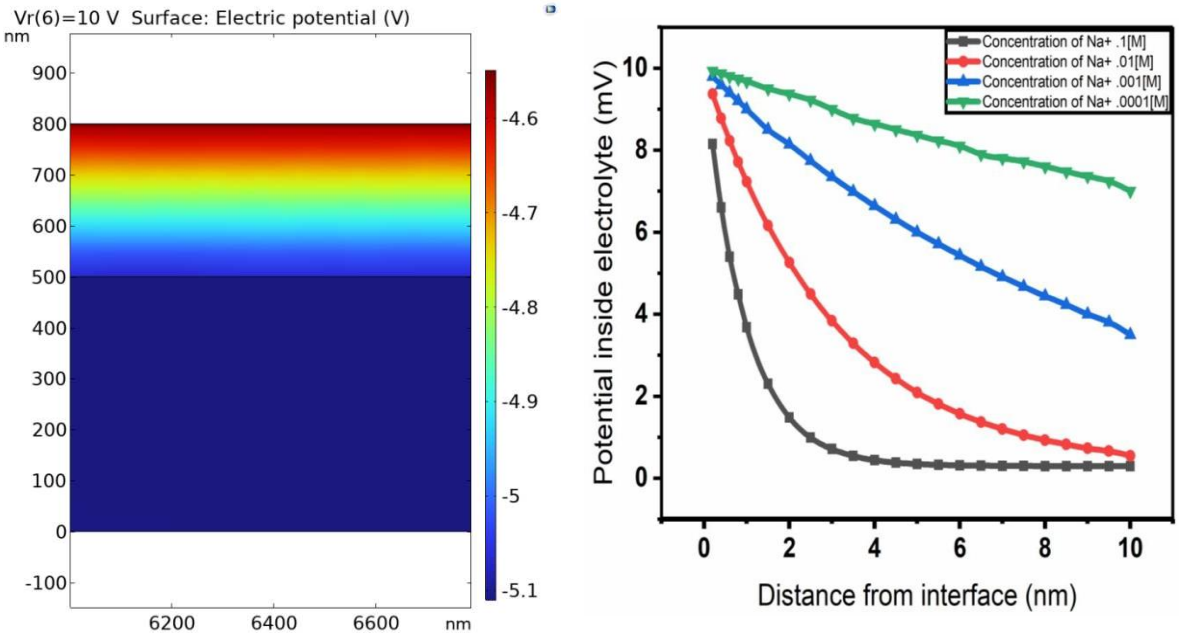

Figure 4.4: Simulated electrostatic potential distribution illustrating exponential decay of the electric field away from the graphene–electrolyte interface.

As shown in figure 4.4, the potential decreases rapidly within a short distance from the graphene surface, reflecting the strong screening effect of mobile ions. This behavior is consistent with the formation of a compact electric double layer, in which the majority of the potential drop occurs within the interfacial region [5,9].

The extent of this potential variation depends on the electrolyte's ionic concentration. Higher ionic strength results in a steeper potential gradient and a more confined electric field due to a reduced Debye length. This directly influences the efficiency of electrostatic gating in the device.

4.4.2 Electrical Characteristics under Electrolyte Gating

The redistribution of ions in the electrolyte directly affects the electrical response of the graphene channel. The accumulation of counter-ions near the graphene surface induces an electrostatic field that shifts the carrier concentration, leading to modulation of the device resistance.

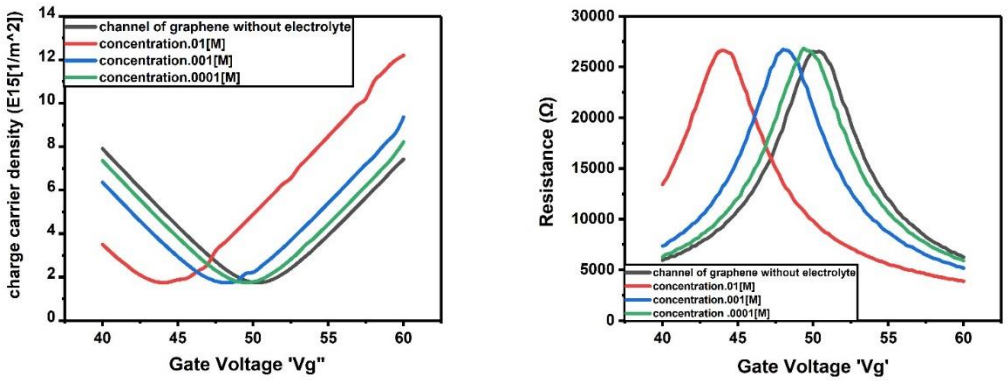

Figure 4.5: Simulated variation of graphene charge carrier density and channel resistance as a function of applied gate voltage under electrolyte-gated conditions.

The simulated transfer characteristics, shown in figure 4.5, exhibit a characteristic peak corresponding to the charge neutrality point (Dirac point). As the ionic environment changes, this peak shifts along the gate voltage axis, reflecting variations in the effective gating field [6].

This behaviour demonstrates that electrolyte gating can effectively tune the electronic properties of graphene through ion-induced electrostatic coupling, without the need for a conventional dielectric layer.

4.4.3 Influence of Ionic Strength

The ionic strength of the electrolyte plays a critical role in determining both the structure of the electric double layer and the resulting device response. As the ion concentration increases, the Debye screening length decreases, leading to a more localized electric field near the graphene surface.

This effect is reflected in the simulated characteristics, where higher ionic concentrations result in sharper potential gradients but reduced sensitivity to changes in surface charge. The enhanced

screening limits the effective range of electrostatic modulation, thereby influencing the magnitude of the Dirac point shift [5].

These results highlight the dual role of ionic strength: while it enhances the capacitance of the electric double layer, it also reduces the device's sensitivity to external perturbations.

4.4.4 Effect of Quantum Capacitance

In addition to the classical electric double-layer capacitance, the quantum capacitance of graphene plays a significant role in determining the overall electrostatic response of the device. Due to the low density of states near the Dirac point, graphene exhibits a finite quantum capacitance that must be considered in series with the EDL capacitace.

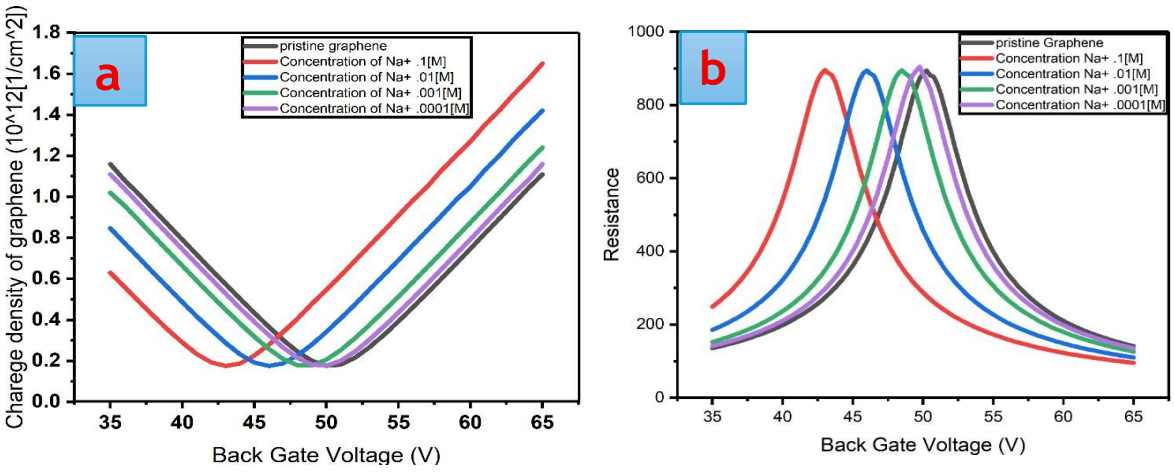

Figure 4.6: Influence of graphene quantum capacitance on (a) charge carrier concentration and (b) channel resistance calculated using the Stern model of the electric double layer

The inclusion of quantum capacitance in the model leads to a modification of the effective gating behaviour, as illustrated in Figure 4.6. In particular, it results in the device's enhanced sensitivity to changes in the electrostatic environment, especially near the charge neutrality point [11,12,13].

4.4.5 Sensitivity Analysis

The device's sensitivity is evaluated by quantifying the shift in the Dirac point as a function of changes in the ionic environment. The model predicts that sensitivity depends strongly on both the electric double-layer capacitance and the quantum capacitance of graphene.

As reported in our work, the inclusion of quantum capacitance leads to a significant enhancement in sensitivity, with higher values observed under conditions where the electrostatic coupling between the electrolyte and graphene is maximized [6].

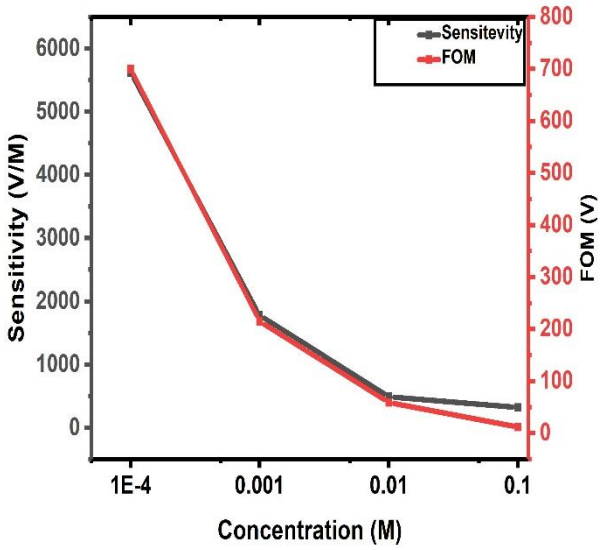

Figure 4.7: Sensitivity and figure of merit (FOM) calculated using the Stern-layer electric double-layer model as a function of electrolyte concentration.

These results establish a direct relationship between electrolyte properties, interfacial electrostatics, and device performance, providing a theoretical basis for interpreting experimental observations. These results provide a reference framework for understanding the influence of electrolyte properties, which will be examined experimentally in subsequent sections. The sensitivity trends observed in the modelling provide a reference for evaluating experimental device performance under varying pH conditions.

4.5 Extension to pH-Based Modelling

The modelling framework is extended here to examine pH-dependent behaviour by considering variations in proton concentration within the electrolyte. The fundamental role of electrolyte-induced charge redistribution in governing the electrical response of graphene field-effect transistors remains central to this analysis. While the framework is developed for monovalent ions

such as Na^+, the same electrostatic principles can be extended to systems in which the ionic environment is modified by varying pH. In such cases, changes in proton concentration introduce additional modulation of the interfacial charge distribution, thereby influencing the device characteristics.

4.5.1 Simulation of pH-Dependent Transfer Characteristics

To investigate the effect of pH on device behaviour, the modelling framework is extended by considering variations in the effective ionic environment associated with proton concentration. Changes in pH correspond to changes in the concentration of H^+ ions, which contribute to the overall charge balance in the electrolyte and modify the structure of the electric double layer [3,4].

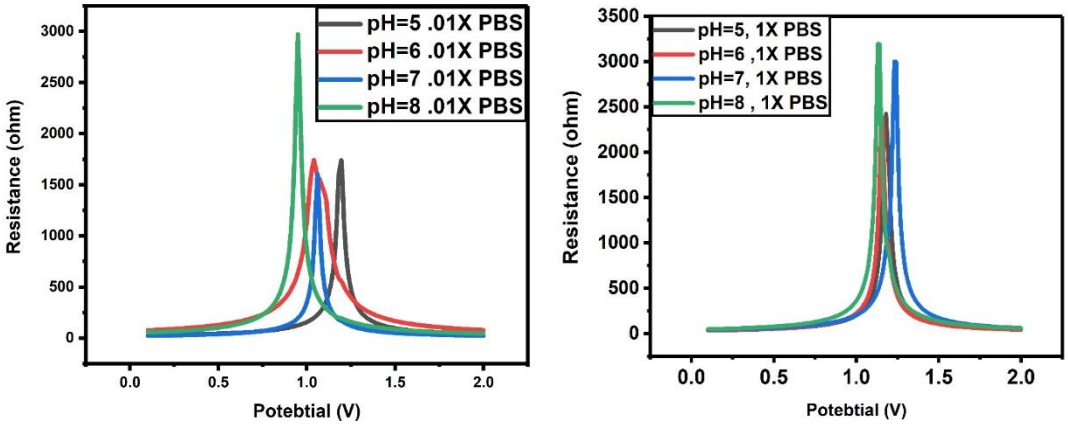

Figure 4.8: Simulated transfer characteristics showing graphene channel resistance as a function of gate voltage for 0.01× PBS and 1× PBS under varying pH conditions

The simulated transfer characteristics under different pH conditions are shown in figure 4.8. The results demonstrate a systematic shift in the position of the resistance peak with pH, indicating modulation of the charge neutrality point. This shift reflects changes in the interfacial electrostatic potential arising from variations in proton concentration. This extension provides a qualitative understanding of pH-induced modulation, which is further validated through experimental measurements.

4.5.2 Influence of Electrolyte Strength

In addition to pH variation, the ionic strength of the electrolyte significantly influences the magnitude of the device response. This effect is particularly evident when comparing simulations

performed under different electrolyte concentrations, such as diluted and standard phosphate-buffered saline (PBS) conditions.Lower ionic strength results in a broader electric double layer and reduced screening, allowing the electric field to penetrate further into the electrolyte. This enhances the device's sensitivity to changes in surface charge. Conversely, higher ionic strength leads to stronger screening and a more confined electric double layer, which reduces the effective modulation of the graphene channel [5,6].

4.5.3 Interpretation of pH-Induced Modulation

The observed shift in the transfer characteristics can be understood in terms of changes in the interfacial charge environment. At lower pH values, the higher proton concentration increases the positive charge near the graphene surface, shifting the Dirac point in one direction. As the pH increases, the reduction in proton concentration alters the charge balance, leading to a corresponding shift in the opposite direction.

This behavior is consistent with the general electrostatic framework established in Section 4.4, in which ion accumulation and depletion govern the modulation of the graphene channel. In this context, protons act as additional mobile charge carriers that influence the electric double layer structure and modify the effective gating field.

4.5.4 Unified Electrolyte Modulation Mechanism

The results presented in this section demonstrate that pH-induced modulation can be interpreted within the same electrostatic framework used to describe ion-driven effects. While Na^+ ions primarily determine the ionic strength and screening behaviour of the electrolyte, H^+ ions introduce a variable component that directly affects the interfacial charge distribution.

Consequently, the overall device response arises from the combined influence of ionic screening and surface charge modulation. This unified perspective provides a consistent basis for understanding both the modelling results and the experimental observations presented in subsequent sections. While the modelling framework captures the primary electrostatic mechanisms governing electrolyte gating, experimental validation is necessary to evaluate the behaviour of practical devices under realistic electrolyte conditions.

4.6 Experimental Methodology

The experimental investigation was carried out to evaluate the pH-sensing performance of electrolyte-gated graphene field-effect transistors under controlled electrolyte conditions. The measurements were designed to systematically examine the electrical response of the devices as a function of pH variation in phosphate-buffered saline (PBS), providing a direct basis for comparison with the modelling framework developed in the preceding sections.

4.6.1 Device Preparation and Cleaning

Prior to measurements, the graphene devices were subjected to a controlled cleaning protocol to ensure surface stability and reproducibility. The mGFET chips were first thermally treated on a hot plate at 110^{o}C for 3 minutes to remove adsorbed moisture and contaminants.

Subsequently, the devices were cleaned using a solvent-based process. The chips were immersed in thermally stabilized acetone at 60^{o}C for to remove organic residues, followed by rinsing in isopropanol under similar conditions to eliminate residual contaminants. The devices were then dried using a nitrogen gun to prevent the presence of liquid residues on the graphene surface.

This preparation step ensures a clean graphene interface, which is essential for reliable electrolyte interaction and stable electrical measurements.

4.6.2 Electrolyte Preparation and pH Control

Phosphate-buffered saline (PBS) solutions were prepared as the electrolyte medium due to their stability and relevance for biological sensing applications. A standard 1XPBS solution was prepared by dissolving sodium chloride (NaCl), potassium chloride (KCl), disodium hydrogen phosphate, and potassium dihydrogen phosphate in distilled water, followed by adjustment of the final volume.

The pH of the solution was controlled within the desired range by the addition of hydrochloric acid (HCl) to lower the pH or sodium hydroxide (NaOH) to increase it. The pH values were verified using a calibrated pH meter.

In addition to the standard solution, a 0.01×PBS (dilluted) solution was prepared to investigate the effect of reduced ionic strength. The dilution was carried out by proportionally reducing the concentration of all constituents while maintaining the same chemical composition.

4.6.3 Measurement Configuration

Electrical measurements were performed using a probe station integrated with a precision source-measurement unit (Keithley Source-meter 2612B). The graphene devices were electrically contacted through micromanipulated probes connected to the source and drain electrodes.

A controlled volume (**5 µL**) of the PBS solution was deposited onto the graphene channel using a calibrated micropipette, ensuring uniform coverage of the active sensing area. The device was then inserted into the measurement platform (Graphenea card), and the electrolyte droplet acted as the gating medium.

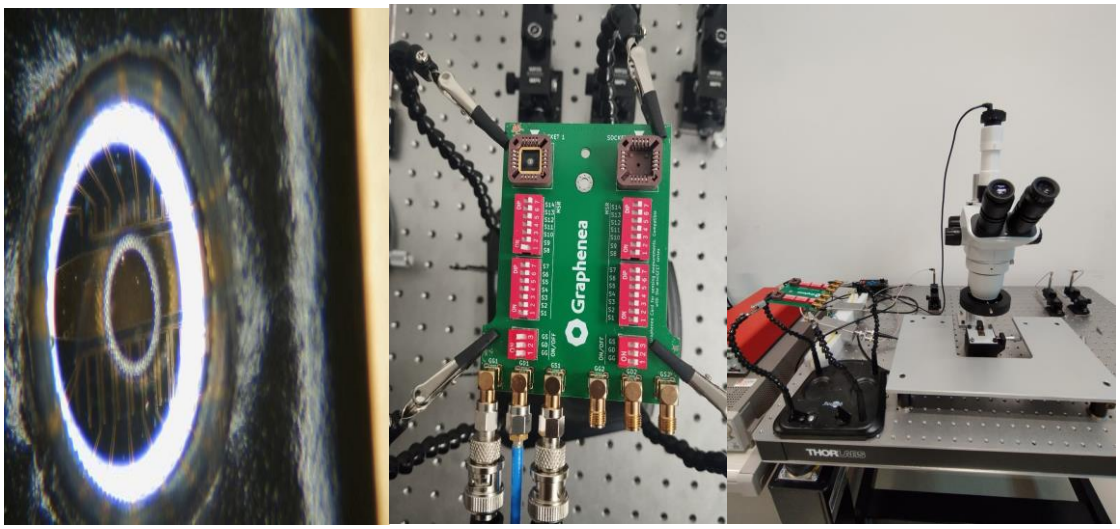

Figure 4.9: Experimental measurement setup used for electrical transport characterization of electrolyte-gated graphene transistors in phosphate-buffered saline solutions.

As illustrated in Figure 4.9, the electrolyte establishes a liquid-gated configuration, enabling modulation of the graphene channel through the electric double layer formed at the graphene-electrolyte interface.

4.6.4 Measurement Protocol and Electrical Conditions

After application of the electrolyte droplet, the system was allowed to stabilize to ensure proper interaction between the graphene surface and the ionic solution. During this process, a gate leakage current was observed, which is characteristic of electrolyte-gated devices.

To ensure stable measurements, the drain bias voltage was set at different fixed values 20mV, 50mV, 100mV and 200 mV during measurements, resulting in a measurable drain current in the micro-ampere (μA) range while maintaining the gate current in the nano-ampere (nA) range. As the electrolyte droplet equilibrated on the graphene surface, the gate leakage current decreased, indicating improved stability of the device response.

Transfer characteristics were obtained by sweeping the gate voltage over a range of 0 to 1 V, beyond which increased gate leakage effects were observed. This voltage window ensured reliable operation while minimizing measurement artefacts.

4.6.5 Measurement Sequence and Data Acquisition

Measurements were performed sequentially for different pH conditions, with intermediate cleaning and stabilization steps to avoid cross-contamination between solutions. For each condition, the drain current was recorded as a function of gate voltage to generate output curves (IV) and transfer curves.

Multiple measurement cycles were conducted to assess repeatability and consistency of the device response. The stabilization time after droplet placement was carefully controlled to ensure reproducible electric double-layer formation and steady-state behavior.

4.6.6 Data Analysis and Parameter Extraction

The measured transfer characteristics were analyzed to extract key sensing parameters. The position of the Dirac point was identified from the maximum resistance in the transfer curve, and its shift was evaluated as a function of pH.

The sensitivity of the device was determined by calculating the change in Dirac voltage per unit change in pH (mV/pH). Additional parameters, including curve symmetry and minimum conductivity, were examined to assess the influence of electrolyte conditions on device performance. These extracted parameters provide the basis for comparison with the modelling results and enable a systematic assessment of the sensing performance of the devices.

4.7 Experimental Results

The electrical response of electrolyte-gated graphene field-effect transistors was investigated under varying pH conditions using phosphate-buffered saline (PBS) solutions. The results are presented in a structured manner, beginning with a controlled study over a limited pH range, followed by extended measurements covering a broader pH range. This approach enables a systematic understanding of the sensing mechanism and its practical performance.

4.7.1 Controlled pH Study: Electrical Characteristics of GFET under pH Variation (pH 5–8)

(a) Output Characteristics (IV Behaviour)

The output characteristics of the graphene field-effect transistor were examined by measuring the drain current I_{ds} as a function of drain voltage V_{ds} at a fixed gate voltage (Vg=0) in 1x PBS under different pH conditions.

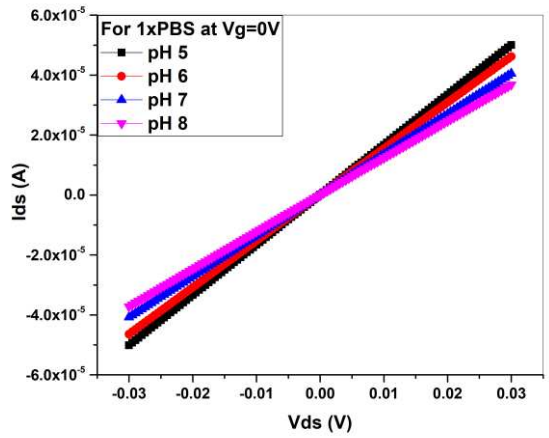

Figure 4.10: Output current–voltage (I–V) characteristics of the electrolyte-gated GFET measured in 1× PBS for pH values ranging from 5 to 8 at Vg = 0 V.

The measured IV curves exhibit a linear dependence of current on voltage across the entire bias range (−0.03 V to +0.03 V), indicating ohmic conduction between the graphene channel and the metal contacts. The curves are symmetric about the origin, confirming uniform charge transport under both positive and negative bias.

A systematic variation in slope is observed with pH. The current magnitude is highest at pH 5 and decreases progressively towards pH 8, indicating an increase in channel resistance with increasing pH. Despite this variation in slope, the overall shape of the curves remains unchanged, suggesting that the fundamental conduction mechanism is not altered.

(b) Transfer Characteristics (Resistance-Gate Voltage Behaviour)

To establish the fundamental sensing behaviour, transfer characteristics were measured over a pH range of 5 to 8 using both 0.01× PBS and 1× PBS solutions. This controlled comparison allows direct evaluation of the influence of ionic strength on device response.

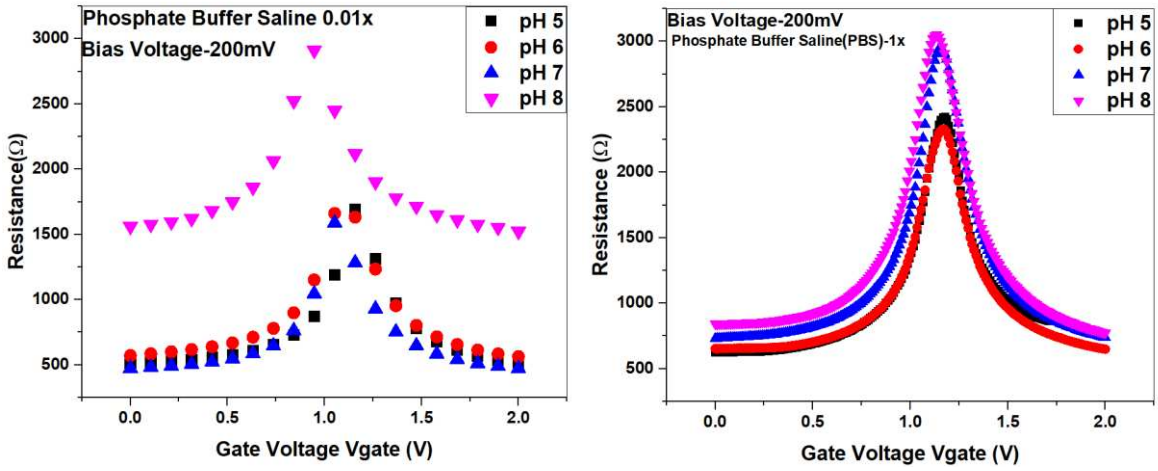

Figure 4.11: Experimental transfer characteristics of electrolyte-gated GFETs measured in 0.01× PBS and 1× PBS under varying pH conditions.

The transfer characteristics measured in 0.01× PBS and 1× PBS show the typical ambipolar behaviour of graphene, with a distinct resistance peak corresponding to the Dirac point.

For the 0.01× PBS solution, the resistance peak is clearly defined and exhibits a systematic shift towards lower gate voltages with increasing pH. The peaks are relatively sharp and maintain a consistent shape across the pH range, indicating efficient electrostatic modulation under reduced ionic screening conditions.

In contrast, the transfer curves in 1× PBS display broader peaks with reduced separation between different pH conditions. The increased width of the peaks and their partial overlap suggest that the electrostatic modulation of the graphene channel is suppressed due to strong ionic screening [5,6].

A notable observation is the increase in peak resistance with increasing pH, particularly in the 1× PBS case, where the peak height becomes significantly larger at higher pH values. This indicates that both the position and magnitude of the Dirac point are influenced by the electrolyte conditions. The symmetry of the curves around the peak remains largely preserved in both cases, although slight deviations are observed at higher ionic strength, suggesting the presence of additional interfacial effects

The extracted Dirac voltages for the 0.01× PBS solution show a consistent decrease from approximately 1.16 V at pH 5 to 0.95 V at pH 8, corresponding to a total shift of ~200 mV. In comparison, the variation in 1× PBS is much smaller and exhibits reduced linearity.

These results confirm that the sensitivity of the GFET is strongly dependent on the ionic strength of the electrolyte, consistent with the electrostatic screening effects described in Section 4.3 and predicted by the modelling results in Section 4.4.

4.7.2 Dirac Point Shift-Controlled Study (pH 5–8)

The position of the Dirac point was extracted from the transfer characteristics as the gate voltage corresponding to the maximum resistance. The variation of this voltage with pH was examined for both **0.01× PBS** and **1× PBS** to evaluate the effect of ionic strength under controlled conditions.

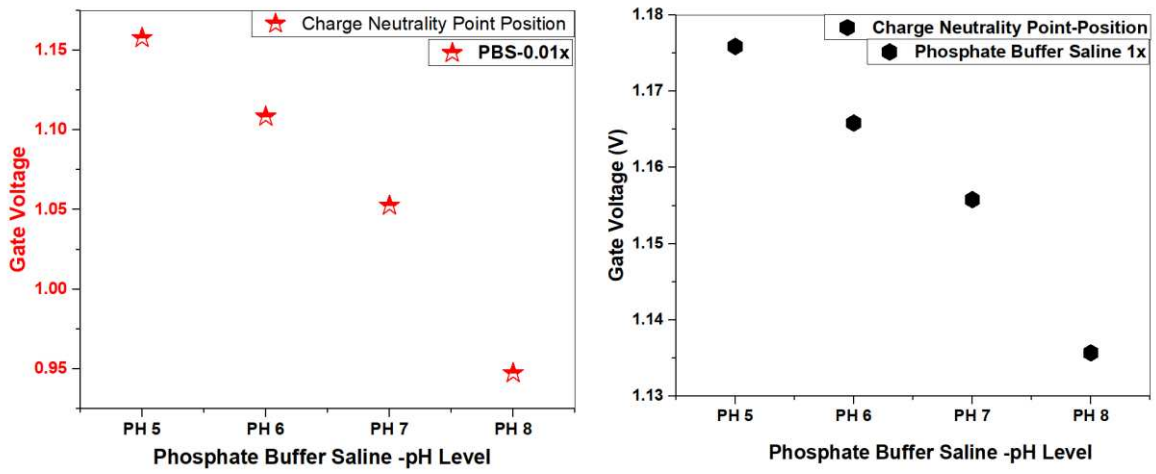

Figure 4.12: Variation of Dirac voltage as a function of pH for electrolyte-gated GFETs measured in 0.01× PBS and 1× PBS solutions.

For the 0.01xPBS solution, the Dirac point exhibits a clear and systematic shift towards lower gate voltages with increasing pH. The extracted values decrease from approximately 1.15–1.16 V at pH 5 to around 0.95 V at pH 8, corresponding to a total shift of nearly 200 mV across the measured range. The change in voltage between successive pH levels is relatively uniform, with distinct separation between the data points.

In contrast, the Dirac point variation in 1xPBS is significantly smaller. The extracted values decrease from approximately 1.17–1.18 V at pH 5 to about 1.13–1.14 V at pH 8, resulting in a total shift of approximately 40–50 mV. The spacing between adjacent pH values is reduced, and the overall variation remains confined within a narrow voltage range.

The difference in the magnitude of the shift between the two electrolyte conditions is evident from the relative slopes of the plots. The steeper variation observed in the diluted electrolyte indicates a stronger dependence of the Dirac voltage on pH, whereas the flatter trend in 1× PBS reflects a weaker response.

The direction of the shift, towards lower gate voltages as pH increases, is consistent in both cases. This behaviour corresponds to a reduction in positive charge density near the graphene surface as the proton concentration decreases, leading to a change in the charge neutrality condition of the channel.

The comparison between 0.01x PBS and 1x PBS indicates that the sensitivity of the Dirac point to pH variation is strongly influenced by ionic strength, with reduced screening in the diluted solution allowing a greater effective modulation of the graphene channel.

4.7.3 Extended pH Response and Electrical Behaviour (pH 2–10, 1xPBS)

(a) Output Characteristics over Extended pH Range

The output characteristics measured over the extended pH range (pH 2–10) exhibit a linear dependence of drain current on drain voltage across the entire bias window. The curves remain symmetric about the origin, indicating stable and uniform charge transport under both positive and negative bias conditions.

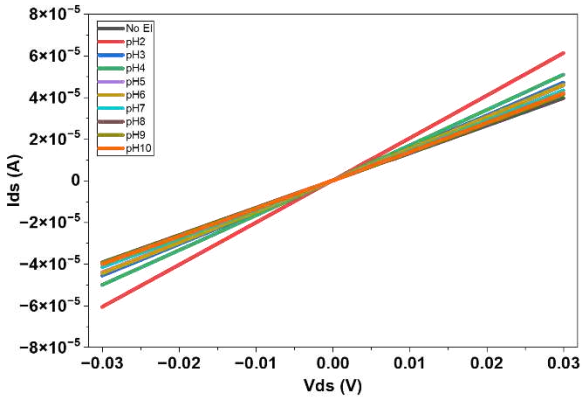

Figure 4.13: Output current–voltage characteristics of the electrolyte-gated GFET measured in 1× PBS over an extended pH range from 2 to 10.

A variation in slope is observed across the pH range. The current magnitude is highest at lower pH values and decreases progressively as the pH increases towards neutral and basic conditions. Beyond pH 7, the variation in slope becomes less pronounced, with the curves showing closer overlap.

The observed trend suggests that the channel conductance decreases with increasing pH, consistent with the reduction in current observed at a fixed bias. The preservation of linearity across all pH

values confirms that the device operates within an ohmic regime, and that the sensing response is not associated with changes in contact behaviour.

(b) Conductance Variation with pH

The variation in output conductance with pH provides a quantitative measure of the change in channel conductivity. The conductance shows a decreasing trend as the pH increases from acidic to neutral conditions.

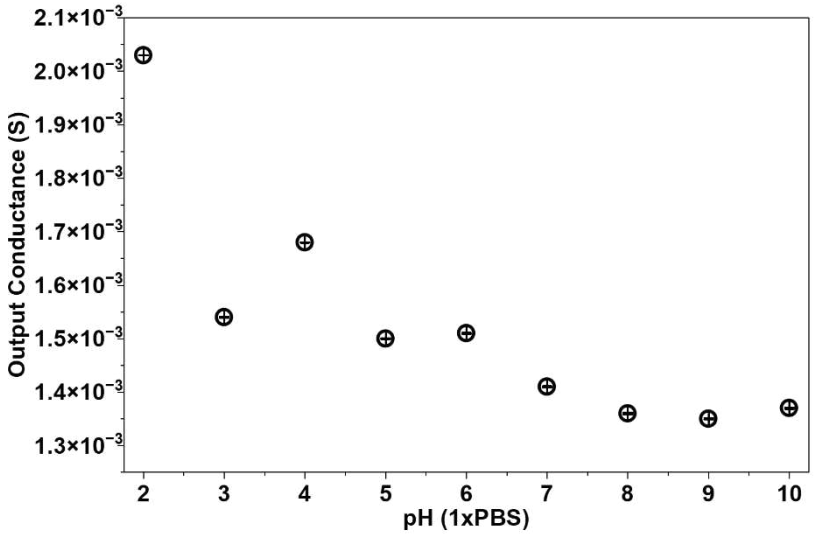

Figure 4.14: Variation of output conductance with pH for electrolyte-gated GFETs measured in 1× PBS.

At lower pH values (pH 2–4), the conductance is relatively high, indicating increased carrier density in the graphene channel. As the pH approaches neutral conditions (pH 6–7), the conductance decreases, and reflecting reduced channel conductivity. Beyond pH 7, the conductance values tend to stabilize, with only minor variations observed in the higher pH range.

The non-uniform spacing between data points suggests that the response is not strictly linear across the entire pH range. The rate of change in conductance is higher at lower pH values and decreases as the pH increases, indicating a saturation-like behaviour at higher pH.

(c) Transfer Characteristics and Dirac Point Evolution

The transfer characteristics over the extended pH range retain the ambipolar behaviour of graphene, with a clear minimum in current corresponding to the Dirac point. However, compared to the controlled study, the evolution of the curves shows several distinct features.

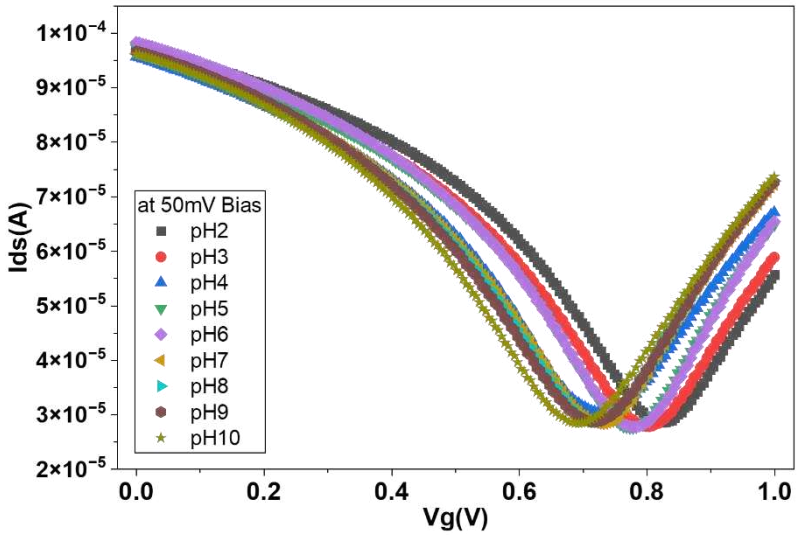

Figure 4.15: Transfer characteristics of electrolyte-gated GFETs measured in 1× PBS over the pH range 2–10 at a fixed drain bias of 50 mV.

The position of the minimum shifts with pH, although the variation is not uniform across the entire range. At lower pH values, the curves are more separated, with a noticeable shift in the position of the minimum. As the pH increases, the separation between the curves reduces, and the minima begin to cluster within a narrower voltage region.

In addition to the shift, a change in the shape of the curves is observed. The curvature around the minimum becomes less sharp at higher pH values, indicating a broadening of the Dirac region. The slopes on either side of the minimum also decrease, suggesting reduced gating efficiency.

The asymmetry between the electron and hole branches becomes slightly more pronounced at higher pH values, indicating that the transport behaviour is influenced by interfacial effects under strongly screened conditions.

The extended pH measurements reveal that the device response is governed by a combination of electrostatic modulation and ionic screening effects. At low pH, the higher proton concentration modifies the interfacial charge environment and influences the effective carrier concentration in graphen. As the pH increases, the reduction in proton concentration modifies the interfacial charge distribution, leading to a decrease in conductance and a shift in the Dirac point.At higher pH values, the influence of ionic screening becomes dominant. The effective electric field is confined near the graphene–electrolyte interface, reducing the sensitivity of the device to further changes in pH. This results in reduced separation of transfer curves, broadening of the Dirac region, and saturation-like behaviour in conductance.

4.7.4 Peak Resistance and Dirac Point Analysis (Extended pH Range)

(a) Peak Resistance Variation with pH

The variation in peak resistance extracted from the transfer characteristics shows a distinct dependence on pH. The resistance at the Dirac point increases as the pH is raised from acidic to neutral conditions, reaching a maximum in the mid-pH range.

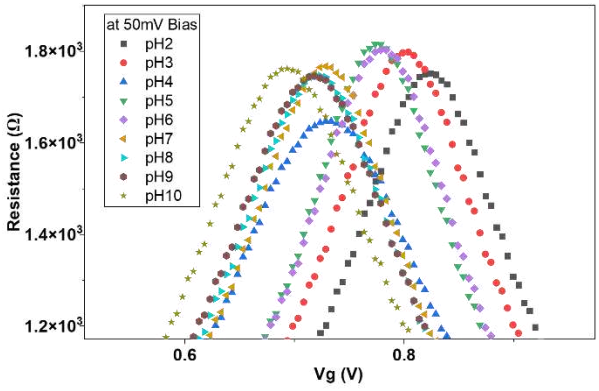

Figure 4.16: Variation of peak resistance extracted from GFET transfer characteristics as a function of pH in 1× PBS solution.

At lower pH values, the peak resistance is comparatively lower, indicating higher conductivity near the charge neutrality point. As the pH increases, the resistance rises, suggesting a reduction in carrier density and increased scattering effects within the graphene channel.

Beyond the mid-pH region, the peak resistance exhibits a tendency to decrease or stabilize, indicating a change in the dominant mechanism governing the channel behaviour. This variation suggests that the relationship between pH and resistance is not strictly monotonic across the entire range.

The broadening of the resistance peak observed in the transfer characteristics at higher pH values is consistent with the increase in peak resistance and reflects reduced gating efficiency under strong ionic screening conditions.

(b) Dirac Point Variation over Extended pH Range

The variation of the Dirac point over the extended pH range (pH 2–10) shows a consistent shift towards lower gate voltages with increasing pH. The data points follow a decreasing trend, with a gradual reduction in the Dirac voltage from acidic to basic conditions.

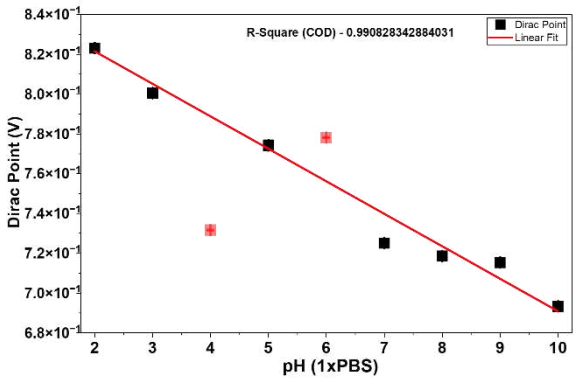

Figure 4.17: Calibration curve showing the variation of Dirac voltage with pH for electrolyte-gated GFET measurements performed in 1× PBS.

At lower pH values, the Dirac point is positioned at higher gate voltages, indicating a higher effective positive charge density at the graphene–electrolyte interface. As the pH increases, the

reduction in proton concentration leads to a corresponding decrease in the gate voltage required to reach the charge neutrality condition.

The trend exhibits an approximately linear behaviour over a significant portion of the pH range, although slight deviations from linearity are observed at higher pH values. The fitted line captures the overall decreasing tendency, while the scatter of the data points reflects the influence of additional interfacial and electrochemical effects under strongly screened conditions.

The magnitude of the shift across the extended range is larger than that observed within the limited pH window, but the rate of change is not uniform, indicating a transition from a more sensitive regime at lower pH to a reduced sensitivity regime at higher pH

(c) Sensitivity Analysis

The sensitivity of the device was evaluated from the variation of the Dirac point with pH, defined as the change in gate voltage per unit change in pH.The extracted data shows an approximately linear dependence of the Dirac voltage on pH over a limited range, with deviations observed at higher pH values. The slope of the fitted line provides an estimate of the sensitivity, which is found to be on the order of tens of millivolts per pH unit.

The variation in slope across the extended pH range indicates that the sensitivity is not uniform. A higher sensitivity is observed in the lower to intermediate pH region, while a reduced slope is observed at higher pH values, consistent with the reduced separation of the transfer curves.The deviation from linear behaviour suggests that the response is influenced by additional factors beyond simple electrostatic modulation, particularly under strongly screened conditions.

The variation of Dirac voltage, peak resistance, and sensitivity with pH reflects the interplay between interfacial electrostatics and carrier transport in the graphene channel [3,4,14].The shift in the Dirac point towards lower gate voltages with increasing pH is associated with a reduction in proton concentration at the graphene–electrolyte interface, leading to a change in the charge

neutrality condition. In parallel, the increase in peak resistance observed in the intermediate pH range indicates a reduction in effective carrier density near the Dirac point.

The sensitivity extracted from the Dirac shift follows a similar trend, with higher values in the lower to intermediate pH region and reduced response at higher pH. This behaviour is consistent with the reduced separation of transfer curves observed in the extended measurements.The combined trends indicate that the device response is strongest when the electrostatic modulation is less affected by ionic screening [5,11]. At higher pH values, the influence of screening becomes more pronounced, limiting both the shift in Dirac voltage and the sensitivity of the device.

4.7.5 Transport Parameter Analysis under Extended pH Conditions

1. Contact Resistance Variation

The variation in contact resistance with pH shows a gradual decrease as the pH increases from acidic to basic conditions. At lower pH values, the contact resistance remains close to 4.0×10^2 Ω with relatively small variation. As the pH increases beyond neutral conditions, a consistent reduction in resistance is observed, reaching values near $3.5\times10^2\Omega$ at higher pH.

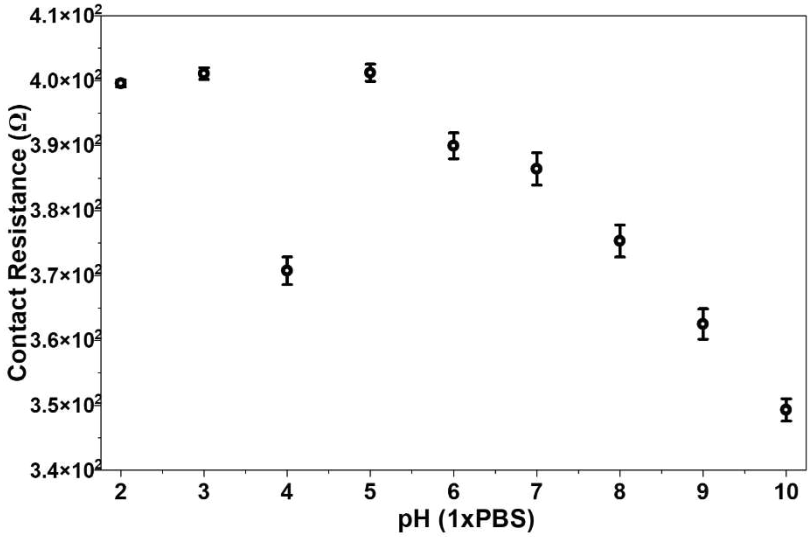

Figure 4.18*: Extracted contact resistance as a function of pH for electrolyte-gated GFET measurements in 1× PBS solution.*

The change is not abrupt, and the data points remain within a narrow range, indicating that the metal–graphene contact interface remains stable across the electrolyte conditions. The presence of error bars suggests minor variations between measurements, which may be attributed to fluctuations in the electrolyte interface or measurement conditions.

The decreasing trend indicates that the effective contact resistance is influenced by the electrostatic environment, although its variation is smaller compared to the changes observed in channel conductance and transfer characteristics.

2. Transconductance Behaviour

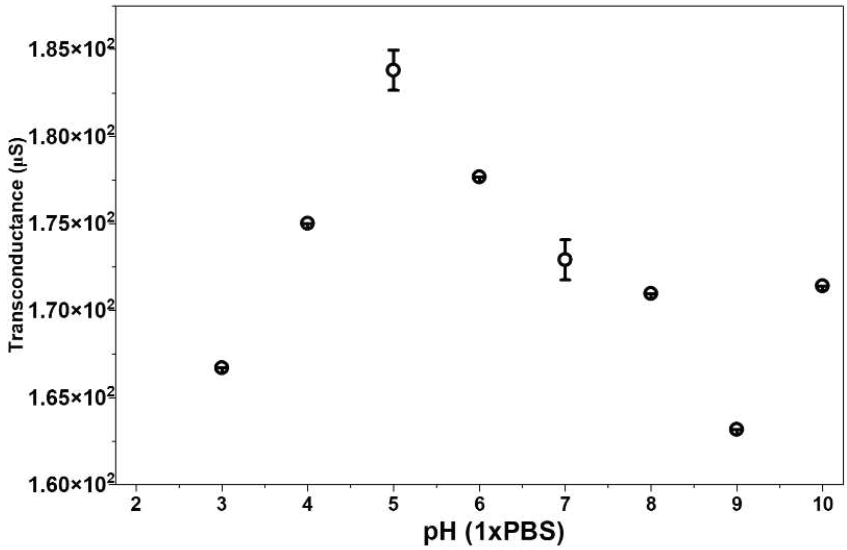

Figure 4.19: Variation of transconductance as a function of pH for electrolyte-gated GFET measurements in 1× PBS solution.

The transconductance(g_m) exhibits a non-monotonic dependence on pH across the measured range. The values increase from lower pH and reach a maximum around the mid-pH region, followed by a gradual decrease at higher pH levels.The variation remains within a relatively narrow range, indicating that the overall transconductive response of the device is maintained across the extended pH range. The peak observed near intermediate pH values suggests that the modulation of channel conductance by the gate is most effective in this region.At higher pH values, the reduction in transconductance reflects a decrease in the sensitivity of the channel conductance to gate voltage, consistent with the reduced slope observed in the transfer characteristics.

3. Field-Effect Mobility Variation

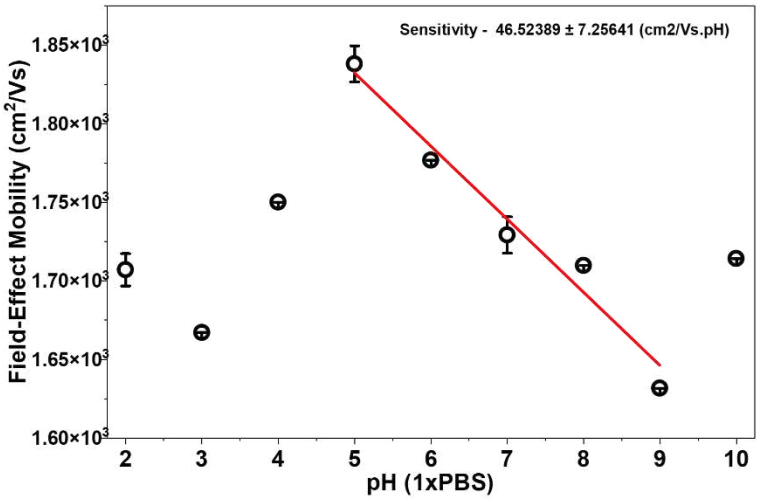

Figure 4.20: Extracted field-effect mobility as a function of pH for electrolyte-gated GFET measurements in 1× PBS.

The field-effect mobility shows a gradual decrease with increasing pH, as indicated by the fitted trend line. The values are relatively higher at lower pH and decrease progressively towards higher pH levels.The variation in mobility is moderate, with the data points distributed around the fitted trend. The decrease in mobility suggests an increase in scattering effects or reduced carrier transport efficiency under higher pH conditions.The slope of the fitted line provides an estimate of the sensitivity of mobility to pH variation, although the scatter in the data indicates that the relationship is not strictly linear across the entire range.

The extracted transport parameters indicate that the variation in device performance with pH is primarily governed by changes in channel properties rather than contact effects.The relatively small variation in contact resistance compared to the more pronounced changes in transconductance and mobility suggests that the sensing response is dominated by modulation of the graphene channel rather than changes at the metal contacts.

The decrease in mobility and transconductance at higher pH values is consistent with the reduced effectiveness of electrostatic gating observed in the transfer characteristics. The combined

behaviour reflects the influence of ionic screening and interfacial charge redistribution on carrier transport within the graphene channel [14,15]

4.7.6 Hysteresis Behaviour and Measurement Stability

The hysteresis behaviour of the graphene field-effect transistor was evaluated by comparing the forward and reverse gate voltage sweeps at different pH conditions. The measurements were performed at a fixed bias voltage of 50 mV, and representative curves for acidic (pH 4), neutral (pH 7), and basic (pH 9) conditions are shown in Figure 4.

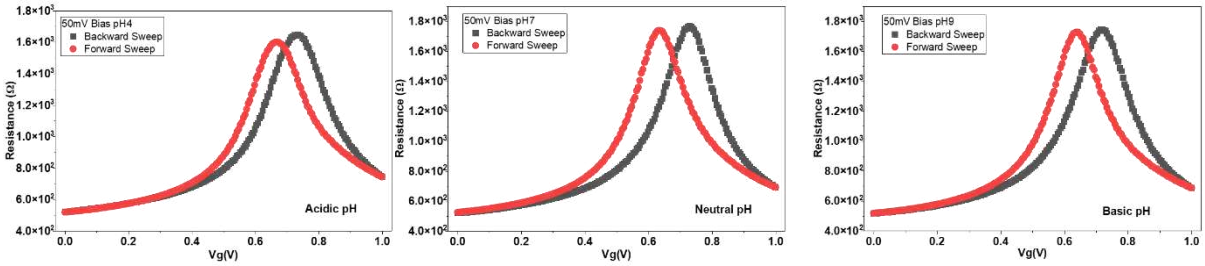

Figure 4.21: Hysteresis behaviour observed during forward and reverse gate-voltage sweeps under acidic (pH 4), neutral (pH 7), and basic (pH 9) conditions.

The transfer characteristics obtained during forward and backward sweeps exhibit a noticeable shift in the position of the resistance peak. For all pH conditions, the peak corresponding to the reverse sweep appears at a higher gate voltage compared to the forward sweep, indicating the presence of hysteresis in the device response.

The magnitude of the hysteresis can be assessed from the separation between the peak positions of the forward and backward curves. At **acidic pH (4)**, the separation is relatively small, with the two curves remaining closely aligned. As the pH increases towards neutral and basic conditions, the separation becomes more pronounced, indicating an increase in hysteresis.

In addition to the peak shift, slight differences in the shape of the curves are observed between the forward and reverse sweeps. The reverse sweep tends to exhibit a broader peak and a slower transition near the Dirac region, suggesting a delayed response of the system to changes in gate voltage.

The observed hysteresis is associated with dynamic processes at the graphene–electrolyte interface. Possible contributions include charge trapping at defect sites, adsorption and desorption of ions, and slow redistribution of ions within the electrical double layer. These processes introduce a time-dependent component to the device response, resulting in a difference between the forward and reverse measurements [16,17].

The increase in hysteresis at higher pH values indicates that interfacial effects become more significant under these conditions. This behaviour is consistent with the extended pH analysis, where reduced electrostatic modulation and increased screening were observed. The presence of hysteresis suggests that the device response is influenced not only by equilibrium electrostatics but also by transient interfacial phenomena.

4.8 Discussion

4.8.1 Correlation between Modelling and Experimental Observations

The experimental results presented in this chapter show clear dependence of the GFET response on pH and ionic strength, which can be interpreted in the context of the modelling framework developed in Chapter 3.

The continuum modelling approach, implemented using COMSOL, describes the electrostatic potential distribution and electric field penetration in the electrolyte–graphene system. The simulations indicate that the effective gating of the graphene channel is strongly influenced by the Debye screening length, which depends on the ionic strength of the electrolyte.

This behaviour is consistent with the experimental observations, where a larger Dirac point shift was obtained in diluted electrolyte conditions compared to standard 1× PBS. The reduced ionic strength increases the Debye length, allowing the gate field to extend further into the electrolyte and interact more effectively with the graphene channel.

At the atomistic level, molecular dynamics simulations provide insight into the structure of the electrical double layer and the arrangement of ions near the graphene surface. The simulations indicate that the distribution of ions at the interface is not static but evolves with changes in pH

and ionic composition. These interfacial effects influence the local electrostatic environment, which in turn affects the charge neutrality condition of the graphene channel.

The combination of continuum and atomistic modelling therefore supports the experimental observation that the GFET response is governed by both long-range electrostatic screening and local interfacial interactions.

4.8.2 Influence of Ionic Strength and Electrostatic Screening

The comparison between 0.01× PBS and 1× PBS highlights the dominant role of ionic strength in determining device sensitivity.

In the diluted electrolyte, the reduced concentration of ions leads to an extended Debye length, resulting in stronger electrostatic coupling between the gate electrode and the graphene channel. This produces a larger shift in the Dirac point and improved sensitivity to pH variations.

In contrast, in 1× PBS, the higher ionic strength results in a shorter Debye length and stronger screening of the electric field. As a result, the effective modulation of the graphene channel is reduced, leading to smaller Dirac shifts and reduced sensitivity.

This effect becomes more pronounced in the extended pH measurements, where the separation between transfer curves decreases at higher pH values. The reduced variation in both Dirac voltage and conductance reflects the limitation imposed by electrostatic screening under realistic electrolyte conditions.

4.8.3 Interfacial Effects and Charge Transport Mechanisms

The variation in peak resistance, mobility, and transconductance indicates that the sensing response is not governed solely by electrostatics but also by changes in carrier transport within the graphene channel.

At lower pH values the higher proton concentration modifies the interfacial charge environment and influences the effective carrier concentration in graphene.As the pH increases, the reduction

in proton concentration alters the interfacial charge distribution, leading to a decrease in carrier density and mobility.

The observed decrease in mobility with increasing pH suggests enhanced scattering effects, which may arise from ion adsorption, surface charge fluctuations, or interactions within the electrical double layer. These effects contribute to the broadening of the Dirac region and reduced transconductance observed in the transfer characteristics.

The relatively small variation in contact resistance compared to the changes in channel parameters indicates that the dominant contribution to the sensing response arises from modulation of the graphene channel rather than changes at the metal–graphene interface.

4.8.4 Nonlinearity and Extended pH Behaviour

The extended pH measurements reveal that the response of the GFET is not strictly linear across the full pH range. While a near-linear relationship is observed over a limited range, deviations become apparent at higher pH values.

The reduction in sensitivity and clustering of Dirac point positions at higher pH indicate a transition to a regime where further changes in proton concentration produce a diminished response. This behaviour is consistent with the combined influence of electrostatic screening and saturation of interfacial charge effects.

The increase in hysteresis observed at higher pH further supports the presence of dynamic interfacial processes. The difference between forward and reverse sweeps suggests that ion redistribution and charge trapping introduce time-dependent effects that influence the device response.These observations indicate that the sensing performance of GFET devices is governed by a combination of equilibrium electrostatics and non-equilibrium interfacial dynamics.

4.8.5 Implications for GFET-Based Biosensing

The results presented in this work highlight several important considerations for the design and application of GFET-based sensors.

The strong sensitivity observed in low ionic strength conditions demonstrates the intrinsic capability of graphene for electrostatic sensing. However, the reduced response in 1× PBS indicates that practical applications in biological environments require careful consideration of ionic screening effects.

The observed dependence of mobility and transconductance on pH suggests that device performance can be influenced by interfacial engineering and surface functionalization. Controlling the interaction between the graphene surface and the electrolyte may provide a route to improving sensitivity under realistic conditions.

The presence of hysteresis and nonlinearity indicates that stability and reproducibility are important factors in sensor design. Minimizing interfacial trapping and optimizing measurement protocols are essential for achieving reliable performance.

4.9 Summary of the Chapter

This chapter investigated the pH response of electrolyte-gated graphene field-effect transistors through a combined modelling and experimental approach, with particular emphasis on the role of electrolyte-induced electrostatic modulation at the graphene–electrolyte interface. The modelling framework established in the earlier sections demonstrated that the electrical response of the device is governed primarily by ion redistribution within the electric double layer and the resulting modulation of carrier concentration in the graphene channel.

The simulations showed that electrolyte properties strongly influence the electrostatic environment near the graphene surface. In particular, the reduction of Debye screening length at higher ionic strength confines the electric field within a narrow interfacial region, limiting the effective penetration of the gating field into the electrolyte. The inclusion of graphene quantum capacitance further demonstrated that the overall device response cannot be described solely by classical electric double-layer effects, especially near the charge neutrality region where the density of states in graphene becomes limited.

Experimental measurements performed in PBS electrolytes confirmed the electrostatic behaviour predicted by the modelling framework. The controlled comparison between diluted and standard

PBS conditions demonstrated that the magnitude of the Dirac point shift is strongly dependent on ionic screening. Under reduced ionic strength, the broader electric double layer enabled stronger electrostatic coupling between the electrolyte and graphene channel, producing larger pH-dependent voltage shifts. In contrast, measurements performed in 1× PBS exhibited reduced modulation due to stronger screening of the applied electric field.

The extended pH measurements further showed that the sensing response is governed by the combined influence of proton-induced interfacial charge variation and electrolyte screening effects. While lower pH conditions produced stronger modulation of the graphene channel, the response gradually approached a reduced-sensitivity regime at higher pH values, where screening and interfacial effects became increasingly dominant. The evolution of peak resistance, mobility, and transconductance indicated that pH sensing affects not only the electrostatic gating behaviour but also the carrier transport properties of the graphene channel.

The hysteresis behaviour observed during forward and reverse gate sweeps demonstrated the presence of dynamic interfacial processes, including ion redistribution and charge trapping within the electrolyte–graphene system. These effects indicate that the electrical response of electrolyte-gated GFETs is influenced by both equilibrium electrostatics and time-dependent interfacial interactions.

The results presented in this chapter show that the response of electrolyte-gated GFETs cannot be interpreted only through pH variation, but must also be understood in terms of electrolyte-dependent electrostatic interactions at the graphene interface. The experimental observations and modelling results consistently indicate that electric double-layer formation, ionic screening, and graphene charge modulation collectively determine the sensing behaviour of the device. Variations in electrolyte concentration alter the effective coupling between the electrolyte and graphene channel, directly influencing the magnitude of the Dirac point shift, transport response, and hysteresis characteristics. These observations provide a physical basis for understanding the operation of electrolyte-gated graphene sensors under physiologically relevant conditions and establish the framework required for the biomolecular sensing investigations discussed in the following chapter.

4.10 REFERENCES

[1] Geim, A. K., & Novoselov, K. S. (2007). The rise of graphene. Nature Materials, 6(3), 183–191. https://doi.org/10.1038/nmat1849

[2] Schwierz, F. (2010). Graphene transistors. Nature Nanotechnology, 5(7), 487–496. https://doi.org/10.1038/nnano.2010.89

[3] Ohno, Y., Maehashi, K., Yamashiro, Y., & Matsumoto, K. (2009). Electrolyte-gated graphene field-effect transistors for detecting pH and protein adsorption. Nano Letters, 9(9), 3318–3322. https://doi.org/10.1021/nl901596m

[4] Ang, P. K., Chen, W., Wee, A. T. S., & Loh, K. P. (2008). Solution-gated epitaxial graphene as pH sensor. Journal of the American Chemical Society, 130(44), 14392–14393. https://doi.org/10.1021/ja806232g

[5] Heller, I., Chatoor, S., Männik, J., Zevenbergen, M. A., Dekker, C., & Lemay, S. G. (2010). Influence of electrolyte composition on liquid-gated carbon nanotube and graphene transistors. Journal of the American Chemical Society, 132(48), 17149–17156. https://doi.org/10.1021/ja105088h

[6] Baridi, G., Liaquat, A., Martini, L., Nappi, L., Rapuzzi, F., Clericò, V., Abidi, E. H., Meziani, Y. M., Amado, M., Diez, E., Brancolini, G., Rovati, L., & Rossella, F. (2026). Graphene-Based Chemical Field-Effect Transistors: Impact of Electric Double Layer Model and Quantum Capacitance on Na+ Detection Capabilities. Micromachines, 17(4), 433.https://doi.org/10.3390/mi17040433

[7] Bard, A. J., & Faulkner, L. R. (2001). Electrochemical methods: Fundamentals and applications (2nd ed.). Wiley.

[8] COMSOL AB. (2024). Electrochemistry module user's guide. COMSOL Multiphysics. COMSOL Electrochemistry Module User Guide

[9] Israelachvili, J. (2011). Intermolecular and surface forces (3rd ed.). Academic Press.

[10]. Bockris, J. O'M., & Reddy, A. K. N. (1998). Modern electrochemistry 2A: Fundamentals of electrodics (2nd ed.). Kluwer Academic Publishers.

[11] Xia, J., Chen, F., Li, J., & Tao, N. (2009). Measurement of the quantum capacitance of graphene. Nature Nanotechnology, 4(8), 505–509. https://doi.org/10.1038/nnano.2009.177

[12] Fang, T., Konar, A., Xing, H., & Jena, D. (2007). Carrier statistics and quantum capacitance of graphene sheets and ribbons. Applied Physics Letters, 91(9), 092109. https://doi.org/10.1063/1.2776887

[13] Luryi, S. (1988). Quantum capacitance devices. Applied Physics Letters, 52(6), 501–503. https://doi.org/10.1063/1.99649

[14] Fu, W., Jiang, L., van Geest, E. P., Lima, L. M. C., & Schneider, G. F. (2017). Sensing at the surface of graphene field-effect transistors. Advanced Materials, 29(6), 1603610. https://doi.org/10.1002/adma.201603610

[15] Hess, L. H., Jansen, M., Maybeck, V., Hauf, M. V., Seifert, M., Stutzmann, M., Sharp, I. D., Offenhäusser, A., & Garrido, J. A. (2011). Graphene transistor arrays for recording action potentials from electrogenic cells. Advanced Materials, 23(43), 5045–5049. https://doi.org/10.1002/adma.201101597

[16] Melzer, K., Uebel, P., Hernández-Rodríguez, J. F., Fischer, S. F., & Kanoun, O. (2015). Hysteresis effects in graphene field-effect transistors under ambient conditions. Sensors, 15(6), 13747–13765. https://doi.org/10.3390/s150613747

[17] Joshi, P., Romero, H. E., Neal, A. T., Toutam, V. K., & Tadigadapa, S. A. (2010). Intrinsic doping and gate hysteresis in graphene field effect devices fabricated on SiO_2 substrates. Journal of Physics: Condensed Matter, 22(33), 334214. https://doi.org/10.1088/0953-8984/22/33/334214

Chapter 5

Label-Free Detection of Human Serum Albumin Using Electrolyte-Gated Graphene Field-Effect Transistors

5.1 Introduction

Human Serum Albumin (HSA) is the most abundant plasma protein in human blood and plays a central role in maintaining osmotic pressure, molecular transport, and biochemical regulation within physiological systems. Abnormal albumin concentrations are frequently associated with renal dysfunction, inflammatory disorders, and metabolic imbalance, motivating the development of sensitive label-free detection platforms for biochemical monitoring [1,2].

Conventional albumin detection techniques are generally based on immunoassays, spectrophotometric analysis, chromatography, or fluorescence-labelled methods. Although these approaches can provide high analytical sensitivity, they often require complex sample preparation, expensive instrumentation, chemical labelling, or long processing times [3]. These limitations have stimulated growing interest in label-free electrical biosensing platforms capable of direct biomolecular detection under physiologically relevant conditions [4].

Graphene field-effect transistors (GFETs) have attracted considerable attention for biosensing applications due to their atomically thin structure, high carrier mobility, and strong sensitivity to local electrostatic perturbations [5,6]. Since every atom in graphene is exposed to the surrounding environment, adsorption-induced charge redistribution at the graphene surface can significantly influence the electrical behaviour of the transistor channel. This property enables direct electrical transduction of biomolecular interactions without the need for fluorescent or enzymatic labels [7].

In electrolyte-gated GFETs, the gate field is established through the electric double layer formed at the graphene-electrolyte interface. Because the effective interfacial capacitance is extremely high, relatively small perturbations in surface charge can produce measurable modulation of the graphene channel [8,9]. Under electrolyte gating conditions, biomolecular adsorption modifies the local electrostatic environment near the graphene surface, leading to changes in the transfer characteristics, Dirac voltage position, transconductance, and carrier transport properties of the

device. However, the sensing response of electrolyte-gated GFETs is also strongly influenced by ionic screening, interfacial disorder, and adsorption-induced scattering effects within the graphene channel [10].

Previous studies on GFET biosensors have primarily focused on Dirac voltage shifts as the main sensing metric for protein detection [11,12]. While this approach provides useful information regarding electrostatic gating effects, it often does not fully capture the transport modifications induced by biomolecular adsorption. In practical electrolyte environments, protein adsorption can generate spatially heterogeneous electrostatic perturbations that modify carrier mobility and influence transport dynamics within the graphene channel. As a result, sensing mechanisms based solely on carrier-density modulation may provide only a partial description of the electrical response of protein-functionalized GFET systems.

In this chapter, electrolyte-gated graphene field-effect transistors are investigated for the label-free detection of Human Serum Albumin through a combined experimental and atomistic analysis framework. Particular attention is devoted to the relationship between protein adsorption, electrostatic modulation, and transport evolution within the graphene channel. Brownian Dynamics simulations are employed to examine the adsorption behaviour and orientation of albumin molecules near the graphene surface, providing atomistic insight into the interfacial interactions governing the sensing process. Experimentally, the electrical response of the devices is analyzed through transfer characteristics, transport parameter extraction, inverse mobility sensing metrics, and ultra-trace calibration analysis over a broad concentration range. The combined experimental and atomistic analysis provides insight into the relationship between protein adsorption, electrostatic perturbation, and transport evolution in electrolyte-gated graphene transistors operating under biologically relevant conditions.

5.2 Electrostatic Biosensing Mechanism and Atomistic Adsorption Framework

5.2.1 Electrolyte-Gated GFET Biosensing Principle

Electrolyte-gated graphene field-effect transistors operate through electrostatic coupling established at the graphene-electrolyte interface. In contrast to conventional dielectric-gated transistors, where the gate field is controlled through a solid insulating layer, electrolyte-gated

devices rely on ion redistribution within the electrolyte to modulate carrier concentration in the graphene channel. When an external gate voltage is applied, oppositely charged ions accumulate near the graphene surface, forming the electric double layer (EDL), which consists of a compact Stern region and a surrounding diffuse ion layer [13,14].

Because the effective thickness of the electric double layer is typically on the nanometer scale, the resulting interfacial capacitance becomes substantially larger than that of conventional oxide gate dielectrics. Under these conditions, relatively small perturbations in interfacial charge distribution can produce measurable modulation of the graphene channel conductivity [15]. The electrical response is commonly observed through variations in the transfer characteristics, including shifts in the Dirac voltage, changes in transconductance, and modifications of channel resistance.

In electrolyte-gated biosensing systems, adsorption of charged or polar biomolecules near the graphene surface perturbs the local electrostatic environment within the EDL region. These perturbations alter the carrier distribution within the graphene channel and influence the overall transport behaviour of the transistor. Since graphene possesses an atomically exposed surface and low density of states near the charge neutrality point, the electrical response becomes highly sensitive to adsorption-induced electrostatic interactions occurring at the graphene–electrolyte interface [16].

The sensing response of electrolyte-gated GFETs is additionally influenced by ionic screening within the electrolyte. Mobile ions present in solution partially screen the electric field generated by adsorbed biomolecules, thereby reducing the effective electrostatic coupling between the biomolecular layer and the graphene channel [17]. The magnitude of this screening effect is governed by the Debye screening length, which decreases with increasing ionic concentration. Consequently, the electrical sensitivity of electrolyte-gated GFETs depends not only on the intrinsic properties of the analyte, but also on the electrochemical environment in which the sensing process occurs.

5.2.2 Electrostatic Effects of Protein Adsorption

Human Serum Albumin is a negatively charged globular protein containing multiple ionizable amino acid residues distributed non-uniformly across its molecular structure. As a result,

adsorption of albumin near the graphene surface produces spatially heterogeneous electrostatic perturbations rather than a uniform surface potential variation [18]. The resulting electrical response therefore depends on several coupled factors, including molecular orientation, local charge distribution, adsorption density, and electrolyte screening conditions.

In many graphene biosensing studies, protein adsorption is primarily interpreted through shifts in the Dirac voltage arising from electrostatic gating effects [19]. However, adsorption-induced perturbations may also modify carrier transport within the graphene channel. Localized charge inhomogeneity generated by adsorbed proteins can alter carrier scattering behaviour, broaden the charge neutrality region, and influence mobility within the graphene layer. Under these conditions, the sensing mechanism extends beyond simple carrier-density modulation and becomes strongly linked to transport disorder at the graphene-electrolyte interface.

The electrostatic influence of adsorbed proteins is further affected by the presence of residual ions within the electrolyte. In liquid-gated systems, the ionic environment partially screens the electric field generated by the biomolecular layer, limiting the penetration of electrostatic perturbations toward the graphene surface. Consequently, proteins adsorbed farther from the graphene channel contribute less effectively to the sensing signal than molecules located within the effective Debye screening region [20].

Because albumin molecules possess non-uniform surface charge distribution and anisotropic dipole characteristics, different adsorption configurations may generate significantly different local electrostatic responses. This heterogeneous adsorption behaviour can produce spatial fluctuations in carrier concentration and contribute to transport non-uniformity within the graphene channel. Such effects become particularly important under low-concentration sensing conditions, where localized adsorption events can strongly influence the overall electrical response of the transistor.

5.2.3 Brownian Dynamics Simulation Framework

To investigate the adsorption behaviour of Human Serum Albumin near the graphene interface, Brownian Dynamics simulations were employed to analyze stochastic biomolecular adsorption under electrolyte conditions. Compared with fully atomistic Molecular Dynamics methods,

Brownian Dynamics enables efficient evaluation of adsorption behaviour over extended temporal and spatial scales while retaining the dominant electrostatic interactions governing biomolecular motion in solution [21].

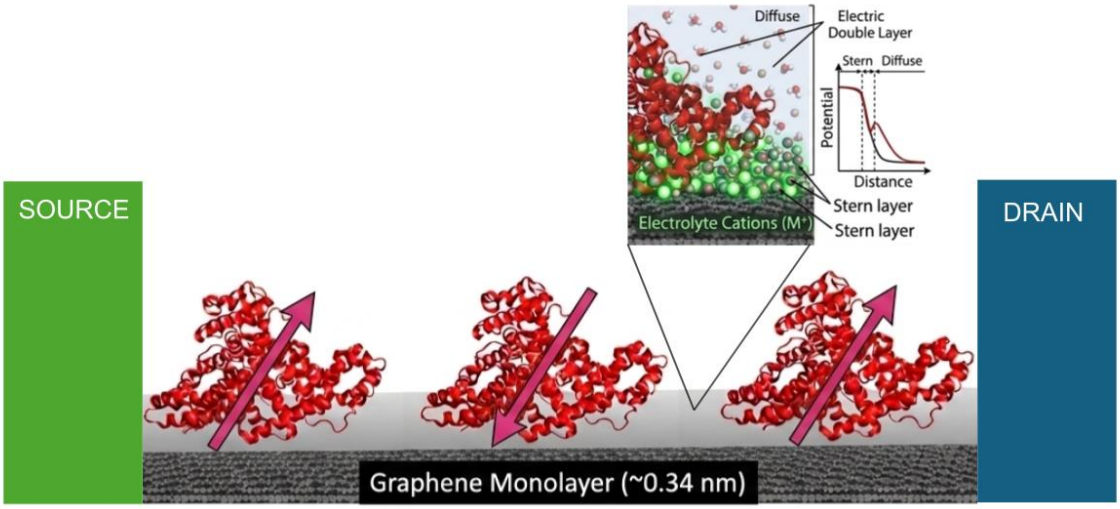

Figure 5.1: Schematic illustration of the electrostatic sensing mechanism in the electrolyte-gated GFET during Human Serum Albumin (HSA) adsorption. The negatively charged HSA molecule perturbs the electric double-layer (EDL) structure near the graphene surface, producing redistribution of electrolyte ions within the Debye screening region (λ_D). The resulting interfacial electrostatic modulation alters the carrier density of the graphene monolayer and influences the conductance of the electrolyte-gated graphene transistor under non-Faradaic sensing condition

In the simulation framework, albumin molecules were treated as rigid bodies interacting with an atomically flat graphene surface under implicit solvent conditions. Electrostatic interactions between the protein and graphene interface were evaluated using the spatial charge distribution of the HSA molecule together with effective electrolyte screening conditions. Since albumin possesses a heterogeneous surface charge distribution, different adsorption configurations generated distinct interfacial interaction behaviour near the graphene surface.

Multiple independent adsorption events were analyzed to investigate the statistical distribution of molecular orientations near the graphene interface. Rather than exhibiting a single preferred adsorption geometry, the simulations revealed heterogeneous adsorption configurations

characterized by substantial orientational variability. These adsorption states produced spatially varying electrostatic interactions within the interfacial region.

The simulations additionally provided insight into dipolar alignment behaviour during adsorption. Depending on molecular orientation and interaction distance, different regions of the albumin molecule approached the graphene surface, producing non-uniform perturbation of the local electric field near the interface. Such variations are expected to influence the carrier environment within the graphene channel during sensing.

The Brownian Dynamics framework therefore provides atomistic insight into the heterogeneous adsorption behaviour governing albumin interactions at the graphene-electrolyte interface. The simulations indicate that adsorption-induced electrostatic modulation arises from dynamically distributed molecular configurations rather than from a uniform biomolecular layer.

5.2.4 Atomistic Interpretation of Adsorption-Induced Perturbation

The atomistic adsorption behaviour observed in the Brownian Dynamics simulations provides important insight into the electrical response of the electrolyte-gated GFET during albumin sensing. Since the electrostatic charge distribution across the HSA molecule is spatially non-uniform, each adsorption configuration generates a distinct perturbation of the local electric field near the graphene interface. Consequently, the sensing response cannot be interpreted solely through average surface charge density, but must also account for orientation-dependent electrostatic interactions occurring within the electric double layer region.

The simulations indicate that albumin adsorption produces localized electrostatic inhomogeneity at the graphene surface. As proteins adsorb with different orientations and interaction distances, spatial fluctuations in the interfacial potential distribution emerge across the graphene channel. These fluctuations modify the local carrier environment and contribute to non-uniform modulation of the graphene conductivity.

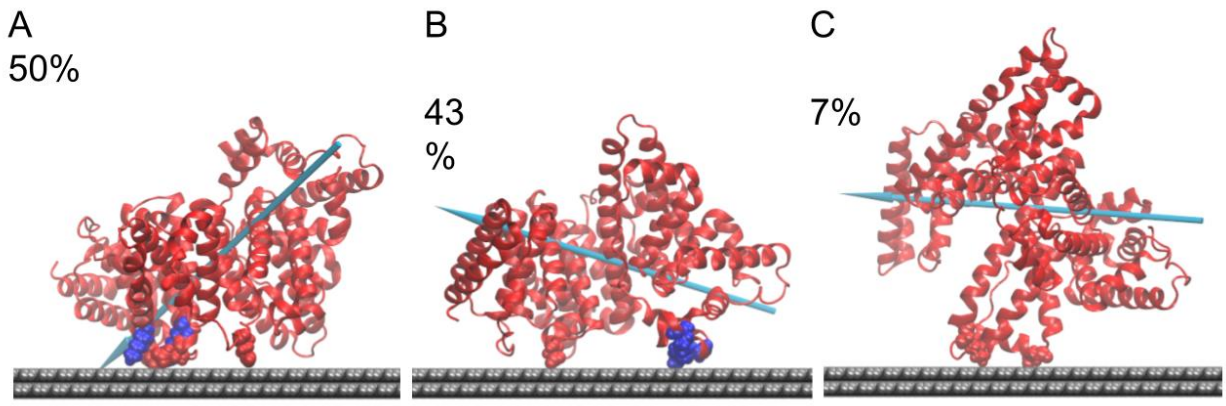

Figure 5.2: Representative adsorption orientations of Human Serum Albumin on the graphene surface obtained from Brownian Dynamics simulations. Interfacial residues located within close proximity to the graphene surface are highlighted according to local charge distribution (positively charged residues: blue; negatively charged residues: red). The cyan arrow indicates the molecular dipole orientation relative to the graphene interface. The figure illustrates the heterogeneous adsorption behaviour and orientation-dependent electrostatic interactions governing interfacial sensing response.

Such adsorption-induced electrostatic disorder is expected to influence carrier scattering within the graphene channel. Local perturbations in surface potential can generate variations in carrier transport pathways, broaden the charge neutrality region, and reduce effective carrier mobility. Under these conditions, the experimentally observed sensing response reflects not only electrostatic gating effects, but also disorder-mediated transport modulation arising from heterogeneous protein adsorption.

The atomistic interpretation additionally provides insight into the concentration-dependent transport behaviour observed experimentally. At low albumin concentrations, isolated adsorption events can produce relatively strong localized perturbations because the graphene surface remains only partially occupied. As concentration increases, the growing population of adsorbed molecules progressively modifies the electrostatic landscape near the graphene interface, resulting in broader transport perturbation and enhanced carrier scattering effects.

The influence of electrolyte screening further complicates this behaviour. Because the electric field generated by adsorbed proteins is partially screened by mobile ions within the electrolyte, the effective electrostatic coupling depends strongly on the distance between the adsorbed molecule and the graphene surface. Proteins positioned closer to the graphene channel therefore contribute more effectively to the sensing signal than molecules located farther from the effective screening region. This distance-dependent interaction contributes to the variability of the adsorption-induced electrical response observed experimentally.

The combined atomistic and electrostatic analysis presented here suggests that albumin sensing in electrolyte-gated GFETs is governed by coupled interfacial mechanisms involving electrostatic modulation, adsorption-induced disorder, and carrier transport perturbation. The sensing response therefore emerges from the interaction between biomolecular adsorption dynamics and the transport properties of the graphene channel rather than from a purely electrostatic carrier-density modulation process alone.

5.3 Device Fabrication and Experimental Methodology

5.3.1 GFET Device Configuration

The experimental investigation was performed using commercially fabricated monolayer graphene field-effect transistor arrays (Graphenea mGFET-4D) operated in a liquid-gated configuration. Each device consisted of a graphene sensing channel integrated between source and drain electrodes on a Si/SiO_2 substrate platform. In the present sensing configuration, electrical modulation of the transistor channel was achieved through electrolyte gating rather than through the underlying oxide dielectric. A droplet-based liquid gate geometry was employed in which the electrolyte solution was directly deposited onto the graphene active region together with an external gate electrode immersed within the electrolyte droplet.

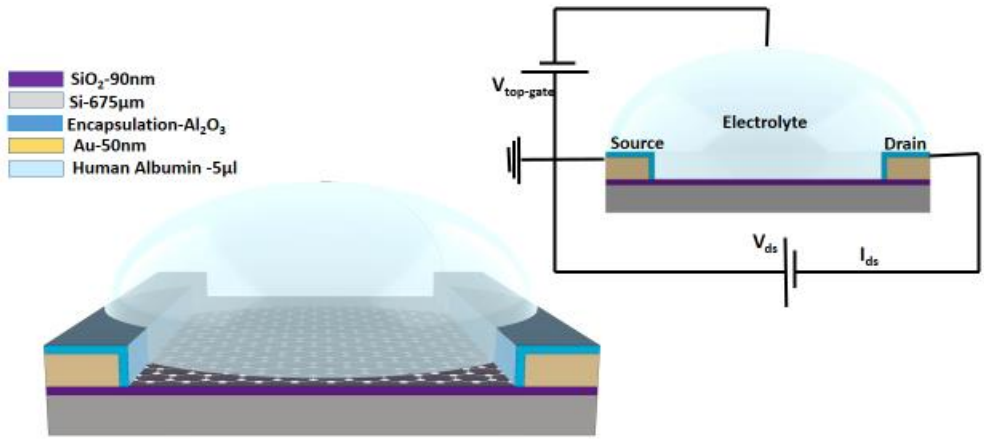

Figure 5.3: Electrolyte-gated graphene field-effect transistor architecture used for albumin sensing. (A) Schematic representation of the monolayer graphene transistor integrated between source and drain electrodes on a Si/SiO_2 substrate. (B) Liquid-gated measurement configuration showing formation of the electric double layer at the graphene–electrolyte interface during Human Serum Albumin adsorption.

The graphene channel served simultaneously as the transport medium and sensing surface, allowing adsorption-induced electrostatic perturbations to directly influence carrier transport within the device. The liquid-gated configuration was selected because the electric double layer formed at the graphene-electrolyte interface provides strong electrostatic coupling and enhanced sensitivity to local interfacial charge variations [22]. All measurements were performed under ambient laboratory conditions.

5.3.2 Albumin Preparation and Measurement Protocol

Human Serum Albumin solutions were prepared through serial dilution of commercial HSA stock solutions using ultrapure deionized water (18.2 MΩ·cm). The investigated concentration range extended from ultra-trace concentrations to physiologically relevant regimes in order to evaluate both low-concentration adsorption behaviour and transport modulation at higher surface coverage conditions. The concentration interval ranged from 0.01 mg mL^{-1} to 30 mg mL^{-1}.

Deionized water was selected as the sensing medium in order to reduce ionic screening effects during electrical measurements. Compared to concentrated physiological buffers, the lower ionic strength environment increases the effective Debye screening length, thereby improving

electrostatic coupling between adsorbed biomolecules and the graphene channel. This configuration enables enhanced sensitivity toward adsorption-induced perturbations while maintaining stable transistor operation during concentration-dependent measurements.

Prior to electrical characterization, a controlled volume of the prepared albumin solution was deposited onto the graphene sensing region to ensure complete coverage of the active device area. After stabilization of the electrolyte droplet, electrical measurements were performed sequentially for each concentration condition.

5.3.3 Electrical Characterization

Electrical characterization was carried out using both output and transfer measurements in order to evaluate the transport behaviour of the electrolyte-gated GFET during albumin adsorption. For the output characteristics, the drain current (I_D) was measured as a function of drain voltage (V_D) under fixed gate bias conditions. These measurements were used to examine the stability of channel transport and verify the linearity of the graphene transistor response across the investigated concentration range.

Transfer characteristics were obtained by sweeping the gate voltage while maintaining a constant drain bias. The resulting transfer curves enabled evaluation of the concentration-dependent modulation of the graphene channel through variations in the Dirac voltage position, transconductance, and channel resistance. Particular attention was devoted to changes occurring near the charge neutrality region, where graphene exhibits enhanced sensitivity to local electrostatic perturbations.

All measurements were repeated under identical experimental conditions in order to minimize variations associated with environmental fluctuations and electrolyte instability. The electrical response was analyzed as a function of albumin concentration to investigate the relationship between biomolecular adsorption and transport modulation within the graphene channel.

5.3.4 Transport Model and Parameter Extraction

The transfer characteristics were analyzed using a nonlinear transport model describing the total device resistance as the combined contribution of graphene channel resistance and contact

resistance. Because electrolyte-gated GFET operation depends strongly on interfacial electrostatics, the effective gate capacitance was treated using a combined capacitance framework that accounts for both electric double-layer capacitance and graphene quantum capacitance [23,24].

The fitting procedure enabled extraction of the principal transport parameters governing the electrical response of the device, including carrier mobility, Dirac voltage, residual carrier density, and contact resistance. Particular emphasis was placed on the evolution of carrier mobility as a function of albumin concentration, since adsorption-induced electrostatic disorder primarily affects carrier scattering and transport behaviour within the graphene channel.

In the present work, the inverse mobility parameter was employed as the principal sensing metric for ultra-trace albumin detection. Unlike sensing approaches based solely on Dirac voltage variation, the inverse mobility framework provides enhanced sensitivity to adsorption-induced disorder and transport perturbations occurring near the graphene interface. This approach allows the sensing response to be interpreted in terms of coupled electrostatic and transport effects rather than through carrier-density modulation alone.

5.3.5 Brownian Dynamics Simulation Procedure

To complement the experimental analysis, Brownian Dynamics simulations were performed to investigate the adsorption behaviour of albumin molecules near the graphene surface. The simulations were used to analyze molecular orientation, adsorption probability, and electrostatic interaction behaviour associated with the graphene interface.

The translational and rotational motion of the albumin molecules was governed by stochastic Brownian trajectories under the combined influence of thermal fluctuations and electrostatic interactions. Multiple independent adsorption trajectories were evaluated in order to investigate the statistical distribution of adsorption configurations and orientation behaviour near the graphene surface.

The simulation framework enabled examination of the relationship between protein adsorption geometry and local electrostatic perturbation at the graphene interface. The resulting atomistic

analysis was subsequently correlated with the experimentally observed transport modulation and sensing response of the electrolyte-gated GFET platform.

5.4 Output Characteristics and Electrolyte-Gated Transport Response

5.4.1 Output Characteristics under Albumin Adsorption

The output characteristics of the electrolyte-gated GFET were measured over the investigated albumin concentration range in order to evaluate the stability of carrier transport within the graphene channel during biomolecular adsorption. Figure 5.4 presents the drain current response as a function of drain voltage for different HSA concentrations.

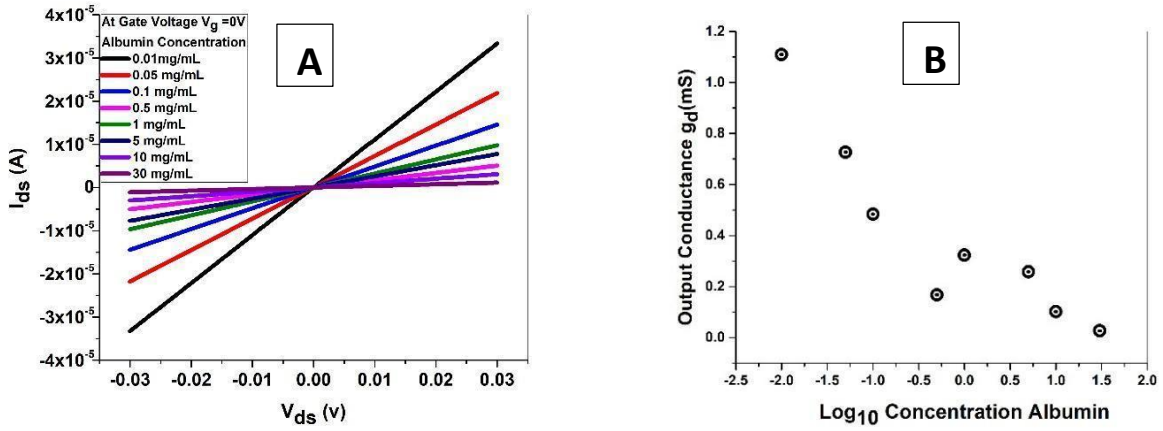

Figure 5.4: Output characteristics of the electrolyte-gated GFET measured under different Human Serum Albumin concentrations. (A) Drain current–drain voltage (I_DV_D) response demonstrating approximately linear transport behaviour and stable ohmic contact characteristics. (B) Concentration-dependent evolution of output conductance with increasing albumin concentration.

The measured output curves exhibit approximately linear behaviour over the investigated drain voltage range, indicating stable ohmic transport between the graphene channel and metal contacts throughout the sensing measurements. The absence of significant nonlinear distortion suggests that albumin adsorption does not strongly disrupt charge injection at the contact interfaces under the investigated operating conditions. Instead, the primary electrical modulation occurs within the graphene transport channel itself.

Although the overall linear transport behaviour is preserved, the magnitude of the drain current varies systematically with albumin concentration. At lower concentrations, the output response

remains comparatively stable, while progressive changes in current magnitude become more pronounced as the concentration increases. This behaviour indicates that adsorption-induced perturbations modify the effective conductivity of the graphene channel during sensing.

The concentration-dependent modulation of the output current is associated with electrostatic perturbations introduced by adsorbed albumin molecules near the graphene surface. Since the graphene channel is directly exposed to the electrolyte environment, adsorption events occurring within the effective screening region can alter the local carrier distribution and influence transport behaviour. The resulting current variation therefore reflects the combined influence of interfacial electrostatic modulation and adsorption-induced scattering effects within the graphene layer.

At higher albumin concentrations, the increased surface coverage of adsorbed proteins contributes to greater electrostatic inhomogeneity near the graphene interface. Under these conditions, localized perturbations in the interfacial potential landscape may modify carrier transport pathways and slightly reduce channel conductivity. The gradual evolution of the output characteristics with concentration is therefore consistent with adsorption-induced modulation of the graphene transport environment rather than with abrupt electrochemical or contact-related effects.

5.4.2 Transfer Characteristics and Dirac Voltage Evolution

The transfer characteristics of the electrolyte-gated GFET were subsequently analyzed to investigate the influence of albumin adsorption on the electrostatic behaviour of the graphene channel. Figure 5.5 presents the transfer curves measured across the investigated concentration range.

The transfer characteristics exhibit clear ambipolar behaviour typical of graphene field-effect transistors operating under electrolyte gating conditions. As the albumin concentration increases, systematic modulation of the transfer response is observed together with progressive displacement of the charge neutrality region. The evolution of the transfer curves indicates that adsorption of albumin molecules modifies the local electrostatic environment near the graphene surface and alters the carrier distribution within the channel.

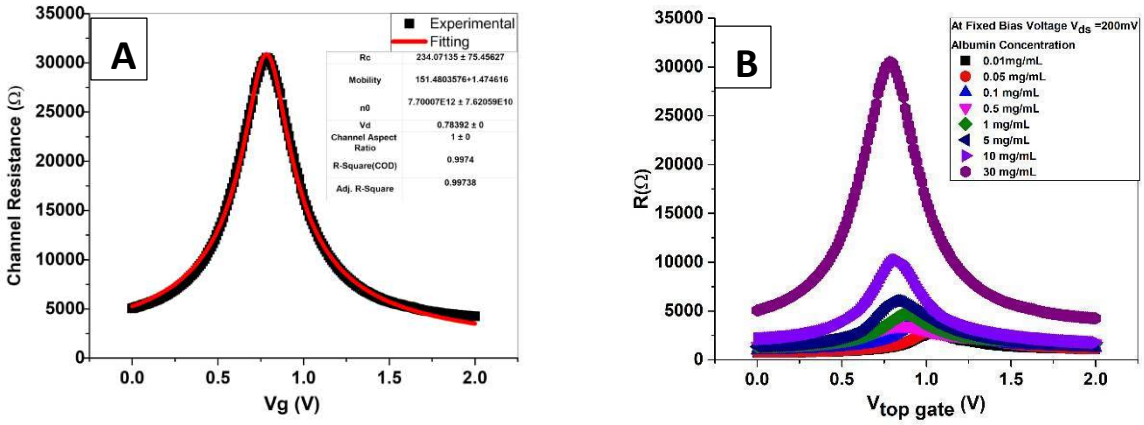

Figure 5.5: Transfer characteristics of the electrolyte-gated GFET during albumin sensing. (A) Nonlinear fitting of the resistance–gate voltage transfer characteristic used for extraction of transport parameters. (B) Evolution of the transfer characteristics with increasing Human Serum Albumin concentration showing systematic modulation of the charge neutrality region and concentration-dependent Dirac voltage displacement.

A concentration-dependent shift in the Dirac voltage is observed throughout the sensing measurements. The shift of the charge neutrality point reflects electrostatic perturbation arising from the adsorption of negatively charged albumin molecules within the electric double-layer region. Because albumin contains multiple ionizable surface residues distributed across the molecular structure, adsorption generates localized variations in interfacial potential that influence the effective gating conditions experienced by the graphene channel.

In addition to the Dirac voltage displacement, progressive broadening of the transfer characteristics is observed at increasing albumin concentrations. The broadening behaviour suggests enhanced carrier scattering and increased electrostatic disorder within the graphene channel during protein adsorption. Under these conditions, the electrical response cannot be interpreted solely through carrier-density modulation but must also account for adsorption-induced perturbations affecting transport uniformity across the graphene surface.

At low albumin concentrations, the transfer characteristics exhibited a moderate shift in the Dirac region accompanied by slight broadening of the conductance profile. In this regime, adsorption events remained relatively sparse, and the interfacial electric field was perturbed primarily by isolated biomolecular interactions near the graphene surface. The sensing response therefore

reflected the initial electrostatic influence of negatively charged albumin molecules within the electric double layer.

As the albumin concentration increased, progressive modification of the transfer characteristics became increasingly pronounced. The gradual broadening of the conductance curve suggested the development of heterogeneous adsorption states across the graphene interface. Under these conditions, the interfacial electrostatic environment became spatially non-uniform due to variations in adsorption orientation, intermolecular separation, and local charge distribution near the sensing surface.

At higher concentrations, the transfer characteristics approached a more stabilized broadening regime in which further increases in albumin concentration produced comparatively smaller variations in the overall response profile. This behaviour indicates partial electrostatic screening saturation within the interfacial region, where accumulation of adsorbed biomolecules increasingly attenuated the effective modulation field near the graphene channel. Because albumin molecules adsorb with varying orientations and interaction distances, the resulting electrostatic perturbations are spatially non-uniform.

5.4.3 Concentration-Dependent Electrostatic Modulation

To further examine the sensing behaviour of the electrolyte-gated GFET, the evolution of the electrical response was analyzed as a function of albumin concentration. The measured transfer characteristics demonstrate that progressive adsorption of albumin molecules near the graphene surface systematically modifies the electrostatic environment within the electric double-layer region.

At low concentrations, isolated adsorption events generate localized variations in interfacial charge distribution near the graphene channel. Because the graphene surface remains only partially occupied, these initial adsorption events can produce measurable shifts in the local gating conditions of the device. As the concentration increases, the growing population of adsorbed albumin molecules progressively alters the interfacial electric field established at the graphene–electrolyte interface.

The concentration-dependent evolution of the transfer characteristics indicates increasing electrostatic coupling between the adsorbed biomolecular layer and the graphene channel. Since albumin contains multiple ionizable surface residues, adsorption modifies the local potential distribution within the electric double layer and influences the charge neutrality condition of the transistor. The gradual displacement of the transfer response with increasing concentration therefore, reflects progressive modulation of the interfacial electrostatic environment during protein adsorption.

The sensing behaviour is additionally influenced by ionic screening within the electrolyte. Although deionized water was employed to minimize screening effects, residual ions present in the sensing environment partially attenuate the electric field generated by adsorbed proteins. Consequently, the effective electrostatic interaction depends strongly on the proximity of the adsorbed molecules to the graphene surface. Proteins located closer to the graphene channel contribute more effectively to modulation of the interfacial electric field than molecules positioned farther from the effective screening region.

As surface coverage increases during concentration-dependent adsorption, the collective electrostatic influence of the adsorbed protein layer becomes progressively more significant. This behaviour is reflected experimentally through systematic evolution of the transfer characteristics and concentration-dependent displacement of the charge neutrality region. The observed response therefore indicates that albumin sensing in electrolyte-gated GFETs is governed by interfacial electrostatic coupling occurring within the electric double-layer environment.

5.5 Adsorption-Induced Disorder and Transport Evolution

5.5.1 Transconductance Evolution during Albumin Adsorption

The evolution of transconductance was analyzed in order to evaluate the influence of albumin adsorption on gate modulation efficiency within the electrolyte-gated GFET. Figure 5.6 presents the transconductance response extracted from the transfer characteristics measured over the investigated concentration range.

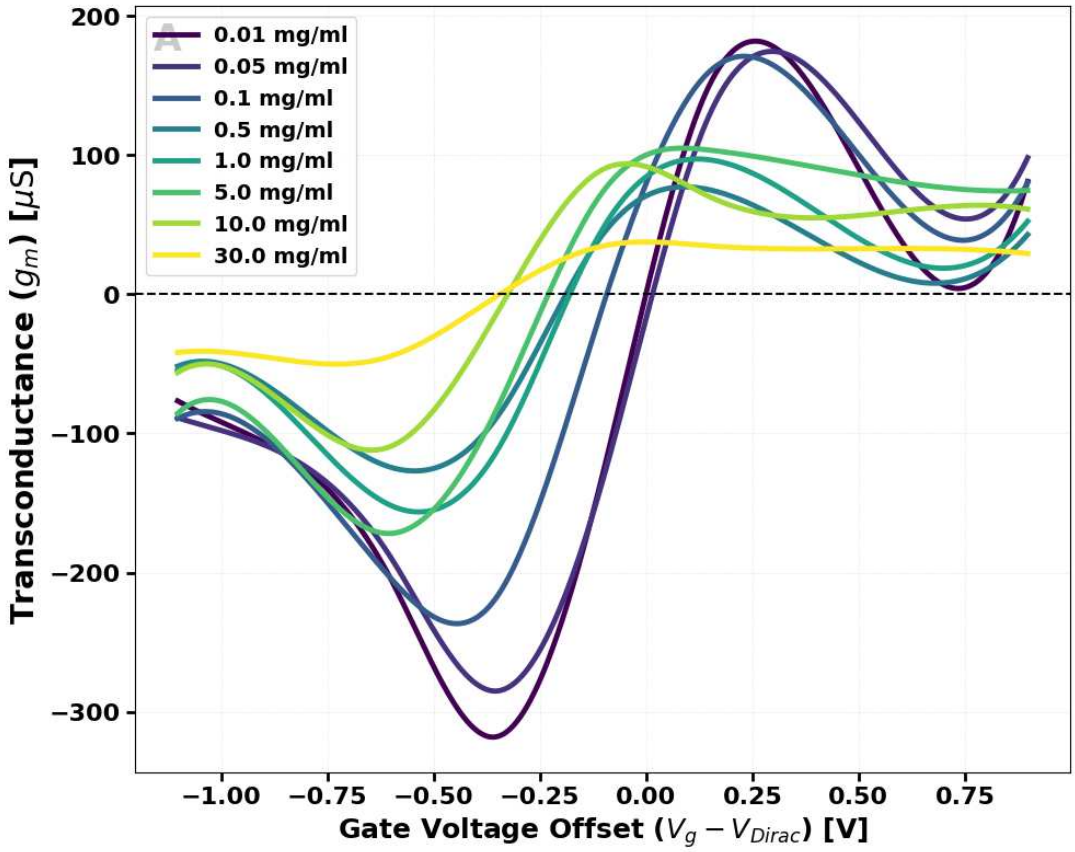

Figure 5.6: Evolution of transconductance as a function of gate voltage relative to the Dirac voltage under increasing Human Serum Albumin concentration, showing progressive broadening and reduction of gate modulation efficiency during adsorption

The transconductance exhibits systematic variation with increasing albumin concentration. At lower concentrations, the device maintains comparatively sharp transconductance behaviour near the charge neutrality region, indicating efficient electrostatic modulation of the graphene channel. As the concentration increases, progressive broadening and reduction of the transconductance peaks are observed.

The reduction in transconductance suggests that adsorption-induced perturbations influence the ability of the gate field to effectively modulate carrier transport within the graphene channel. Since transconductance is directly related to the sensitivity of the drain current to gate voltage variation, the observed decrease indicates reduced modulation efficiency arising from increasing electrostatic disorder at the graphene interface.

The broadening of the transconductance response further suggests the development of spatially non-uniform carrier transport conditions within the graphene layer. Adsorbed albumin molecules generate localized perturbations in the interfacial potential landscape, producing variations in carrier concentration and transport pathways across the graphene channel. Under these conditions, the electrical response becomes increasingly governed by heterogeneous interfacial interactions rather than by uniform electrostatic gating alone.

The concentration-dependent evolution of transconductance therefore indicates that albumin adsorption modifies both the electrostatic environment and the transport uniformity of the graphene channel during sensing.

5.5.2 Broadening of the Charge Neutrality Region

To further investigate adsorption-induced transport perturbation, the evolution of the charge neutrality region was analyzed through the variation of ΔVpp and full-width at half-maximum (FWHM) extracted from the transfer characteristics. Figure 5.7 presents the concentration dependence of the extracted broadening parameters.

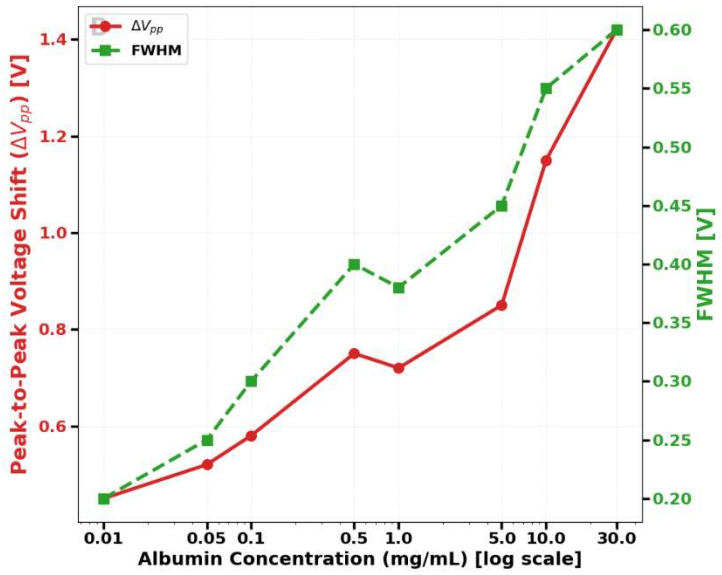

Figure 5.7: Concentration-dependent broadening of the charge neutrality region during albumin adsorption. Evolution of peak-to-peak voltage separation (ΔV_{pp}) and full width at half maximum (FWHM) extracted from the transfer characteristics as a function of Human Serum Albumin concentration

As the albumin concentration increases, progressive broadening of the transfer characteristics is observed together with an increase in the width of the charge neutrality region. The increase in ΔVpp and FWHM indicates that the transition between hole-dominated and electron-dominated transport becomes less abrupt during protein adsorption.

This broadening behaviour is consistent with the development of electrostatic inhomogeneity across the graphene surface. Adsorption of albumin molecules with different orientations and interaction distances generates spatially varying perturbations in the local electrostatic potential. As a result, different regions of the graphene channel experience non-uniform carrier modulation, producing broadened transport characteristics near the charge neutrality condition.

The broadening of the transfer response additionally suggests the presence of increased carrier scattering and disorder-mediated transport effects. Localized electrostatic fluctuations generated by adsorbed proteins can modify carrier trajectories within the graphene layer and reduce transport uniformity across the channel. These effects become progressively stronger as surface coverage increases during concentration-dependent adsorption.

The evolution of ΔVpp and FWHM therefore provides experimental evidence that albumin sensing in electrolyte-gated GFETs involves substantial transport perturbation associated with adsorption-induced electrostatic disorder at the graphene–electrolyte interface.

5.5.3 Mobility Suppression and Disorder-Mediated Scattering

Carrier mobility was subsequently analyzed to evaluate the influence of albumin adsorption on transport dynamics within the graphene channel. Figure 5.8 presents the extracted mobility values as a function of albumin concentration.

The measured mobility decreases progressively with increasing concentration, indicating that adsorption-induced perturbations increasingly influence carrier transport within the graphene layer. At low albumin concentrations, the graphene channel maintains comparatively high mobility, consistent with relatively limited interfacial perturbation. As the concentration increases, the growing population of adsorbed molecules contributes to enhanced carrier scattering and reduced transport efficiency.

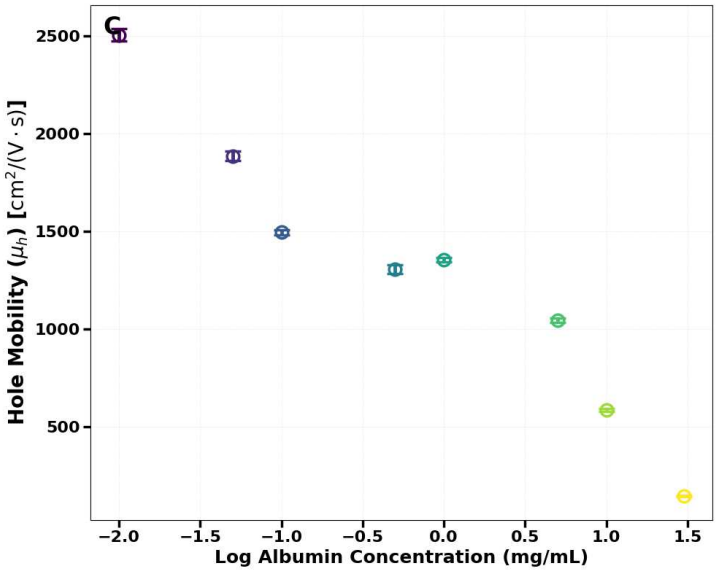

Figure 5.8: Concentration-dependent suppression of hole mobility during Human Serum Albumin adsorption, indicating progressive transport perturbation and adsorption-induced carrier scattering within the graphene channel.

The observed mobility suppression is associated with disorder-mediated scattering arising from heterogeneous electrostatic perturbations near the graphene interface. Because albumin molecules adsorb with variable orientations and charge distributions, localized fluctuations in interfacial potential develop across the graphene surface. These fluctuations act as scattering centres that perturb carrier transport pathways and reduce effective mobility within the channel.

The mobility evolution additionally supports the interpretation that the sensing response cannot be fully described through electrostatic carrier-density modulation alone. While Dirac voltage shifts reflect changes in the charge neutrality condition, mobility suppression indicates that biomolecular adsorption also modifies the transport landscape of the graphene channel through adsorption-induced disorder.

The concentration dependence of mobility therefore provides important evidence that protein adsorption affects both electrostatic gating and carrier transport dynamics within electrolyte-gated GFET systems.

5.5.4 Charge Puddles and Local Electrostatic Fluctuations

The adsorption of albumin molecules near the graphene interface produced substantial spatial variation in the local electrostatic environment. Because the adsorbed biomolecules exhibited heterogeneous charge distributions and orientation-dependent interactions, the resulting interfacial field became highly non-uniform across the graphene surface. These local electrostatic fluctuations promoted the formation of carrier-density inhomogeneities commonly associated with charge puddles in graphene systems.

The emergence of these localized charge regions introduced additional transport instability within the graphene channel. Spatial fluctuations in carrier concentration generated variations in local conductivity, thereby enhancing carrier scattering and disrupting uniform charge transport along the sensing interface. The effect became increasingly significant as adsorption density increased and intermolecular electrostatic interactions became more spatially correlated near the graphene surface.

Such transport inhomogeneity is expected to contribute directly to the experimentally observed broadening of the transfer characteristics at elevated albumin concentrations. Rather than arising solely from uniform electrostatic gating, the sensing response reflects the combined influence of interfacial charge redistribution, conductivity fluctuation, and adsorption-induced transport disorder within the graphene channel.

5.6 Analytical Calibration and Ultra-Trace Albumin Detection

5.6.1 Concentration-Dependent Sensing Response

The concentration-dependent sensing behaviour of the electrolyte-gated GFET was evaluated using the transport parameters extracted from the transfer characteristics. Particular attention was devoted to the extraction of Responsivity as a function of albumin concentration, since adsorption-induced disorder was found to strongly influence carrier transport within the graphene channel.

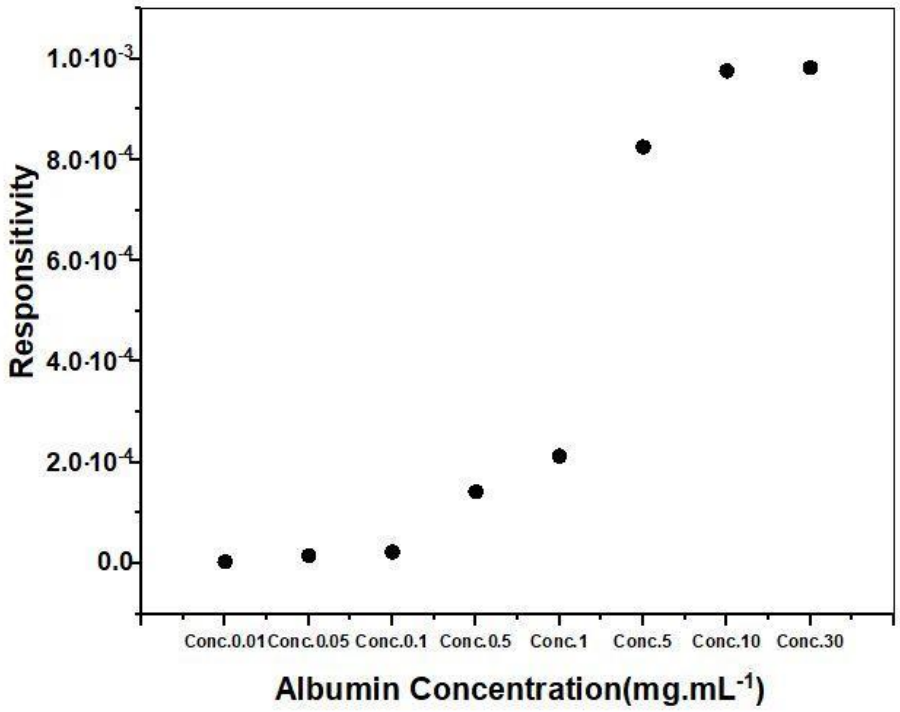

Figure 5.9: Concentration-dependent sensing response of the electrolyte-gated GFET measured at the charge neutrality region during Human Serum Albumin adsorption.

Figure 5.9 presents the variation of the extracted sensing response across the investigated concentration range. A systematic increase in the sensing signal is observed with increasing albumin concentration, indicating progressive modulation of the graphene transport environment during biomolecular adsorption.

At low concentrations, relatively small changes in albumin coverage produce measurable variation in the electrical response of the device. This behaviour reflects the high sensitivity of the electrolyte-gated graphene channel to localized electrostatic perturbations occurring near the graphene surface. Because graphene exhibits strong transport sensitivity near the charge neutrality region, isolated adsorption events can generate detectable modulation of carrier transport even under ultra-trace concentration conditions.

As the concentration increases, the sensing response evolves progressively due to the growing population of adsorbed proteins at the graphene interface. The increasing surface coverage contributes to enhanced electrostatic disorder and stronger perturbation of carrier transport

pathways within the graphene channel. Under these conditions, the measured response reflects the combined influence of electrostatic gating, adsorption-induced scattering, and transport broadening effects.

The concentration-dependent behaviour additionally indicates that the sensing mechanism is not governed solely by uniform surface charge accumulation. Instead, heterogeneous adsorption and localized electrostatic fluctuations contribute significantly to the evolution of the transport response during albumin adsorption.

5.6.2 Inverse Mobility as a Sensing Metric

To quantify the adsorption-induced transport perturbation, the inverse mobility parameter was employed as the primary sensing metric for albumin detection. In contrast to conventional GFET biosensing approaches based primarily on Dirac voltage shifts, the inverse mobility framework directly reflects modifications in carrier transport arising from adsorption-induced disorder within the graphene channel.

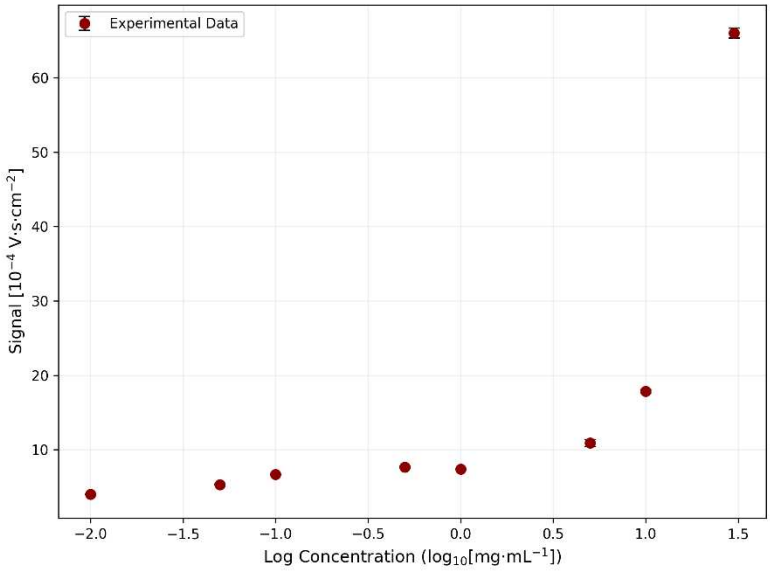

Figure 5.10: Evolution of inverse mobility as a function of Human Serum Albumin concentration, demonstrating adsorption-induced transport perturbation and carrier scattering within the graphene channel.

Figure 5.10 presents the variation of inverse mobility as a function of albumin concentration. The inverse mobility increases systematically with concentration, indicating progressive degradation of carrier transport associated with increasing protein adsorption at the graphene interface.

The use of inverse mobility provides enhanced sensitivity to local electrostatic fluctuations generated by heterogeneous adsorption behaviour. Since adsorbed albumin molecules introduce localized perturbations in the interfacial potential landscape, carrier scattering within the graphene channel becomes increasingly sensitive to surface disorder as concentration increases. Under these conditions, mobility degradation becomes a more direct indicator of adsorption-induced transport perturbation than simple Dirac voltage displacement alone.

The inverse mobility response additionally exhibits comparatively stable monotonic behaviour across the investigated concentration range. This behaviour suggests that transport-based sensing metrics may provide improved robustness for biosensing analysis under conditions where electrostatic gating effects alone do not fully describe the device response.

The results therefore indicate that adsorption-induced disorder plays a central role in determining the sensing behaviour of electrolyte-gated GFETs during albumin detection.

5.6.3 Calibration Behaviour and Detection Sensitivity

The analytical calibration behaviour of the device was evaluated using the extracted sensing response over the investigated concentration interval. Figure 5.11 presents the calibration curve obtained from the concentration-dependent transport analysis.

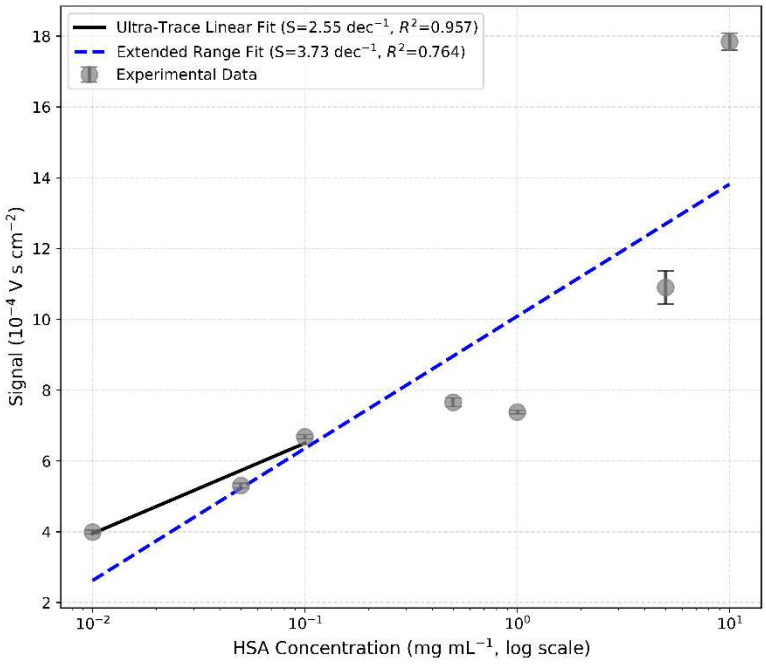

Figure 5.11: Evolution of inverse mobility as a function of Human Serum Albumin concentration, demonstrating transport-sensitive detection of adsorption-induced disorder and carrier scattering effects within the graphene channel

The measured response exhibits a monotonic concentration dependence over a broad dynamic range, demonstrating the capability of the electrolyte-gated GFET platform for quantitative albumin detection. At lower concentrations, the sensing response evolves rapidly due to the strong influence of isolated adsorption events on the graphene transport environment. As the concentration increases, the response gradually approaches a reduced-slope regime associated with increasing surface coverage and adsorption saturation effects.

The nonlinear behaviour of the calibration response is consistent with heterogeneous adsorption processes occurring at the graphene interface. Since albumin molecules adsorb with varying orientations and interaction strengths, the resulting transport perturbation does not evolve linearly with concentration. Instead, the sensing behaviour reflects the collective influence of adsorption statistics, electrostatic screening, and disorder-mediated scattering within the graphene channel.

The sensitivity of the device remains sufficiently high to enable detection within the ultra-trace concentration regime. This behaviour is primarily associated with the strong electrostatic coupling

established through electrolyte gating together with the high transport sensitivity of graphene to local interfacial perturbations.

The calibration analysis therefore demonstrates that electrolyte-gated GFETs can provide stable concentration-dependent albumin detection through transport-based sensing mechanisms governed by adsorption-induced electrostatic disorder.

5.6.4 Freundlich Adsorption Analysis

To further investigate the adsorption behaviour associated with the sensing response, the concentration-dependent data were analyzed using the Freundlich adsorption model. The Freundlich framework is commonly employed to describe heterogeneous adsorption processes occurring on non-uniform surfaces where adsorption energies vary across different interaction sites.

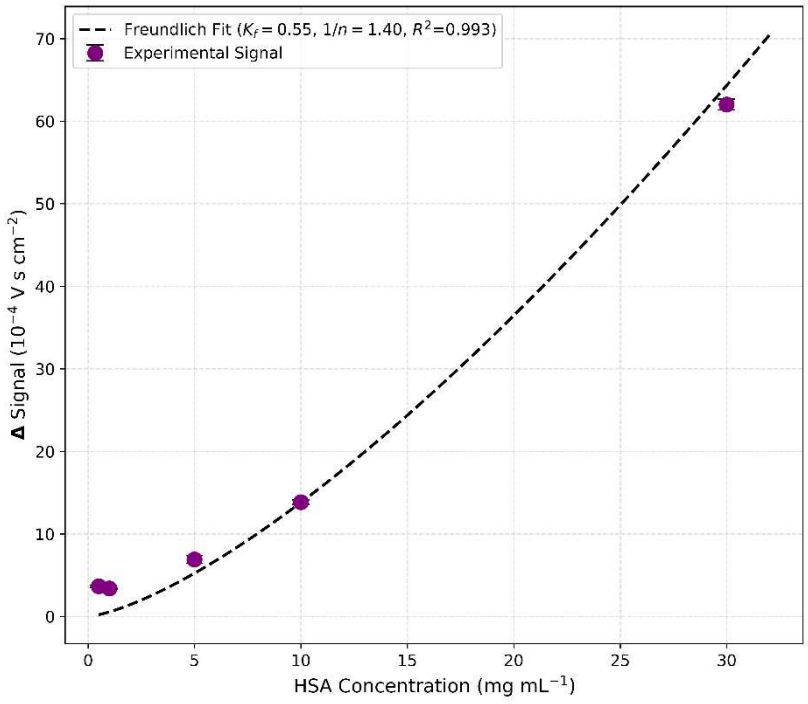

Figure 5.12: Freundlich fitting of the experimentally measured sensing response showing nonlinear concentration-dependent adsorption behaviour associated with heterogeneous albumin adsorption at the graphene interface.

Figure 5.12 presents the Freundlich fitting obtained from the experimental sensing response. The measured behaviour exhibits good agreement with the heterogeneous adsorption model, indicating that albumin adsorption on graphene occurs through a distribution of interaction strengths rather than through uniform monolayer adsorption.

The applicability of the Freundlich model is consistent with the atomistic adsorption behaviour observed in the Brownian Dynamics simulations. Since albumin molecules adsorb with variable orientations and localized interaction geometries, the resulting adsorption landscape at the graphene interface becomes spatially heterogeneous. Different adsorption configurations therefore contribute differently to the overall transport perturbation observed experimentally.

The heterogeneous adsorption behaviour additionally supports the experimentally observed broadening of the transfer characteristics and mobility suppression discussed in the previous section. Because different regions of the graphene surface experience distinct electrostatic perturbations during adsorption, the resulting carrier transport behaviour becomes increasingly non-uniform as concentration increases.

The combined calibration and adsorption analysis therefore indicates that albumin sensing in electrolyte-gated GFETs is governed by coupled electrostatic and disorder-mediated transport mechanisms associated with heterogeneous biomolecular adsorption at the graphene interface.

5.7 Discussion

5.7.1 Electrostatic Origin of the Sensing Response

The sensing behaviour of the electrolyte-gated GFET originates from electrostatic coupling established at the graphene-electrolyte interface through the electric double layer. When a gate potential is applied, redistribution of ions within the electrolyte forms an interfacial capacitive region consisting of the Stern layer and the surrounding diffuse layer. The resulting electric field modulates the Fermi level of graphene and controls the carrier population within the channel [31].

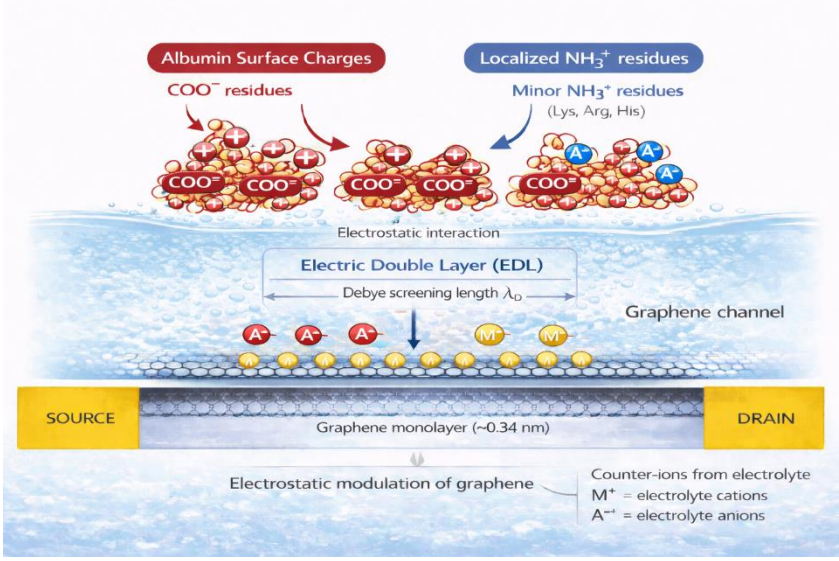

Figure 5.13: Schematic illustration of electrostatic coupling and electric double-layer modulation during Human Serum Albumin adsorption at the electrolyte-gated graphene interface. Heterogeneous albumin surface charge distributions perturb the interfacial ionic environment within the Debye screening region, producing electrostatic modulation of the graphene channel under electrolyte-gated sensing conditions.

Because the effective thickness of the electric double layer is on the nanometer scale, electrolyte-gated graphene transistors exhibit substantially higher interfacial capacitance than conventional dielectric gated devices. Under these conditions, relatively small variations in interfacial charge distribution can produce measurable changes in the electrical characteristics of the graphene channel. This strong capacitive coupling is responsible for the high sensitivity of electrolyte-gated GFETs to surface-bound biomolecular interactions.

During albumin adsorption, charged and Polar Regions of the protein modify the local electric field within the interfacial region near the graphene surface. These adsorption-induced variations alter the electrostatic boundary conditions experienced by the graphene channel and shift the charge neutrality condition of the transistor. The experimentally observed evolution of the transfer characteristics and Dirac voltage therefore reflects modulation of the interfacial electric field during protein adsorption.

The sensing response is additionally influenced by the spatial proximity of the adsorbed proteins to the graphene surface. Since electrostatic coupling occurs primarily within the effective electric double-layer region, proteins located closer to the graphene interface contribute more strongly to

modulation of the local gating environment. The measured electrical response, therefore, depends on the interaction between the adsorbed biomolecular layer and the interfacial electric field established within the electrolyte-gated structure.

The observed sensing behaviour demonstrates that electrolyte-gated GFET biosensors operate through direct modulation of the interfacial electrostatic environment at the graphene–electrolyte interface. Under these conditions, biomolecular adsorption influences the electrical response of the device through electric double-layer coupling and local field redistribution near the graphene channel.

5.7.2 Ionic Screening and Interfacial Coupling

The sensing response of electrolyte-gated GFETs is strongly influenced by ionic screening within the electrolyte environment. In liquid-gated systems, mobile ions present in the solution partially attenuate the electric field generated by adsorbed biomolecules, thereby reducing the effective electrostatic coupling between the protein layer and the graphene channel [32]. The extent of this attenuation is governed by the Debye screening length, which defines the characteristic distance over which electrostatic fields decay within the electrolyte.

The Debye screening length depends primarily on the ionic strength of the sensing medium. As ionic concentration increases, the population of mobile ions near the graphene interface also increases, leading to stronger electrostatic screening and shorter effective field penetration distance. Under highly concentrated electrolyte conditions, the electric field generated by adsorbed biomolecules becomes rapidly attenuated, reducing the effective interaction between the biomolecular layer and the graphene surface.

In the present work, deionized water was employed as the sensing medium in order to minimize ionic screening effects and increase the effective Debye length within the interfacial region. The reduced ionic concentration allows electrostatic fields generated by adsorbed albumin molecules to extend farther toward the graphene channel, thereby improving interfacial coupling during sensing measurements.

The effectiveness of electrostatic coupling additionally depends on the spatial separation between the adsorbed proteins and the graphene surface. Biomolecules positioned within the effective screening distance contribute more significantly to modulation of the interfacial electric field than molecules located farther from the graphene interface. Consequently, adsorption geometry and interaction distance play important roles in determining the magnitude of the electrical response observed during sensing.

Hydration layers and interfacial electrolyte structure further influence the effective coupling distance within the electric double-layer region. Even when proteins are adsorbed near the graphene surface, the presence of solvated ions and structured water layers partially separates the biomolecular charge distribution from the graphene channel. This interfacial separation contributes to attenuation of the electric field reaching the graphene surface during sensing.

The experimental behaviour observed in the present work indicates that electrolyte screening and interfacial coupling represent critical factors governing biomolecular detection in electrolyte-gated graphene transistors. The measured sensing response therefore reflects the balance between adsorption-induced electric field generation and electrolyte-mediated field attenuation within the interfacial region.

5.7.3 Adsorption-Induced Disorder and Transport Perturbation

Adsorption-induced transport perturbation originates from the heterogeneous distribution of albumin molecules near the graphene surface. Since the adsorbed biomolecules possess non-uniform surface charge distributions and variable adsorption orientations, the resulting interfacial environment becomes electrostatically disordered at the nanoscale.

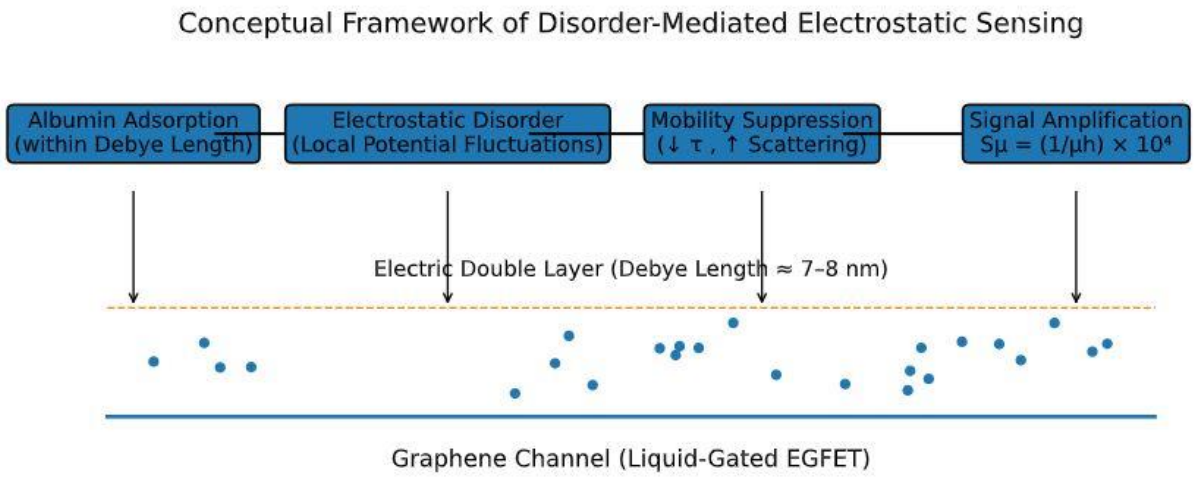

Figure 5.14: Conceptual framework illustrating disorder-mediated electrostatic sensing in electrolyte-gated graphene biosensors. Biomolecular adsorption within the Debye screening region produces localized electrostatic perturbations and transport disorder, leading to carrier mobility suppression and amplified transport-sensitive electrical response.

This spatial disorder modifies the local carrier landscape within the graphene channel. Variations in interfacial charge density generate localized fluctuations in carrier concentration, producing enhanced scattering regions and disrupting the uniformity of charge transport across the sensing surface. The effect becomes increasingly pronounced at higher adsorption densities where intermolecular electrostatic interactions contribute to additional carrier inhomogeneity.

The resulting transport perturbation contributes directly to degradation of carrier mobility and broadening of the transfer characteristics observed experimentally. Under these conditions, the sensing response no longer reflects purely ideal electrostatic gating behaviour, but instead incorporates the influence of adsorption-induced disorder on channel conductivity.

Consequently, the GFET sensing mechanism should be interpreted as a coupled electrostatic–transport process in which biomolecular adsorption simultaneously modifies interfacial electric fields and perturbs carrier transport within the graphene layer. This combined behaviour provides a physically consistent explanation for the nonlinear response evolution observed during albumin sensing.

5.7.4 Correlation between Atomistic Adsorption and Electrical Response

The combined experimental and atomistic analysis reveals strong correlation between the adsorption behaviour observed in the Brownian Dynamics simulations and the transport perturbations measured experimentally. The simulations demonstrate that albumin adsorption occurs through dynamically distributed molecular orientations rather than through a single preferred adsorption geometry. Different adsorption configurations therefore, generate distinct local electrostatic perturbations near the graphene surface.

This heterogeneous adsorption behaviour is consistent with the experimentally observed broadening of the transfer characteristics and concentration-dependent mobility degradation. As the population of adsorbed proteins increases, the interfacial electrostatic landscape becomes progressively more non-uniform, leading to enhanced carrier scattering and disorder-mediated transport modulation within the graphene channel.

The atomistic analysis additionally explains the nonlinear calibration behaviour observed experimentally. Since different adsorption configurations contribute differently to the interfacial electrostatic perturbation, the electrical response evolves through collective statistical adsorption behaviour rather than through simple linear surface charge accumulation. The applicability of the Freundlich adsorption model further supports the presence of heterogeneous adsorption interactions at the graphene interface.

The agreement between simulation and experiment therefore indicates that the sensing response of electrolyte-gated GFETs is governed by coupled multiscale processes involving molecular adsorption dynamics, electrostatic perturbation, and carrier transport evolution within the graphene channel.

5.7.5 Implications for Electrolyte Gated Graphene Biosensing

The results presented in this chapter demonstrate that electrolyte-gated GFET biosensors can achieve highly sensitive label-free detection of biomolecules through transport-based sensing mechanisms governed by interfacial electrostatic interactions. In contrast to conventional sensing approaches that primarily focus on Dirac voltage displacement, the present work shows that

adsorption-induced disorder and transport perturbation provide additional information regarding biomolecular interactions occurring at the graphene surface.

The combined electrostatic and transport interpretation developed here may therefore provide a broader framework for understanding sensing behaviour in electrolyte-gated graphene devices operating under biologically relevant conditions. Because many biomolecules exhibit heterogeneous charge distributions and orientation-dependent adsorption behaviour, transport perturbation effects are expected to play an important role in a wide range of graphene biosensing applications.

The integration of atomistic simulation with experimental transport analysis additionally provides a useful multiscale approach for investigating biomolecular interactions in graphene-based sensing platforms. By correlating adsorption dynamics with experimentally observed transport evolution, the sensing response can be interpreted in terms of physically meaningful interfacial mechanisms rather than through empirical signal variation alone.

The results therefore indicate that adsorption-induced electrostatic disorder represents an important component of the sensing behaviour of electrolyte-gated graphene transistors and may provide a useful basis for the development of future ultra-sensitive graphene biosensing platforms.

5.8 Summary of the Chapter

This chapter investigated the label-free detection of Human Serum Albumin using electrolyte-gated graphene field-effect transistors through a combined experimental and atomistic analysis framework. The sensing response of the devices was examined in terms of electrostatic modulation, adsorption-induced transport perturbation, and concentration-dependent evolution of the graphene channel characteristics under liquid-gated operating conditions.

The electrical measurements demonstrated that albumin adsorption systematically modifies both the output and transfer characteristics of the electrolyte-gated GFET. Progressive evolution of the Dirac voltage, transconductance, and transport broadening was observed with increasing protein concentration, indicating that adsorption of albumin molecules perturbs the local electrostatic environment at the graphene-electrolyte interface. The experimental results additionally showed

that the sensing response extends beyond simple carrier-density modulation and involves substantial modification of carrier transport within the graphene channel.

Analysis of the transport parameters revealed progressive suppression of carrier mobility together with broadening of the charge neutrality region during albumin adsorption. These observations indicate the development of adsorption-induced electrostatic disorder within the graphene channel arising from heterogeneous protein adsorption behaviour. The inverse mobility sensing framework demonstrated strong sensitivity to concentration-dependent transport perturbation and provided an effective metric for ultra-trace albumin detection. The electrolyte-gated GFET platform demonstrated concentration-dependent albumin detection over the range of 0.01–30 mg mL^{-1}, with a calculated limit of detection of 0.0087 mg mL^{-1} under low ionic-strength conditions.

Brownian Dynamics simulations were employed to investigate the adsorption behaviour of albumin molecules near the graphene surface. The simulations demonstrated that adsorption occurs through heterogeneous molecular orientations rather than through a single preferred adsorption configuration. Because albumin possesses a non-uniform surface charge distribution, different adsorption geometries generate distinct local electrostatic perturbations at the graphene interface. The atomistic analysis therefore supports the experimentally observed transport broadening and mobility degradation associated with adsorption-induced scattering effects.

The combined experimental and atomistic analysis presented in this chapter demonstrates that albumin detection in electrolyte-gated GFETs is governed by coupled interfacial mechanisms involving electric double-layer modulation, adsorption heterogeneity, ionic screening, and transport perturbation within the graphene channel. Rather than behaving as a purely electrostatic gating system, the sensing response evolves through spatially distributed adsorption-induced variations in the local carrier environment near the graphene surface. The results further indicate that transport-sensitive analysis provides a physically meaningful framework for interpreting biomolecular interactions in electrolyte-gated graphene biosensors, particularly under conditions where heterogeneous adsorption and interfacial screening dominate the sensing behaviour.

5.9 References

[1] Peters, T. (1995). *All about albumin: Biochemistry, genetics, and medical applications*. Academic Press.

[2] Quinlan, G. J., Martin, G. S., & Evans, T. W. (2005). Albumin: Biochemical properties and therapeutic potential. *Hepatology, 41*(6), 1211–1219. https://doi.org/10.1002/hep.20720

[3] Doweiko, J. P., & Nompleggi, D. J. (1991). Role of albumin in human physiology and pathophysiology. *JPEN Journal of Parenteral and Enteral Nutrition, 15*(2), 207–211. https://doi.org/10.1177/0148607191015002207

[4] Justino, C. I. L., Rocha-Santos, T. A. P., & Duarte, A. C. (2010). Review of analytical figures of merit of sensors and biosensors in clinical applications. *TrAC Trends in Analytical Chemistry, 29*(10), 1172–1183. https://doi.org/10.1016/j.trac.2010.07.008

[5] Novoselov, K. S., Geim, A. K., Morozov, S. V., Jiang, D., Zhang, Y., Dubonos, S. V., Grigorieva, I. V., & Firsov, A. A. (2004). Electric field effect in atomically thin carbon films. *Science, 306*(5696), 666–669. https://doi.org/10.1126/science.1102896

[6] Schwierz, F. (2010). Graphene transistors. *Nature Nanotechnology, 5*(7), 487–496. https://doi.org/10.1038/nnano.2010.89

[7] Fu, W., Jiang, L., van Geest, E. P., Lima, L. M. C., & Schneider, G. F. (2017). Sensing at the surface of graphene field-effect transistors. *Advanced Materials, 29*(6), 1603610. https://doi.org/10.1002/adma.201603610

[8] Ohno, Y., Maehashi, K., Yamashiro, Y., & Matsumoto, K. (2009). Electrolyte-gated graphene field-effect transistors for detecting pH and protein adsorption. *Nano Letters, 9*(9), 3318–3322. https://doi.org/10.1021/nl901596m

[9] Baridi, G., Liaquat, A., Martini, L., Nappi, L., Rapuzzi, F., Clericò, V., Abidi, E. H., Meziani, Y. M., Amado, M., Diez, E., Brancolini, G., Rovati, L., & Rossella, F. (2026). Graphene-based

chemical field-effect transistors: Impact of electric double layer model and quantum capacitance on Na^+ detection capabilities. *Micromachines, 17*(4), 433. https://doi.org/10.3390/mi17040433

[10] Heller, I., Chatoor, S., Männik, J., Zevenbergen, M. A., Dekker, C., & Lemay, S. G. (2010). Influence of electrolyte composition on liquid-gated carbon nanotube and graphene transistors. *Journal of the American Chemical Society, 132*(48), 17149–17156. https://doi.org/10.1021/ja105088h

[11] Ohno, Y., Maehashi, K., & Matsumoto, K. (2010). Label-free biosensors based on aptamer-modified graphene field-effect transistors. *Journal of the American Chemical Society, 132*(51), 18012–18013. https://doi.org/10.1021/ja108127r

[12] Ping, J., Johnson, A. T. C., & Andrews, A. M. (2016). Quantifying the effect of ionic screening with protein-decorated graphene transistors. *Nano Letters, 16*(7), 4415–4421. https://doi.org/10.1021/acs.nanolett.6b01612

[13] Bard, A. J., & Faulkner, L. R. (2001). *Electrochemical methods: Fundamentals and applications* (2nd ed.). Wiley.

[14] Fu, W., Feng, P., Mayer, D., Panaitov, G., Kireev, D., Offenhäusser, A., & Krause, H. J. (2021). Electrolyte-gated graphene field-effect transistors for biosensing applications: A review. *Micromachines, 12*(10), 1205. https://doi.org/10.3390/mi12101205

[15] Schmickler, W., & Santos, E. (2010). *Interfacial electrochemistry* (2nd ed.). Springer.

[16] Xia, J., Chen, F., Li, J., & Tao, N. (2009). Measurement of the quantum capacitance of graphene. *Nature Nanotechnology, 4*(8), 505–509. https://doi.org/10.1038/nnano.2009.177

[17] Peters, T. (1995). *All about albumin: Biochemistry, genetics, and medical applications*. Academic Press.

[18] Ping, J., Johnson, A. T. C., & Andrews, A. M. (2016). Quantifying the effect of ionic screening with protein-decorated graphene transistors. *Nano Letters, 16*(7), 4415–4421. https://doi.org/10.1021/acs.nanolett.6b01612

[19] Fu, W., Jiang, L., van Geest, E. P., Lima, L. M. C., & Schneider, G. F. (2017). Sensing at the surface of graphene field-effect transistors. *Advanced Materials, 29*(6), 1603610. https://doi.org/10.1002/adma.201603610

[20] Ermak, D. L., & McCammon, J. A. (1978). Brownian dynamics with hydrodynamic interactions. *The Journal of Chemical Physics, 69*(4), 1352–1360. https://doi.org/10.1063/1.436761

[21] Graphenea. (2024). *mGFET-4D Graphene transistor array datasheet*. Graphenea.

[22] Xia, J., Chen, F., Li, J., & Tao, N. (2009). Measurement of the quantum capacitance of graphene. *Nature Nanotechnology, 4*(8), 505–509. https://doi.org/10.1038/nnano.2009.177

[23] Fang, T., Konar, A., Xing, H., & Jena, D. (2007). Carrier statistics and quantum capacitance of graphene sheets and ribbons. *Applied Physics Letters, 91*(9), 092109. https://doi.org/10.1063/1.2776887

[24] Ermak, D. L., & McCammon, J. A. (1978). Brownian dynamics with hydrodynamic interactions. *The Journal of Chemical Physics, 69*(4), 1352–1360. https://doi.org/10.1063/1.436761

[25] Fu, W., Jiang, L., van Geest, E. P., Lima, L. M. C., & Schneider, G. F. (2017). Sensing at the surface of graphene field-effect transistors. *Advanced Materials, 29*(6), 1603610. https://doi.org/10.1002/adma.201603610

[26] Ping, J., Johnson, A. T. C., & Andrews, A. M. (2016). Quantifying the effect of ionic screening with protein-decorated graphene transistors. *Nano Letters, 16*(7), 4415–4421. https://doi.org/10.1021/acs.nanolett.6b01612

[27] Adam, S., Hwang, E. H., Galitski, V. M., & Das Sarma, S. (2007). A self-consistent theory for graphene transport. *Proceedings of the National Academy of Sciences, 104*(47), 18392–18397. https://doi.org/10.1073/pnas.0704772104

[28] Martin, J., Akerman, N., Ulbricht, G., Lohmann, T., Smet, J. H., von Klitzing, K., & Yacoby, A. (2008). Observation of electron–hole puddles in graphene using a scanning single-electron transistor. *Nature Physics, 4*(2), 144–148. https://doi.org/10.1038/nphys781

[29] Freundlich, H. (1906). Über die adsorption in lösungen. *Zeitschrift für Physikalische Chemie, 57*, 385–470.

[30] Fu, W., Jiang, L., van Geest, E. P., Lima, L. M. C., & Schneider, G. F. (2017). Sensing at the surface of graphene field-effect transistors. *Advanced Materials, 29*(6), 1603610. https://doi.org/10.1002/adma.201603610

[31] Ohno, Y., Maehashi, K., Yamashiro, Y., & Matsumoto, K. (2009). Electrolyte-gated graphene field-effect transistors for detecting pH and protein adsorption. *Nano Letters, 9*(9), 3318–3322. https://doi.org/10.1021/nl901596m

[32] Ping, J., Johnson, A. T. C., & Andrews, A. M. (2016). Quantifying the effect of ionic screening with protein-decorated graphene transistors. *Nano Letters, 16*(7), 4415–4421. https://doi.org/10.1021/acs.nanolett.6b01612

CHAPTER 6

CONCLUSIONS AND FUTURE PERSPECTIVES

6.1 Conclusions

This thesis investigated electrolyte-gated graphene field-effect transistors as label-free biosensing platforms through a combination of continuum electrostatic modelling, experimental transport analysis, and atomistic adsorption interpretation. The work focused on understanding how interfacial electrostatic interactions, ionic screening, and adsorption-induced transport perturbations collectively govern the sensing behaviour of graphene biosensors operating under electrolyte-gated conditions.

A multiscale framework was developed to analyze the coupled physical mechanisms involved in electrolyte-gated GFET sensing. Continuum electrostatic simulations based on the Poisson-Nernst-Planck formalism were employed to investigate electric double-layer formation, ion redistribution, and electrostatic modulation near the graphene interface. The analysis demonstrated that electrolyte-gated graphene devices exhibit strong sensitivity to small interfacial perturbations because of the large capacitance associated with the nanometer-scale electric double layer.

The experimental and computational investigation of pH sensing demonstrated that variations in proton concentration systematically modify the interfacial electrostatic environment near the graphene surface. The finite element simulations showed that the sensing response strongly depends on electric double-layer coupling and ionic screening behaviour within the electrolyte region. These results established the importance of electrostatic modulation in governing the electrical response of electrolyte-gated graphene transistors.

The label-free detection of Human Serum Albumin was subsequently investigated through combined experimental characterization and atomistic adsorption analysis. The experimental results demonstrated systematic evolution of the transfer characteristics, transconductance, charge neutrality region, and carrier mobility with increasing albumin concentration. The observed response indicated that protein adsorption modifies not only the carrier density of the graphene

channel, but also the transport uniformity of the device through adsorption-induced disorder and scattering effects.

Brownian Dynamics simulations further demonstrated that albumin adsorption occurs through heterogeneous molecular orientations and dynamically distributed adsorption configurations near the graphene surface. Because albumin possesses a non-uniform molecular charge distribution, different adsorption geometries generated distinct local electrostatic perturbations within the interfacial region. The atomistic analysis therefore provided physical insight into the experimentally observed transport broadening and mobility suppression measured during sensing.

The combined results of this thesis indicate that electrolyte-gated GFET biosensors operate through coupled electrostatic and transport-mediated interfacial mechanisms spanning continuum and atomistic scales. The sensing response therefore emerges from the interaction between electric double-layer modulation, ionic screening, heterogeneous adsorption behaviour, and carrier transport perturbation within the graphene channel.

6.1.1 Key Scientific Findings and Device Performance

One of the principal findings of this work is that electrolyte-gated graphene biosensors cannot be interpreted solely through conventional electrostatic carrier-density modulation models based only on Dirac voltage shifts. Although interfacial electrostatic coupling remains the dominant gating mechanism in electrolyte-gated GFETs, the experimental and atomistic analyses presented in this thesis demonstrate that adsorption-induced transport perturbation also plays a major role in determining the sensing response.

The finite-element electrostatic analysis demonstrated that the electric double layer strongly governs the interfacial modulation behaviour of electrolyte-gated graphene transistors. Because the effective gate capacitance is dominated by the nanometer-scale electric double layer, relatively small perturbations in interfacial charge distribution produce measurable changes in the electrical response of the graphene channel. The simulations further showed that ionic screening significantly influences the penetration of electrostatic fields toward the graphene surface and therefore strongly affects sensing sensitivity under electrolyte conditions.

The experimental analysis of albumin sensing revealed systematic broadening of the transfer characteristics together with concentration-dependent suppression of carrier mobility and transconductance. These observations indicate that biomolecular adsorption progressively modifies the local transport landscape of the graphene channel during sensing. Rather than behaving as a uniformly gated conductor, the graphene surface develops spatially distributed conductivity fluctuations associated with heterogeneous adsorption-induced electrostatic perturbations.

The electrolyte-gated GFET platform demonstrated stable concentration-dependent electrical modulation across the investigated albumin concentration range, with a calculated limit of detection of **0.0087 mg.mL^{-1}** under the experimental conditions employed in this work. Progressive evolution of the transfer characteristics, systematic broadening of the charge neutrality region, and concentration-dependent suppression of carrier mobility collectively indicated strong sensitivity of the graphene channel to adsorption-induced interfacial perturbations.. The observed transport behaviour further demonstrated that inverse mobility analysis provides enhanced sensitivity to adsorption-induced disorder and conductivity fluctuation compared with sensing interpretation based solely on Dirac voltage displacement. These results indicate that transport-sensitive electrical analysis provides an effective framework for investigating heterogeneous biomolecular interactions in electrolyte-gated graphene biosensors.

The Brownian Dynamics simulations additionally demonstrated that albumin adsorption occurs through heterogeneous molecular configurations rather than through a single preferred adsorption geometry. Different adsorption orientations generated spatially varying interfacial electrostatic perturbations near the graphene surface, producing non-uniform modulation of the carrier environment within the graphene channel. The atomistic interpretation therefore provided direct physical support for the experimentally observed transport broadening and disorder-mediated sensing behaviour.

The combined electrostatic, experimental, and atomistic analyses developed in this thesis therefore suggest that electrolyte-gated GFET sensing is governed by coupled multiscale processes involving electric double-layer modulation, ionic screening, adsorption heterogeneity, and transport perturbation. These results demonstrate that transport-sensitive analysis provides a

physically meaningful framework for interpreting biomolecular interactions in graphene biosensors operating under electrolyte-gated conditions.

6.1.2 Limitations and Future Perspectives

Although the present work provides insight into electrostatic and transport-mediated sensing mechanisms in electrolyte-gated GFETs, several limitations remain that may be addressed in future investigations. The experimental measurements were primarily performed under simplified low-ionic-strength conditions in order to minimize electrolyte screening and isolate interfacial electrostatic effects. Future studies performed under physiologically relevant electrolyte environments may provide deeper understanding of sensing behaviour under realistic biological conditions where strong ionic screening influences biomolecular coupling near the graphene surface.

The atomistic analysis employed Brownian Dynamics simulations using rigid-body adsorption behaviour and implicit solvent approximations. While this approach enabled efficient investigation of adsorption statistics and orientation-dependent interactions, fully coupled Molecular Dynamics simulations may provide additional insight into hydration effects, conformational flexibility, and dynamic interfacial restructuring occurring during biomolecular adsorption near graphene interfaces.

The present work additionally focused on Human Serum Albumin as a model biomolecular system for investigating adsorption-induced transport perturbation in electrolyte-gated GFETs. Future investigations involving multiple biomarkers with different molecular charge distributions and adsorption geometries may further clarify the role of heterogeneous adsorption behaviour in determining sensing performance in graphene biosensors.

Further development of coupled multiscale simulation frameworks integrating continuum electrostatics with atomistic transport analysis may also improve understanding of the relationship between molecular adsorption dynamics and experimentally observed carrier transport evolution in graphene-based sensing platforms. Such approaches may contribute toward the development of physically grounded biosensing models capable of describing complex electrolyte–biomolecule–graphene interactions under realistic operating conditions.

The integration of electrolyte-gated graphene biosensors with flexible and wearable electronic platforms additionally represents an important future direction for portable and real-time biochemical sensing technologies. Because graphene devices exhibit strong interfacial sensitivity under low-voltage electrolyte gating conditions, such systems may provide promising opportunities for future biomedical monitoring applications.

6.1.3 Final Remarks

The present work demonstrates that electrolyte-gated graphene field-effect transistors provide a highly sensitive platform for investigating biomolecular interactions through coupled electrostatic and transport-mediated sensing mechanisms. The combined continuum, experimental, and atomistic framework developed in this thesis establishes a physically grounded interpretation of graphene biosensing behaviour spanning electric double-layer modulation, ionic screening, heterogeneous adsorption, and carrier transport perturbation near the graphene interface.

The results further indicate that transport-sensitive analysis provides important insight into adsorption-induced disorder within graphene biosensors beyond conventional electrostatic gating interpretation alone. The multiscale approach presented in this work, therefore, contributes toward improved physical understanding of electrolyte-gated graphene sensing systems and may support the future development of highly sensitive and physically interpretable graphene-based biosensing technologies.

LIST OF PUBLICATIONS AND CONTRIBUTIONS

1. Arslan Liaquat*, Ghaseem Baridi, Federico Rapuzzi, Daniele Goldoni, Vito Clericò, El Hadj Abidi, Yahya Moubarak Meziani, Mario Amado, Enrique Diez, Camilia Coletti, Giorgia Brancolini, Leonardo Martini, Luigi Rovati, Francesco Rossella, Graphene Electric Double Layer Transistor for enhanced sensitivity label-free detection of Human Serum Albumin (HSA), **ACS Applied Materials & Interfaces,** Submitted
2. Arslan Liaquat*, Ghaseem Baridi, Federico Rapuzzi, Daniele Goldoni, Vito Clericò, El Hadj Abidi, Yahya Moubarak Meziani, Mario Amado, Enrique Diez, Camilia Coletti, Giorgia Brancolini, Leonardo Martini, Luigi Rovati, Francesco Rossella, Electrolyte Gated Graphene Field Effect Transistor for pH Sensin **ACS Applied Nanomaterials,** Submitted
3. Liaquat, A.**,** Carella, A., Prete, D., Demontis, V., Martini, L., Menozzi, C., & Rossella, F. (2023, October). Impact of counter-electrode and device architecture on the gating performance of iontronic transistors. In *2023* ***IEEE Nanotechnology Materials and Devices*** 785-786 IEEE.
4. Muhammad Isram, Elaheh Abdollahzadeh, Flavia Valentini, Arslan Liaquat, Francesco Rossella, Somayeh Asgary, MgO, CaCo3, and zeolite nano absorbers for NOx, SO2, and CO gases, NanoTrends (Manuscript Number: **NANTRE-D-26-00193).** (Under Review)
5. Ghassem Baridi, Arslan Liaquat, Leonardo Martini, Federico Rapuzzi, Herath Mudiyanselage Kasun Gayanga Anuradha Herath, Maria Celeste Maschio, Vito Clericò, El Hadj Abidi Yahya Moubarak Meziani, Mario Amado, Enrique Diez, Stefano Corni, Luigi Rovati, Giorgia Brancolini and Francesco Rossella, Nonlinear Optical Detection of β2-Microglobulin Using Graphene-Enhanced Third-Harmonic Generation, **Sensors** (Under Review).
6. Ghassem Baridi, Arslan Liaquat, Leonardo Martini, Federico Rapuzzi, Herath Mudiyanselage Kasun Gayanga Anuradha Herath, Maria Celeste Maschio, Vito Clericò, Yahya Moubarak Meziani, Mario Amado, Enrique Diez, Stefano Corni, Giorgia Brancolini, El Hadj Abidi, Luigi Rovati and Francesco Rossella, Multiscale Molecular Dynamics and Quantum–Electrostatic Modelling of Graphene Electric Double-Layer Transistors for β2-Microglobulin Biosensing, **Electronics** (Under Review)

7. Baridi, G., Liaquat, A., Martini, L., Nappi, L., Rapuzzi, F., Clericò, V., Abidi, E. H., Meziani, Y. M., Amado, M., Diez, E., Brancolini, G., Rovati, L., & Rossella, F. (2026). Graphene-Based Chemical Field-Effect Transistors: Impact of Electric Double Layer Model and Quantum Capacitance on Na+ Detection Capabilities. **Micromachines**, 17(4), 433. https://doi.org/10.3390/mi17040433
8. Baridi, G., Liaquat, A., Martini, L., Rapuzzi, F., Clericò, V., Amado, M., Diez, E., Abidi, E. H., Maschio, M. C., Corni, S., Meziani, Y. M., Brancolini, G., Rossella, F., & Rovati, L. (2026). Computational Simulation of a Surface Plasmonic Resonance Biosensor for β2-Microglobulin Based on Electrolyte-Gated Graphene. **Sensors**, 26(9), 2815. https://doi.org/10.3390/s26092815.